2020-08

HYDROLOGICAL MODELING OF CLIMATE CHANGE IMPACTS IN AWASH RIVER BASIN: A CASE OF BORKENA RIVER CATCHMENT, ETHIOPIA

TESHOME, KIFLE WONDIE

BAHIR DAR UNIVERSITY

BAHIR DAR INSTITUTE OF TECHNOLOGY

SCHOOL OF RESEARCH AND POSTGRADUATE STUDIES

CIVIL AND WATER RESOURCE ENGINEERING FACULTY

HYDROLOGICAL MODELING OF CLIMATE CHANGE IMPACTS IN AWASH RIVER BASIN: A CASE OF BORKENA RIVER CATCHMENT, ETHIOPIA

BY

TESHOME KIFLE WONDIE

Bahir Dar, Ethiopia

AUGUST, 2020

HYDROLOGICAL MODELING OF CLIMATE CHANGE IMPACTS INAWASH RIVER BASIN: A CASE OF BORKENA RIVER CATCHMENT, ETHIOPIA.

BY

TESHOME KIFLE WONDIE

Email- Teshome.kif@gmail.com

MSc Thesis Submitted to School of Graduate Studies of Bahir Dar University, Institute of Technology in Partial Fulfillment of the Requirements for the Degree of Masters of Science in Hydraulic Engineering in the Civil and Water Resource Engineering.

Advisor Name: Dr. Mamaru A. Moges

CO- Advisor Name: Dr. Dejne Sahilu

Bahir Dar, Ethiopia

AUGUST, 2020

DECLARATION

I, the undersigned, hereby declare that this thesis submitted for the partial fulfillment of the requirements for the Masters of Science in Hydraulic Engineering is the original work done by me under the supervision of Dr.Mamaru A.Moges and Dr.Dejnie Sahilu and this thesis is my original work and has not been published or submitted elsewhere for the requirement of a degree program to the best of my knowledge and belief. Materials or ideas of other authors used in this thesis have been properly acknowledged and referenced

Name of the student Teshome Kifle Signature

Date of submission: 11/03/2020

Place: Bahir Dar

This thesis has been submitted for examination with my approval as a university advisor.

Advisor Name: Mamaru A. (PhD)

Advisor's Signature:

Bahir Dar University

Bahir Dar Institute of Technology

School of Research and Postgraduate Studies

Faculty of Civil and Water Resource Engineering

THESIS APPROVAL SHEET

Student:

Teshome Wifle Tefera

Name Signature Date

The following members certify that this student has successfully presented the necessary written final thesis and oral presentation for partial fulfillment of the thesis requirements for the Degree of Master of Science in Hydraulic Engineering.

Approved By:

Advisor:

Mamaru A. 07/08/2020

Name Signature Date

External Examiner:

Hanibal Lemma 6/08/2020

Name Signature Date

Internal Examiner:

Biftew Ceneff 06/08/2020

Signature Date

Chair Holder:

Asegdew G. (PhD) 11/08/2020

Name Signature Date

Faculty Dean: Nemesgen Enku Nigussie (PhD) Faculty Dean

Aug. 11, 2020

Name Signature Date

iii

ACKNOWLEDGMENTS

First and foremost, thanks to the Almighty God for granting me his limitless care, love, and blessings all along the way. And I would like to convey my deep-hearted appreciation to Woldia University for providing me financial support for the academic admission to attend this MSc Program at Bahir Dar University. I have special and truthful gratitude to my advisor Dr.Mamaru Ayalew, for his encouragement, insight guidance, and professional expertise to clear out my doubts and I am deeply besieged in his tireless help and assistance for the overall success of this study. Secondly, my special thanks go to my Co-advisor Dr.Dejne sahilu for his inspiration, guidance, and valuable suggestions that led to the start and completion of this thesis work. He has provided me invaluable support starting from giving me materials, documents and related information about the study. Correspondingly I would like to acknowledge the Ethiopian Meteorological Agency, Ministry of Water Resources, for providing the required data and information to fulfill this research work during data collection. Finally, I would like to express my deep feeling of appreciation and thank my family and friends who are always encouraging and rendering me the necessary services and are taking care of some of my responsibilities.

ABSTRACT

Regional and local hydrological regimes are expressively exposed to global climate change, which is considered to be one of the major problems threating water resources and flood security. This research has been done aimed at the examination of the effect of climate change on the hydrology of Borkena watershed, Awash River Basin during 2030s (2021-2040), 2050s (2040-2060), and 2070s (2061-2080) future periods. To realize this, the distributed hydrological SWAT Model driven by three different Global Circulation Models (MIROC5, MPI, and IPSL) under two Representative Concentration Pathway emission scenarios (RCP4.5 and RCP8.5) was used. As result, the GCM projection indicated that, the mean annual maximum and minimum temperature projected to increases by 0.56°c and 0.31°c respectively while the mean annual rainfall has no a significant change in the coming decades. The study also resulted in a considerable average monthly and seasonal, rainfall change in magnitude and direction. Relative to the baseline period the changes in mean annual stream flow from (2021-2080) are mostly negative and indicate a reduction in volume of discharge available in the Borkena river. In addition, trends in the extreme flow are also determined for high and low flows and the results show a forceful negative trend for extreme stream flows and flood volumes may decrease by 43.1% in RCP4.5 under MPI (2021–2040), 38.6% (2041–2060) and 49.4% (2061–2080) in RCP8.5 under IPSL and MIROC5 respectively. These findings will serve as a nearly warning for the alarming extreme weather events for the future period in Borkena watershed as well as Awash River basin which require sustainable and effective adaptive measures for future water resource management.

Key words: Climate Change, SWAT, CORDEX Awash, Borkena

Table of Contents

LIST OF FIGURES

LIST OF TABLES

LIST OF ABBREVATIONS

AR4	Assessment report No.4
AR5	Assessment report No 5
Arc SWAT	ArcGIS Integrated SWAT Hydrological Model
Asl	above sea level
CDF	Cumulative Distribution Function
CMIP5	Coupled Model Inter-comparison Project Phase5
CORDEX	Coordinated Regional Downscaling Experiment
DEM	Digital elevation model
DMC	Double Mass Curve
FAO	Food and Agricultural Organizations
FDC	Flow duration curve
GCM	Global circulation Model
GHG	Green House Gas
GIS	Geographic Information System
GLUE	Generalized Likelihood Uncertainty Estimation
GPS	Global Positioning System
HRU	Hydraulic Response Units
IPCC	Inter-Governmental Panel on Climate Change
IWMI	International Water Management Institute
MoWIE	Ministry of Water, Irrigation & Electricity
NMA	National Metrological Agency
Parasol	Parameter Solution
PET	Potential Evapotranspiration
RCA4	Rossby Center Regional Atmospheric model
RCM	Regional Climate Models
RCP	Representative Concentration pathway
RMSE	Root Mean Square Error
SMHI	Swedish meteorological and hydrological institute

SRES	Special Report on Emission Scenario
SRTM	Shutter Radar Topography Mission
SUFI-2	Sequential Uncertainty Fitting version-2
SWAT	Soil and Water Assessment Tool
SWAT-CUP	SWAT Calibration and Uncertainty Program
USAID	United States Agency for International Development
USBR	United States Bureau of Reclamation
USGS	United States Geology Survey
WCRP	World Climate Research Program
WMO	World Metrological organization

1. INTRODUCTION

1.1. Background of the Study

With the development of economy and industry, greenhouse gases especially co_2 are emitted continuously to the atmosphere, which leads to global climate change (sui, et al, 2010). The atmospheric concentration of co_2 and other trace gases has increased substantially over the last century and double concentration of co_2 is expected by the middle or latter part of the next century if no control measures are adopted (singh & kumar, 1997). The earth's warming of a half-degree Celsius during the 20th century can be explained simply by asserting the trend to be a natural fluctuation in the climate. Climate is usually defined as the average weather or more rigorously, as the statistical description of the weather in terms of the mean and variability of relevant quantities(rainfall and temperature) over periods of several decades (Houghton et al., 1997). Climate change is often taken to mean climate fluctuations of a global nature, including effects from human activities such as the enhanced greenhouse effect and natural causes such as volcanic aerosols. This alteration of the global atmosphere includes changes in land use as well as anthropogenic emissions of greenhouse (Penner et al 1999).

Changes to climate and climate variability will impact on hydrological systems and affect the flow in rivers(Graham, et al, 2007). Impacts of climate change and climate variability on the water resources are likely to affect irrigated agriculture and installed power capacity. Changes in flow magnitudes are likely to raise tensions among the provinces, in particular with the downstream areas concerning reduced water flows in the dry season and higher flows and resulting flood problems during the wet season (Bogner et al., 2008).

The IPCC finding indicates that developing countries, such as Ethiopia will be more vulnerable to climate change because of the less flexibility to adjust the economic structure and is largely dependent on agriculture; the impact of climate change has far reach implication in Ethiopia. In Ethiopia, climate change is expected to intensify the great hydrological variability and frequency of extreme events, and drought and flood may have a significant negative effect on the development of the agriculture sector and the economy as a whole. Therefore, the projection of climate change impact on water resources of the country should not be deserted on the future development plan

(You & Ringler, 2010). Therefore, there is a need to quantify and assess the future scenarios of climate change and its impact on water resources of the country as a whole and in each catchment in particular, because the country s future development relies on this resource. Even though much research has been done in continental or global scale studies related to climate change, the magnitude and type of impact at the regional-catchment scale are not investigated in many parts of the world that includes Ethiopia.

In addition to this reason; one of the climate change studies in water resources of Ethiopia has focused on existing information over large river basins and not much research has been conducted in a different part of the country at the catchment scale. Investigating climate change at the local level allows defining the degree of vulnerability of local water resources and plan appropriate adaptation measures that must be taken ahead of time. Moreover, this will give enough opportunity to consider possible future risks in all phases of water resource development at the local scale (Kim et al., 2014).

To investigate the impact of climate change on future water resources a hydrological model can be driven with the output from a regional climate model (Akhtar, et al.,2008). Borkena River is one of the main tributaries of the Awash River basin, found in Amhara region, and has been chosen as a study area for this research. Some high intensity could produce local floods, but most heavy runoffs come from highland humid regions of Awash River basin causing lowland inundation and sedimentation lowland region.

Therefore quantitative estimates of hydrologic effects of climate change are essential for understanding and solving the potential water resource management problems associated with water supply for domestic and industrial water use, power generation, and agriculture as well as for future water resource planning, reservoir design and management, and protection of the natural environment (Hailemariam, 1999). This research aims to generate climate scenarios from precipitation and temperature over the Awash River basin representative catchment to assess the potential impact of climate change on surface runoff in the catchment. The precipitation and temperature scenarios were generated from three representative dynamically downscaled regional climate models on behalf of coordinated regional downscaling experiment (CORDEX) project under two representative concentration pathways (RCP4.5 and

RCP8.5) and the outputs were changed to fine resolution for the hydrologic model using bias correction methods. In general investigating climate change impact on the Borkena river catchment, in particular, was very important because of the research has addressed assessing of the general trends of the future climate variables such as Precipitation, Maximum and Minimum temperature and the possible future potential impacts of climate change on the stream flow of Borkena catchment using Regional Climate Model outputs by integrating with the soil and water assessment tool (SWAT).

1.2. Statement of the problem

Climate change has a profound impact on natural resources, of which water is one of the most important. With climate change, the amount of rainfall in many parts of Africa is expected to decline while variability may increase dramatically (IPCC, 2007). Due to climate change and variability, there is an increase in the severity of extreme events which results in fluctuation of storages. This may lead to an increase in floods and droughts. Ethiopia has plentiful water resources, which can be appropriately utilized to enhance the socio-economic development of its people but due to the lack of development of this resource, the people of Ethiopia have been exposed to major problems such as impacts of drought and flood; shortage of clean water supply, and inadequate energy supply (Hailemariam, 1999).

Awash River Basin is one of the most utilized Rivers in Ethiopia that serves as drinking water, hydropower industrial consumption, and irrigation (Hemel et., al, 2013).The development of irrigation projects in the upper reaches of the basin, coupled with drought occurrences have caused a serious threat to the region's water resources, affecting the socio-economic activity of the people and the diversity of ecosystem especially in the lower reach of the basin (Edossa et al., 2010). As it is the case in other Rivers, the major tributaries have been subjected to major environmental stress and climate change, frequent and persistent droughts and the associated flood insecurity have drastically affected the human and livestock population, especially in the middle and lower basins of Awash River. Even though, Awash River Basin is intensively utilized and has a vast potential for irrigation and other developmental activities there is little and fragmented information on the impact of climate change on the Basin hydrological process. The Borkena watershed in the Awash River basin

is one prominent example where no information exists regarding climate change, and its impact on hydrological processes and sediment loss, while the stream is a major tributary to the Awash River. In general, even if the water resource in the Borkena watershed is a fundamental basis for the economic growth and social development of the communities and also the source of instability in the case of flooding during summer. Therefore, modeling of water resources in light of future climate change is very important for sustainable planning and management of the water resources in the watershed as well as the Basin based on the information obtained. Hence the present study is designed to determine the sensitivity of hydrological processes to climate change in Borkena watershed using Representative concentration pathways (RCP).

1.3. Objective of the study

1.3.1. General Objective

The main objective of this study was to evaluate the hydrological impacts of climate change on the extreme hydrology in the catchment of the Borkena River.

1.3.2. Specific objectives

- To evaluate the significance of trends in hydro climatological variables.
- To evaluate the Performance of Global climate models (MPI, MIROC5 and IPSL) to simulate climatological variables in Borkena watershed.
- To develop a hydrologic SWAT model for the Borkena watershed.
- To evaluate climate change impacts on extreme hydrology for future RCP scenarios.

1.4. Research question

- What are the trends of climatological variables in the present and future scenarios?
- How does the Global climate model data downscale to statistical level using observed climate variables (Rainfall, Temperature)?
- How much the extreme flow, will likely be changed in the future as compared to the baseline period?

1.5. Scope of the Study

This study was a step towards analyzing climate change impacts on the hydrology of the study area especially to the rainfall-runoff characteristics of the Borkena river watershed. Inanition this study was limited to analyzing the feedback mechanism of the impact of climate change on the rainfall-runoff of the watershed for different scenarios which were considered in this study.so based on the objective of the study scope of this study would have gone on overseeing how climate is changed and how its change will affect the rainfall run-off response of the watershed.

1.6. Significance of the Study

This research would have a contribution for addressing valuable information on the projected climate change impact in the catchment of Borkena river and assessing future water resources availability that helps to know what changes in climate means may be expected in the future and will provide enough information about the variability and methodological status of the watershed which will be very essential for watershed development and management options, and decision-makers will be beneficiaries on decision making based on the outcome of this Research.

1.7. Thesis structure

This thesis contains five chapters organized as follows. The first chapter gives a general introduction to the study with its background of the statement of the problems, objective of the research, research questions, and significance of the study. The second chapter summarizes the reviewed literature regarding the subject of climate change in terms of global, continental, and regional aspects, major previous studies conducted in the Awash basin, recent climate change scenarios, and overview of the SWAT model. The third chapter presents a brief description of the study area, data availability, and sources and dealing with the methodology adopted for this thesis. Chapter four one of the main parts of this studies presents the outcome of the model application to assess the impact of climate change. It gives a detailed account of the model set up, the sensitivity of model par ammeters, calibration, validation, and interpretation of results. Finally, in chapter five, conclusion, recommendations, reference and appendix are presented respectively.

2. LITERATURE REVIEW

2.1. Climate Change

Based on IPPC (IPPC, 2007), the climate is defined as describing weather elements by way of average and variation for the duration from months to decades and century with thirty years being classical averaging period for most of its weather element to properly describe the climate of that particular region. And climate change is changes in climatic variables or an element through time (USAID, 2007. It is the current serious issue though out the world and widely accepted that climate change has already happened and further change also expected.

Over the last century, between 1906 and 2005, the average global temperature was risen by about 0.74 ^{0}C. This climate change has happened in two phases, which is from the 1910s to the 1940s and more strongly from the 1970s to the present-day. Everything around us is now dedicated to future considerable environmental change throughout the following thirty years what's more, past. This change is liable to quicken over whatever remains of the 21st century (Barker et al., 2007). The negative impacts of climate change on freshwater systems will most likely outweigh its benefits. Current projections show that crucial changes in the temporal and spatial distribution of rainfall and the frequency and intensity of water-related disasters have risen significantly with increasing greenhouse gas emissions (Water, 2015)

2.2. Climate Change and Water Resources in Ethiopia

Ethiopia is among those countries, which are most vulnerable to climate risks in Africa. Its high vulnerability derives in large measure from the country's heavy dependence on rain-fed, subsistence agriculture Ethiopia is a country where about 80% of the population is engaged in the agricultural sector (Dile et al., 2013) and the main source of income for rural communities (Bryan et, al, 2009). Around 90% of the country's grain is produced by smallholder farms. Subsistence and rain-fed farming systems dominate and, with few exceptions, irrigation is not practiced (Ahmed et al., 2009). Consequently, agricultural and livestock production, people's livelihoods and food security depend strongly on weather conditions mainly on rainfall patterns such as amounts and timing. Hence, a large share of Ethiopia's population is very vulnerable to climate change and in particular to its interred annual variability

(Liersch et al., 2018). The Ethiopian Highlands, from which most water resources obtained considered as the water tower in East Africa. Most of the rivers like Borkena are the most important water resource. With the growth of the number of populations, industrialization, climate change, and its variability the situation becomes more and tenser (Abtew & Dessu, 2019).

Nowadays Climate modeler carried out new atmosphere demonstrate tests utilizing the time arrangement of emanations and focuses related with the four RCPs, as a feature of the preliminary stage for the advancement of new situations for the IPCC's Fifth Assessment Report and future. Therefore, Knowledge about the availability of future water resources in this area and studies providing insights into climate change, and their impacts on hydrology are of utmost importance.

2.3. Representative Concentration Pathway (RCPs)

RCPs are time and space-dependent trajectories of concentrations and emission of greenhouse gases and pollutants resulting from human activities, including changes in land use. RCPs provide a quantitative description of concentrations of the climate change pollutants in the atmosphere over time, as well as their radiative forcing in 2100. RCP is the latest generation of scenarios that provide input to climate models in climate research. The RCPs were developed by the combined efforts of the researchers from different disciplines involved in climate research (Van Vuuren al., 2011).

A total of four pathways RCP2.6, RCP4.5, RCP6, and RCP8.5 were developed. They were named based on the radiative forcing target levels of 2.6, 4.5, 6 and 8.5 Watt/m2, by the end of the 21st century (Meinshausen et al., 2011).The estimation of radiative forcing is based on the forcing of GHGs and other agents. All these four pathways were considered to be representative of all the literature pertinent to change in climate (Van Vuuren et al., 2014). And each RCP defines a specific emissions trajectory and subsequent radiative forcing (McPherson et al., 2017).

2.3.1. RCP2.6 (mitigation scenario)

The RCP 2.6 was developed by using the MESSAGE model and the Integrated Assessment Framework by the International Institute for Applied Systems Analysis (IIASA) (McPherson et al., 2017). This RCP2.6 is representative of the mitigation scenarios, which aims to limit the increase of global mean temperature to 2^{o}c. This

pathway is also referred to as RCP3PD in which PD stands for peak and decline. This pathway indicates that radiative forcing will reach around 3 W/m2 in the mid-century and decline afterward to 2.6 W/m by the end of the 21st century (Van Vuuren et al., 2011).To achieve this, the emission would need to be significantly reduced. The important assumption in this scenario is that new energy-efficient technologies can be rapidly transferred to all over the world and implement immediately (Van Vuuren, Stehfest, et al., 2011).

2.3.2. RCP4.5 (stabilization scenario)

The RCP4.5 was developed by the global change assessment model (GCAM) modeling group at the Pacific Northwest National Laboratory's Joint Global Change Research Institute (JGCRI) in the United States. It is the stabilization scenario (Wayne,2013) in which radiative forcing stabilizes at 4.5W/m2 (approximately 650 ppm CO2-equivalent) in 2100 without ever exceeding that value (Thomson et al., 2011).However, it doesn't mean that the GHG emissions and concentrations are stable. The major assumptions of this scenario are the global population reaches a maximum of 9 billion by 2065 and then declines to 8.7 billion in 2100, declines in energy consumption, increase in fossil fuel consumption, the substantial increase in renewable energy and nuclear energy use, and the large increase in forest area as a mitigation strategy (Thomson et al., 2011).

2.3.3. RCP6 (stabilization scenario)

The RCP6 was developed by the Asia-Pacific Integrated Model (AIM) modeling team at the National Institute for Environmental Studies (NIES) in Japan. It is a stabilization scenario in which total radiative forcing is stabilized shortly after 2100, without overshoot, by the application of a range of technologies and strategies for reducing greenhouse gas emissions. It is a stabilization scenario like RCP4.5 but here relative forcing stabilizes at 6.0 W/m2 in the year 2100 without exceeding that value in prior years (Masui et al., 2011). It is a climate policy intervention scenario in which climate policies are implemented to restrain radiative forcing not to exceed 6.0 W/m2. In this scenario, the GHG emissions will be the highest in 2060 and then decline thereafter. The primary assumptions of this RCP increased in energy demand, shift from coal-based to gas-based production technologies, increase in the use of non-fossil fuel energy type and increase in population and economic growth in the urban

area, expansion of cropland and forest area, and decrease in grassland (Masui et al., 2011).

2.3.4. RCP8.5 (high emission scenario)

The RCP8.5 was developed by Integrated Assessment Framework by the International Institute for Applied System Analysis (IIASA) using the MESSAGE model (Riahi et al., 2011).This pathway is also called a baseline scenario without including any mitigation target or without explicit climate policy. GHG emissions increase significantly over time leading to 8.5 W/m2 of radiative forcing by the end of the 21st century. The important assumptions in this pathway are a continuous increase in global population reaching 12 billion by 2100, slow income growth with modest rates of technological progress, long-term high energy demand, moving towards coal intensive technologies and high emission in the absence of climate change policies (Riahi et al., 2011)

2.4. Global Climate Models

A global climate model represents numerically the characteristics of the global climate system, how they interact and respond mechanism (Vermeer & Rahmstorf, 2009). They are used to examine the influence of increased concentrations of GHGs and aerosols in the atmosphere through simulation of the processes and interactions that define the global climate. Essentially, GCMs are used to study large scale phenomena such as global circulation of the atmosphere, land, and ocean as well as at the continental scale of rainfall and temperature but cannot represent the fine-scale details that characterize local climates in many regions of the world (Whitehead, et al., 2009). One of the widely accepted methods of adding the finer details that are missed out by GCMs is the use of Regional Climate Models (RCMs) which are the subject of the next section.

2.5. Regional Climate Models

Regional Climate Models (RCMs) works by increasing the resolution of the GCM in a small, limited area of interest. Assumptions in regional models are that the data used are drawn from the global climate model over a limited area such as East Africa (IPCC, 2007). Essentially, there is a connection between the local climate and the global climate events such that the enormous global circulations interfere with domains such as the East African region, the boundary conditions of the RCMs

consist of the information drawn from the GCM outputs. Since two models have different resolutions, the RCM s domain should larger for it to accommodate the climactic event concerning the orographic influence and other small atmospheric processes to grow and the domain should not be too large as to allow the flow to deviate too much in the running model (Samuelsson et al., 2011).

To get regional climate model projections for purposes of impacts studies, regional climate model runs are normally done on time-slice modes Therefore, regional climate forecast is important in modeling influence on hydrological conditions of river basins and catchment worldwide (Feser et al., 2011), and thus Coordinated Regional climate Downscaling Experiment (CORDEX) climate data for studies on climate change is very essential.

2.6. Coordinated Regional Climate Downscaling Experiment (CORDEX)

A World Climate Research Program (WCRP) intends to coordinate and provide regional climate forecasts in the world that will be useful for studies on impacts, adaption, and mitigation of changing climate and for the preparation of IPCC 5th Assessment Report. In CORDEX, ensemble dynamical and statistical models are normally produced by looking at global models resulting from the 5th Climate Intercom paring Project with an initial project being started in Africa since there are already other projects running. The output from CORDEX provides timely access to changes in climate scenarios which is vital for developing countries like Ethiopia where economic stresses are likely to increase vulnerability to influence of climatic conditions especially on the hydrology of a river basin from a given rainfall event (Giorgi et al, 2009).

2.7. Downscaling Climate Models

Downscaling is a technique for exploring the regional and local-scale response to global climate change as simulated by comparatively low-resolution global climate models (GCMs) (Jones et al, 2009). Downscaling is commonly done either by using Regional Climate Downscaling (RCD) or Statistical Downscaling Methods (SDSM). RCD has been increasingly used to address a variety of climate-change issues and have by now become an important method in climate change research (WMO, 2008). GCM‟s are coarse in resolution and are unable to resolve significant sub-grid scale features such as topography, clouds, and land use (Ramírez Villegas & Jarvis, 2010).

There are two main approaches available for the downscaling of large spatial resolution GCM outputs to a finer spatial resolution, termed dynamical and statistical downscaling.

2.7.1. Dynamical downscaling

It is a higher resolution climate model or regional climate model that is forced using a GCM. The statistical approach establishes empirical relationships between GCM-resolution climate variables and local climate. Dynamical downscaling is usually based on the use of regional climate models (RCMs), which generate finer resolution output based on atmospheric physics over a region using GCM fields as boundary conditions (Pielke Sr & Wilby, 2012). Thus, this method is also called the 'nested' RCM approach, which was first applied in climate change studies in the late 1980s by (Gustafson Jr & Leung, 2007). RCMs also referred to as Limited-Area Models (LAMs), produce highly resolved spatial and temporal climate information (Schmidli et al, 2006; Wilby et al., 2004).

Dynamical downscaling seeks to couple large scale climate dynamics and local climate and hydrological features. It does so by utilizing higher-resolution regional climate models (RCMs) that respond to the output of GCMs. The GCM output is provided as boundary conditions, which are the values at the edges of the spatial domain of the RCM. RCMs are used for downscaling seasonal climate forecasts and for diagnostic studies of regional climate in addition to their use with climate change projections. The main drawbacks are the requirement of powerful computing capacities and the dependency on initial and boundary conditions. There is also still a lack of readily available climate scenario ensembles for most regions in the world, although the number of publically available ensemble archives from European projects on a similar grid size is increasing, e.g., (Mearns et al., 2003).

2.7.2. Statistical downscaling

Based on particular statistical relationships between the coarse GCMs and fine observed data, statistical downscaling is a straightforward means of obtaining high-resolution climate projections. Statistical downscaling may be used whenever impacts models require small-scale data, provide suitable observed data are available to derive the statistical relationships, and covers all kinds of locations. The output obtained is generally small scale information on future climate or climate change (maps, data,

etc.), the key input being appropriate observed data to calibrate and validate the statistical model(s) and GCM data for the future climate to drive the model(s) (Wilby & Dawson, 2013). It is a tool for downscaling climate information from coarse spatial scales to finer scales. The underlying concept is that local climate is conditioned by large-scale climate and by local physiographical features such as topography, distance to coast, and vegetation. At a specific location, therefore, links should exist between large-scale and local climatic conditions.

Statistical downscaling consists of identifying empirical links between large-scale patterns of climate elements (predictors) and local climate (the predicted), and applying them to output from global or regional models. Successful statistical downscaling is thus dependent on long, reliable series of predictors and predictands statistical downscaling is less technically demanding than regional modeling; it is thus possible to downscale from several GCMs and several different emissions scenarios relatively quickly and inexpensive; it is possible to tailor scenarios for specific localities, scales, and problems.

2.8. Bias correcting climate models

If the output from a GCM or RCM is not corrected for biases, the model will produce simulations that are not realistic (Piani et al., 2010). Bias correction methods use a transformation algorithm to adjust RCM and GCM outputs. The purpose of bias correction is to identify possible biases between observed and simulated climate variables. It is assumed that the correction algorithms and its parameterization for current climate conditions are also valid for future conditions. Multiple bias correction methodologies have been developed and those that have been used in research include power transformation and (Barlow et al., 2011), stochastic weather generators (Teutschbein & Seibert, 2012), cumulative distribution functions (Turco et al., 2011), change factor for temperature and quintile mapping for precipitation (Kumar et al., 2015), artificial neural networks (Najafi & Moradkhani, 2015) or through the use of a fitted histogram equalization function (Jakob et al., 2011) and daily bias-corrected and constructed analogs (Maurer et al., 2015).

The six main methods of bias correcting are linear scaling, local intensity scaling (LOCI), power transformation, variance scaling, delta change, and distribution mapping. Linear scaling corrects the RCM data by adjusting the mean monthly values

with a correction factor. While the bias correction is fairly simple to perform, it adjusts all events, including extreme weather events, with the same correction factor. It also cannot correct for the frequency of which precipitation events occur. Local intensity scaling attempts to make up for the disadvantages of linear scaling by adjusting the RCM data to have the same mean, wet-day frequencies, and intensity as the observed data (Ehret et al., 2012).

However, local intensity scaling cannot reproduce the effect of regional processes and does not allow for precipitation variances to be corrected. Power transformation and variance scaling adjust both the variance and mean of precipitation and temperature respectively. However, the power transformation of precipitation is unable to accurately correct the probability of dry days and precipitation intensity. The delta-change approach does not account for potential future changes in climate. In other words, the delta change approach does not allow the number of dry vs wet days to change (Graham et al., 2007).

2.9. Baseline scenario

In the assessment of future impacts of climate change studies, before considering future climate it is important to characterize the present-day or recent climate in a region referred to as the climatological baseline. The need for this baseline period is to define the observed climate with which climate change information is usually combined to create climate scenarios. The choice of baseline period has often governed by the availability of the required climate data. The baseline period usually selected according to Representativeness for the present-day, recent average climate in the study region, Sufficient duration to encompass a range of climatic variations including the number of different Weather conditions, Including data of sufficiently high quality for use in evaluating climate impacts, Covering a period for which data on all climatological variables available, adequately distributed over space and readily available the following criteria(Carter, 2007).

2.10. Previous climate studies in the Awash River Basin

Numerous studies regarding climate (precipitation, temperature, and stream flow) change have been conducted in the Awash River basin with most studies focusing on annual and seasonal total precipitation and stream flow. Studies that explicitly considered, extreme conditions are limited and the results of these investigations are often divergent and inconsistent. The precipitation prediction over the Awash River basin, the results of the various authors are different.

Tesema et al., (2020) studied and quantify the impacts of climate change on stream flow in Kesem sub-basin, Middle Awash River basin, Ensemble mean of four Coordinated Regional Climate Downscaling Experiment (CORDEX) Africa regional climate models operating under two alternative scenarios of Representative Concentration Pathways (RCP 4.5 and RCP 8.5) was used. The impact assessment on stream flow was done using soil and water assessment tool (SWAT) hydrological model. Mean monthly changes in precipitation and temperature (maximum and minimum) were used to quantify these impacts. The result of bias-corrected precipitation and temperature disclosed a logical increase in all future periods for both RCP 4.5 and RCP 8.5 scenarios. These changes in climate variables created an increase in mean annual stream flow by 14.5 and 19.1% for RCP 4.5 and by 4.7 and 6.9% for RCP 8.5 scenarios of the 2050s and 2080s, respectively.

Getahun & Lanen (2016) studied the Impact of Climate Change on Hydrology of the Upper Awash River Basin in the selected watershed (Intercomparison of old SRES and new RCP scenarios) on Awash River basin. The study used HBV hydrological model and selected GCMs correspondence with SRES A2, RCP4.5, and RCP8.5 scenarios considering the periods as intermediate future (2021-2050) and far future period (2071-2100). The result of the study indicated that the predicted precipitation increase using RCP was 18% for intermediate and 34% for the far future, whereas using SRES it was increased by 3% for intermediate and 4% for the far future. The possible increase of evapotranspiration was also estimated to be 11% for intermediate and 24% for the far future using all GCMs.

The increase of evapotranspiration using RCP was 17% for intermediate and 34% for the far future, whereas using SRES it was 6% for intermediate and 13% for the far

future. The projected stream flow also was projected to increase using RCP by 12% for intermediate and 29% for the far future, whereas using SRES it was projected to decrease in 2% for intermediate and an increase in 4% for the far future. The maximum temperature increase was 1.8°C by intermediate and 4.5°C by far future, whereas the minimum temperature increase was 2.3°C by intermediate and 5.7°C by far future.

Hailemariam (1999) assessed the impact of climate change on the water resources of Awash River Basin using GCM (both transient and CO2 doubling) and incremental scenarios. The International Institute for Applied System Analysis (IIASA) integrated water balance model was used to estimate runoff under a changing climate. The study found that the results of the impact assessment over the basin showed a projected decrease in runoff which ranged from (–10 to –34%. And a 20% decrease in rainfall coupled with a 2°C increase in a temperature decrease in the annual runoff. Even a temperature increase of 2°C without precipitation change would result in a 9% decrease in the annual runoff. On the other hand, an increase of precipitation by 10% would counterbalance a 2 to 4°C increase in temperature and result in a surplus of runoff ranging from (4 to 12%).

Taye et al.,(2018) studied the Climate Change Impact on Water Resources in the Awash Basin. The study used an improved change factor method to estimate future water availability and three well-performed GCMs in conjunction with the RCP8.5 scenario. The study concluded that the projections for the future three periods (006–2030, 2031–2055, and 2056–2080) show an increase in water deficiency in all seasons and for parts of the basin, due to a projected increase in temperature and decrease in precipitation.

Daba,(2018) assessed SWAT simulated hydrological response to climate change impacts and its adaptation strategies in the upper Awash River basin. The study used the Soil and Water Assessment Tool (SWAT) hydrological model and Regional Climate Model (RCM). To investigate the hydrological impact of a possible future climate change scenario; downscaling of regional climate model (ECHAM5 with A1B emission scenario) to meteorological variables at local scale was applied for three time periods (the 2020s, 2050s, and 2080s.

The results show that average annual maximum temperature changes for the basin were the 2020s: 0.53°C, 2050s: 1.18°C and 2080s: 1.87°C relative to the historical

climate (1980-2010). The average annual minimum temperature change was 0.58°C, 0.82°C, and 2.14°C in the 2020s, 2050s and 2080s respectively. Basin average annual rainfall based on the ECHAM5 downscaling was 2.40, -2.14, and -10.11% for future periods of the 2020s, 2050s and 2080s respectively. The annual stream flow of upper awash sub-basin is reduced by 2.46% and 18.14% in 2050s and 2080s respectively, while the stream flow increased in 2020s by 4.90% for A1B scenario.

The simulated flow at the 2050s and 2080s with A1B scenario from RCM shows a reduction of runoff by 1.52% and 3.50% in the sub-basin and it is directly related to the reduction in precipitation, while the annual runoff increase in 2020s by 8%. The model result shows that about 44.36% of annual rainfall contributes to stream flow as surface runoff. Generally, the results revealed that change in climate variables such as a decrease in rainfall and increase in temperature would have a significant impact on the stream flow and surface runoff, causing a possible reduction in the total water availability in the sub-basin.

Bekele et al., (2019) analyzed impact of climate change on hydrological processes of the Keleta watershed in the Awash River .Delta statistical downscaling methods were used to downscale 20 global circulation models (GCMs) and two representative concentration pathways (RCPs) (RCP 4.5 and RCP 8.5) over the study periods of 2050s and 2080The Soil and Water Assessment Tool (SWAT) model was used to simulate hydrological processes. The results show that RCP 4.5 predicts an average precipitation increase of 15.2 and 17.2% for midland end-of-century data, respectively.

Similarly, RCP 8.5 predicts an average precipitation increase of 19.9 and 34.4% for midland end-of-century data, respectively. Mid-century minimum and maximum temperature increases range from 1.8 to 1.6 °C (RCP 4.5) to 2.6 to 2.1 °C (RCP 8.5), respectively, while end-of-century increases vary from 2.4 to 2.0 °C (RCP 4.5) and 4.6 to 3.7°C (RCP 8.5), respectively. This leads to an average increase in runoff by 70%. On the other hand, the mean monthly surface runoff reaches maximum value during the main rainy season (July, August and September) followed by the short rain y season (March, April and May).

And he summarized that, the hydrologic component of the watershed is highly sensitive for precipitation change than temperature change such that the increased rainfall, warmer temperature, significant increment in the hydrologic component

particularly the surface runoff and associated extreme peak flows over the coming decades. Most of the studies result over the Awash indicated that the temperature increase from and the magnitude varies depending on the type of GCMs. Even though the above-mentioned reasons which cause uncertainties of the prediction of future climate variables over the Awash River Basin, it is not clear which combination of input would give a good insight for the understanding of future plausible climate conditions where the current hydrological and meteorological parameter values are different in most of the studies mentioned.

Most of the previous studies used gridded data sets which are constructed based on the interpolation of a few climate stations distributed sparsely across Ethiopia. The investigations typically address results of mean annual and seasonal scale by using statistical downscaling or bias correction techniques of GCM outputs based on SRES. Due to the high spatial variability of climate in the Awash River basin, incorporating only a few stations may not be reasonable for such a large area. To fill the gap for the inconsistency of studies detail investigation and evaluation of climate changes on an extreme state on a hydrological variable on specific watershed using up to date emission scenarios and appropriately tested hydrological model to be used. The uniqueness of this study is the use of i) Parameter Efficient semi Distributed (SWAT) hydrological water balance model which was verified for Ethiopian watersheds having different geographical climate patterns ii) up to dated Representative Concentration Pathway (RCP) scenarios and iii) using different RCMs at small scale watershed.

2.11. Hydrological modeling

There are many models for evaluating basin hydrology, which is used by water resource managers and researchers. These models help to estimate and specify the effect on runoff from a special development program. Continuous flow models can provide a better understanding of basin hydrological responses due to its climate and vegetation changes. Watershed models are used for a better understanding of hydrological processes role that control the movement of surface and subsurface water.

Choosing a proper model strongly depends on several factors such as simulation of design parameters(surface-runoff, groundwater, sediment load) accuracy, available

data, and temporal and spatial scales (Shiklomanov et al., 2013). The watershed models can be classified into two major groups based on their performance on spatial components. Lumped models, consider the basin as an integrated unit without considering the spatial changes in the processes, inputs, boundary conditions, or hydrological characteristics of the basin. In contrast, the distributed models consider the spatial changes by solving the equations of each pixel in the basin network (Strauch et al., 2012).

2.12. Soil and Water Assessment Tool (SWAT)

The Soil and Water Assessment Tool (SWAT) is a physical hydrological model developed by United States Department of Agriculture-Agricultural Research Service (USDA-ARS) to study the influence of land use on hydrology, sedimentation, and chemical yields from agriculture in watersheds with distinct physiographic parameters and management conditions over some time. Currently, the model is being used to estimate the impacts of climate change and land use management on water resources (Gassman et al, 2007). In SWAT a catchment is divided into sub-basins based on the type of soil, land use/cover, and slope for simulating runoff. SWAT model has been used widely in the world to study various aspects of hydrological processes (Chekol et al., 2007) but specific application on climate change was reviewed in this study. SWAT operates on a daily time step and is composed of eight major model components including weather, hydrology, soil temperature and properties, plant growth, nutrients, pesticides, bacteria and pathogens, and land management. Currently, the model is being used to estimate the impacts of climate change and land use management on water resources (Tibebe et al., 2016).Arc SWAT is a geographic information system (GIS) interface for SWAT.

2.12.1. Hydrologic components of the SWAT model

Water balance is the driving force behind everything that happens in the watershed. SWAT simulation of the hydrology of the watershed can be separated into two major divisions. The first division is the land phase of the hydrologic cycle controls the amount of water, sediment, nutrient, and pesticide loadings into the main channel in each sub-basin. The second division is the routing phase of the hydrological cycle which can be defined as the movement of water, sediments, etc. through the channel network of the watershed to the outlet (Neitsch et al., 2002). As far as this research

work is concerned the hydrologic cycle mainly focused only on the movement of water, which is the runoff generation. The hydrologic cycle simulated by SWAT is based on the following water balance equation:

$$\mathrm{SW_{t=}}SW_0 + \sum_{i=1}^{t}(R_{day} - Q_{surf} - E_a - W_{seep} - Q_{Qw} \qquad (2\text{-}1)$$

Where: SWt (mm) is the final soil water content at time *t* (day), SWo (mm) is the initial soil water content on day *i*, and Rday (mm), Qsurf (mm), Ea(mm), WSeep(mm), and Qgw(mm) are the amount of precipitation, surface runoff, evapotranspiration, percolation, and return flow (or base flow) on day *i*, respectively.

2.12.2. Surface runoff

Surface runoff occurs whenever the rate of water application to the ground surface exceeds the rate of infiltration. SWAT p provides two methods for estimating surface runoff: the SCS curve number and plant ET method. For this research work, the SCS curve number method has been designated

$$\mathrm{Q_{surf}} = \left[\frac{(R_{day} - I_a)^2}{(R_{dsay} - I_a + S)}\right] \qquad (2\text{-}2)$$

Where: Q_{surf} is the accumulated runoff of rainfall excess (mm) R_{day} is the rainfall depth for the day (mm), Ia is the initial abstractions which include surface storage, interception, and infiltration before runoff (mm), S= is the retention parameter (mm).The retention parameter varies spatially due to changes in soils, land use, management, and slope and temporally due to changes in soil water content. The retention parameter is defined as:

$$\mathrm{S} = 25.49\left[\frac{1000}{CN} - 10\right] \qquad (2\text{-}3)$$

Where: CN is the curve number or the day. The initial abstraction, Ia, is commonly approximated as 0 .2 S and Eq. (2.3) becomes,

$$\mathrm{Q_{surf}} = \left[\frac{(R_{day} - 0.2S)^2}{(R_{dsay} - 0.8S)}\right] \qquad (2\text{-}4)$$

The runoff will only occur when Rday> Ia.

2.12.3. Routing

The routing phase is the second division of the hydrological cycle which can be defined as the movement of water, sediments, etc. through the channel network of the watershed to the outlet. Two options are available to route the flow in the channel network: the variable storage and Muskingum methods. The variable storage method uses a simple continuity equation in routing the storage volume, whereas the Muskingum routing method models the storage volume in a channel length as a combination of wedge and prism storages. The variable storage method was used for this study

2.12.4. Peak Runoff Rate

The peak discharge or the peak surface runoff rate is the maximum volume of flow rate passing a particular location during a storm event. SWAT calculates the peak runoff rate with a modified rational method it assumed that a rainfall of intensity I begin at time t=0 and continuous indefinitely, the rate of runoff will increase until the time of concentration t= t_{con} and mathematically expressed as:

$$q_{peak} = \left(\frac{\alpha_{tc} * Q_{surf} * Area}{3.6 * t_{con}}\right) \quad (2\text{-}5)$$

Where: q_{pea} is the peak runoff rate (m3/s), is the fraction of daily rainfall that occurs during the time of concentration, Q_{surf} is the surface runoff (mm), Area is the sub-basin area in (km2), and α_{tc} is the time of concentration(hr), and 3 .6 is the conversion factor.

2.12.5. Potential Evapotranspiration

Potential evapotranspiration (PET) was originally introduced by (Sanderson, 1948) as part of a climate classification scheme. He defined PET is the rate at which evapotranspiration would occur from a large area uniformly covered with growing vegetation that has access to an unlimited supply of soil water and that was not exposed to advection or heat storage effects. Because the evapotranspiration rate is strongly influenced by several vegetative surface characteristics, Penman (1956) redefined PET as “the amount of water transpired by a short green crop, completely shading the ground, of uniform height and never short of water”. Penman used grass

as his reference crop, but later researchers (Budinger & Jensen, 1990) have suggested that at a height of 30 to 50 cm may be a more appropriate choice.

Numerous methods have been developed to estimate PET. Three of these methods have been incorporated into SWAT: the Penman-Monteith method (Hatfield & Allen, 1996), the Priestley -Taylor method (Priestley & Taylor, 1972) and the Hargreaves method (Balint Jr & Hargreaves, 1987). The three PET methods included in SWAT vary in the number of required inputs. The Penman-Monteith method requires solar radiation, air temperature, and relative humidity and wind speed. The Priestley-Taylor method requires solar radiation, air temperature, and relative humidity. The Hargreaves method requires air temperature only (Price-Williams, 1969)

2.12.6. Groundwater

To simulate the groundwater, SWAT partitions groundwater into two aquifer systems: a shallow, unconfined aquifer which contributes return flow to streams within the watershed and a deep, confined aquifer which contributes return flow to streams outside the watershed. (Arnold & Allen, 1999) In SWAT the water balance for a shallow aquifer is calculated with equation

$$aq_{sh,i} = aq_{sh,i-1} + W_{rchrg} - Q_{qw} - W_{revap} - W_{deep} - W_{pump,sh} \quad (2\text{-}6)$$

Where: $\alpha q_{sh,i}$ is the amount of water stored in the shallow aquifer on day i (mm) , $\alpha q_{sh,i-1}$ is the amount of water stored in the shallow aquifer on day i-1 (mm),W_{rechrg} is the amount of recharge entering the aquifer on day i (mm), Q_{gw} is the groundwater flow, base flow, into the main channel on day i (mm), W_{revap} is the amount of water moving into the soil zone in response to water-deficient on day i (mm), W_{deep} is the amount of water percolating from the shallow aquifer into the deep aquifer on day i (mm), and $W_{pump,sh}$ is the amount of water removed from the shallow aquifer by pumping on day.

3. MATERIALS AND METHODOLOGY

3.1. Study area description

3.1.1. Location of the study area

Borkena River originates from Kutaber Woreda, at the boundary of two big River Basins, Abay and Awash. Borkena River is one of the main tributaries of the Awash River Basin. It drains from the mountainous chains and escarpments found in the northern plateau which is adjacent to the Afar rift down to south eastern direction and after joining the Jara River around Chefa at the swamp, it finally enters the Awash River (Sahele, 2001. The total area of the catchment is 1655 km^2 and geographically it lies between 39º35’ 0´E and 40 º 50´0¨ E and 10º20˙ 0´´ and 11º20˙ 0´N.

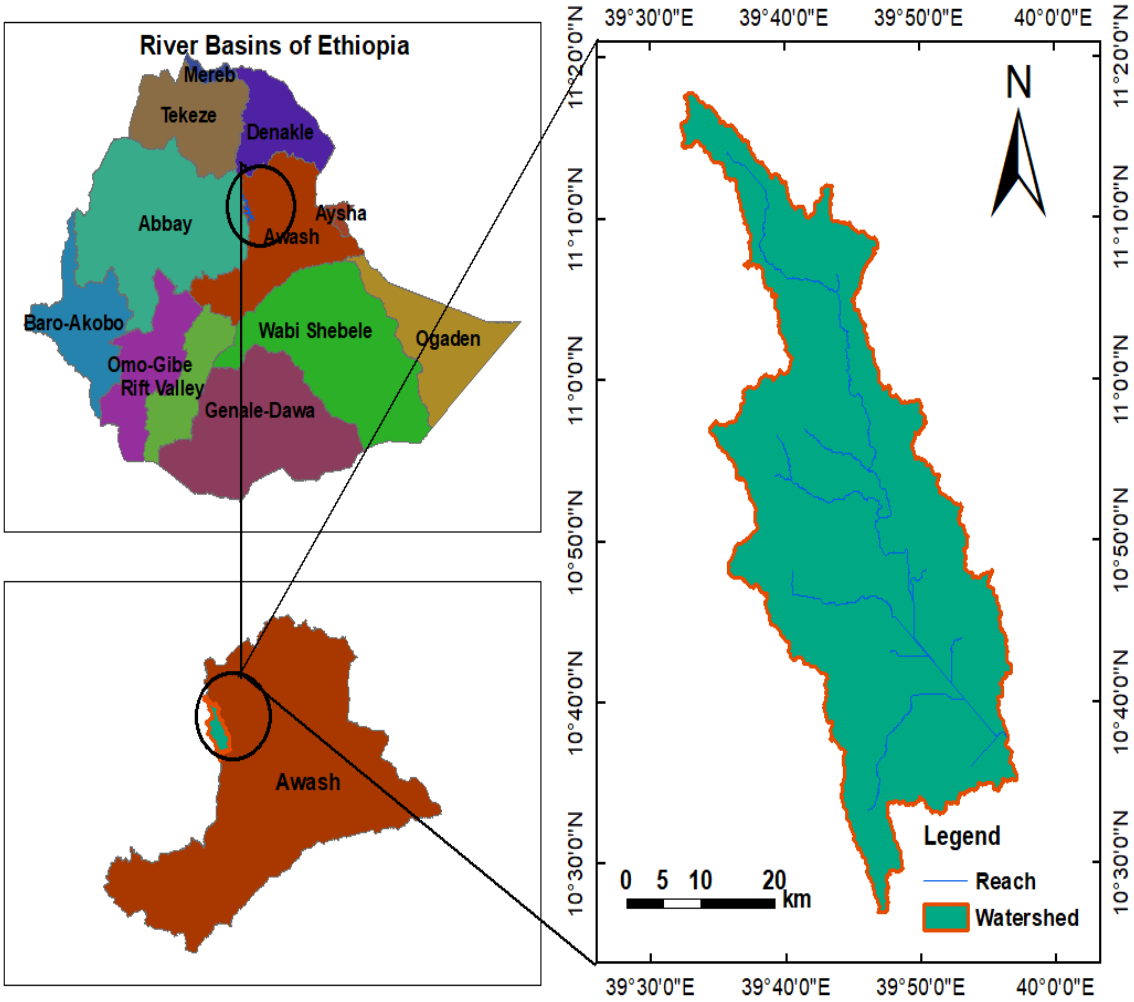

Figure 3-1 Location map of Borkena watershed

3.1.2. Elevations and topography

The topographic of the Borkena watershed varieties from the top of the ridge around the northwest of the water divide at Kutaber, to the floor of the swamp area around Chefa. The elevation of the study area is ranged from 1357 to 3510 m a. s.l. The elevation of the catchment is developed from ArcGIS10.3 version software by using the 30m X 30m resolution DEM of the study area. The higher elevation is found at the south-eastern part of the watershed, Tossa Mountain. The lower elevation is found at the western part of the catchment. The mean elevation of the catchment is 2434m. The large parts of the catchment are found below the mean elevation. The higher elevation areas are also found at the Northern and North Eastern tips of the catchment.

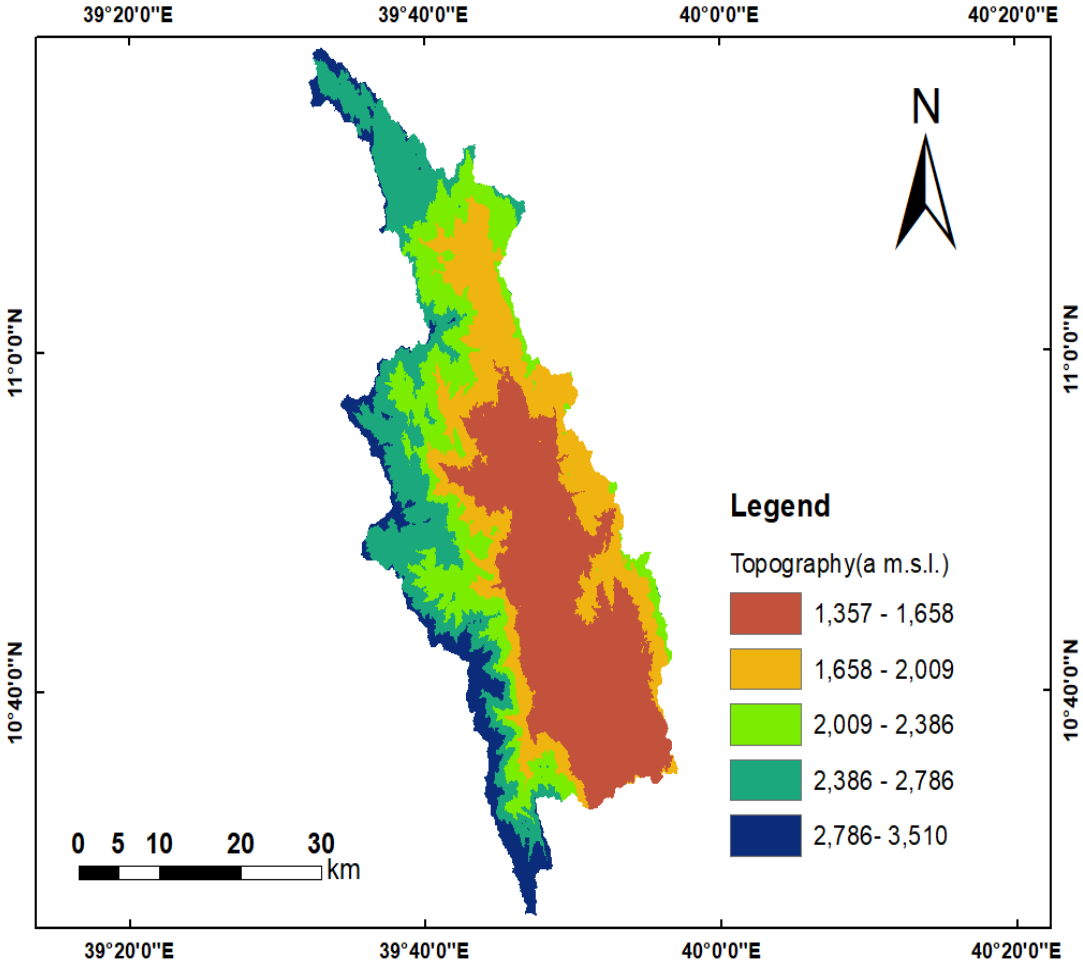

Figure 3-2.Elevation map of Borkena watershed

3.1.3. Climate

The climate of Ethiopia is mainly controlled by the seasonal migration of Inter-tropical Convergence Zone (ITCZ) and its associated atmospheric circulation but the topography has also an effect on the local climate(Sahele, 2001.The climate of the study area upstream of the town of Kombolcha varies between sub humid and subtropical, and according to the traditional classification of climate which is mainly based on altitude variation, the study area falls in the climate of a Dega, Weyna Dega, kola and wurch. The sub humidity area covers about 50.3% and the subtropical aerial coverage is about 49.7% of the total catchment area (Sahele, 2001)

3.1.3.1. Rainfall

The rainfall pattern in the study area is distinctively Bi-modal such that with two peak values observed during the dry season (March to May) and rainy season especially from July to September. The range of average annual precipitation in the watershed was found to be 996 -1272mm per year. Since the study is considering the watershed is getting the same amount of rainfall to the nearest meteorological station, the maximum annual rainfall is 1646.3mm, and the minimum rainfall of 502.9 mm. It was analyzed for the simulation period of (1986-2005.) and the mean monthly rainfall distribution of the area is illustrated in Fig 3-3.

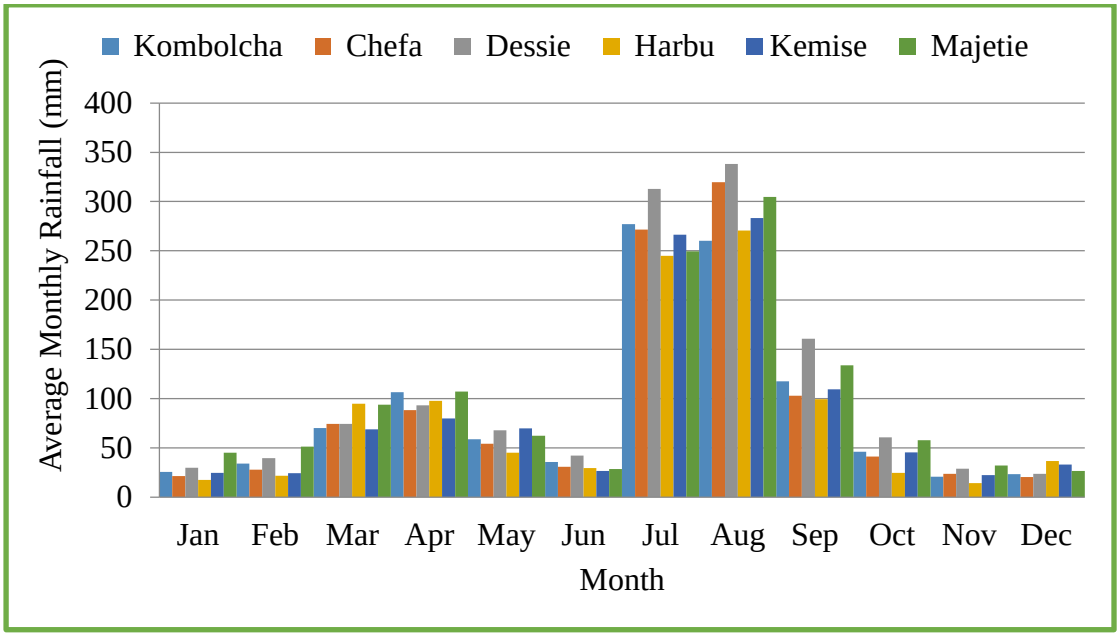

Figure 3-3 Mean monthly Rain Fall of Each station in Borkena watershed

3.1.3.2. Temperature

The information found from the observed minimum and maximum temperature data of the stations (Kombolcha, Majtie Chef, and kemise) clearly showed as the temperature of the area is very spatially, temporally, and seasonally. The twenty years (1986-2005) mean daily minimum and maximum temperature information of the stations point out that the catchment exhibits a range of an average annual temperature of (6.78- 29.86°c). In the maximum temperature records, all the stations in area record the highest value in May and June. The lowest maximum temperature is recorded in December and January. In the minimum temperature, the highest record occurred in June and July and the lowest record is showed in November, December, and January. And the mean monthly maximum and minimum temperatures of the catchment at different stations are illustrated in fig 3-4.

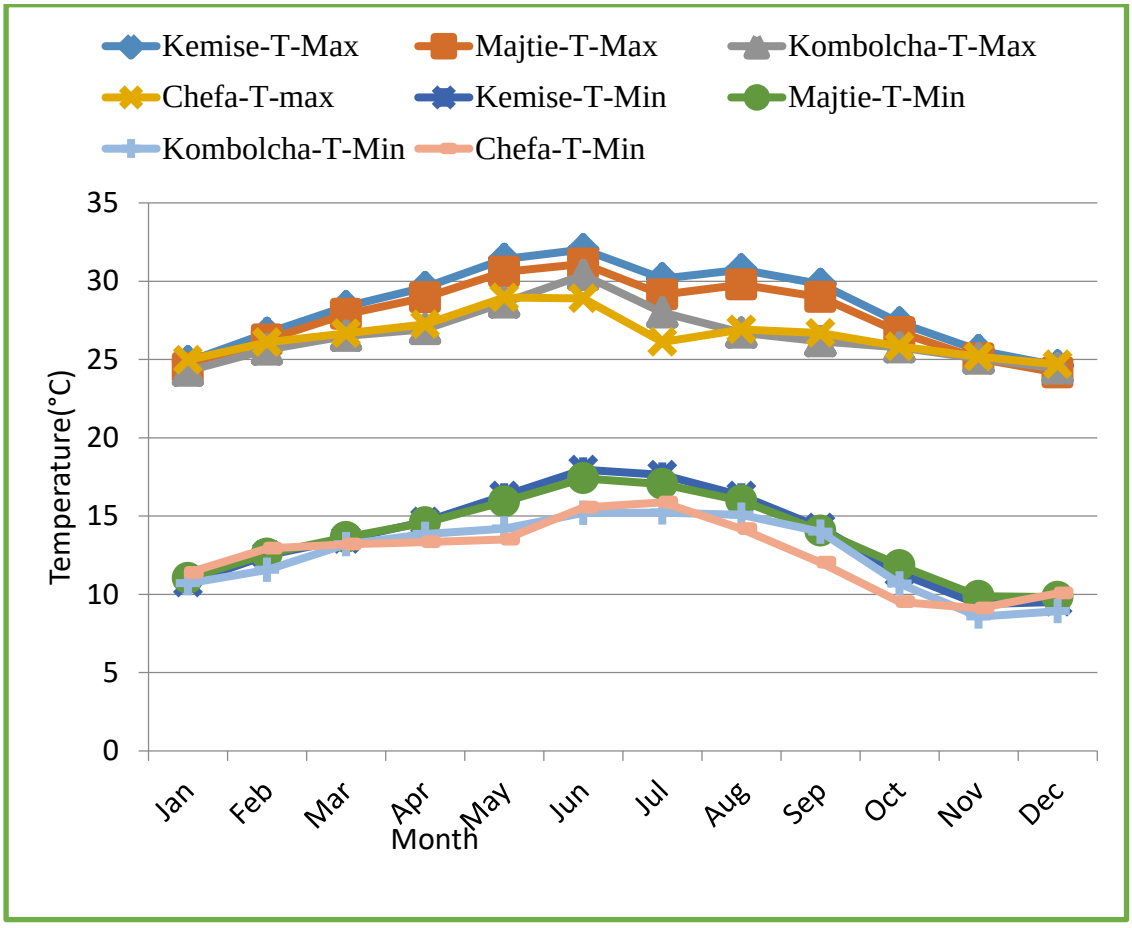

Figure 3-4 Mean monthly minimum and maximum temperature of each station in for Borkena watershed.

3.1.3.3. Hydrology

There are three main hydrological gauging stations in Borkena watershed. These are Borkena at Borumeda, Borkena at Kombolcha, and Borkena at swamp with upstream area of 50, 281 and 1655km2 respectively. The gaging station, Borkena at swamp which is found close to Ataye (Efeson) town near the Bridge of Borkena River on the road from Addis to kombolcha was used for this study. These stations are located near or inside the watershed. Of the total annual discharge, 80% to 90% occurs in the June to September rainy season. The distribution of monthly average discharge of Borkena River at swamp (outlet) is illustrated below in Fig.3-5.

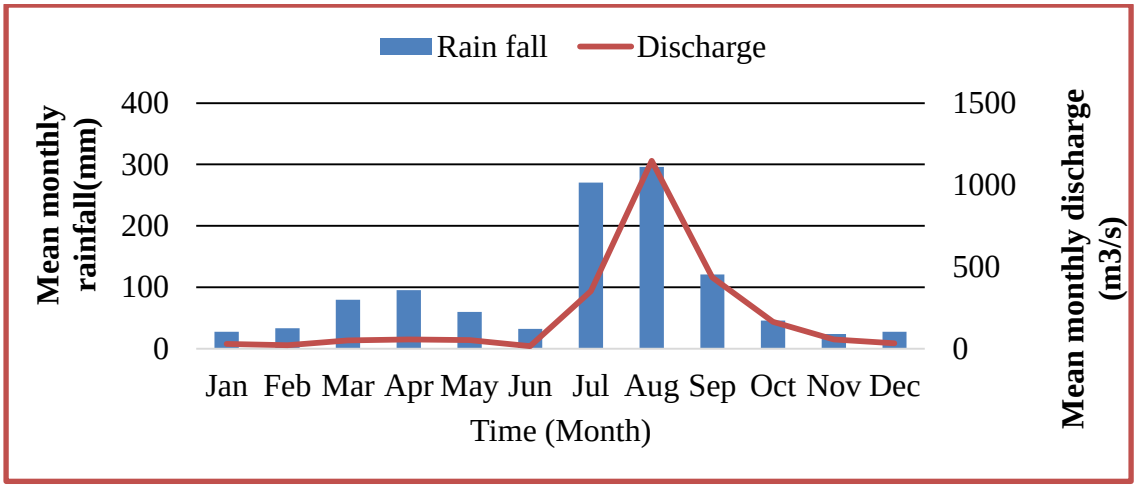

Figure 3-5.Mean monthly observed Rainfall-Runoff distribution in Borkena watershed

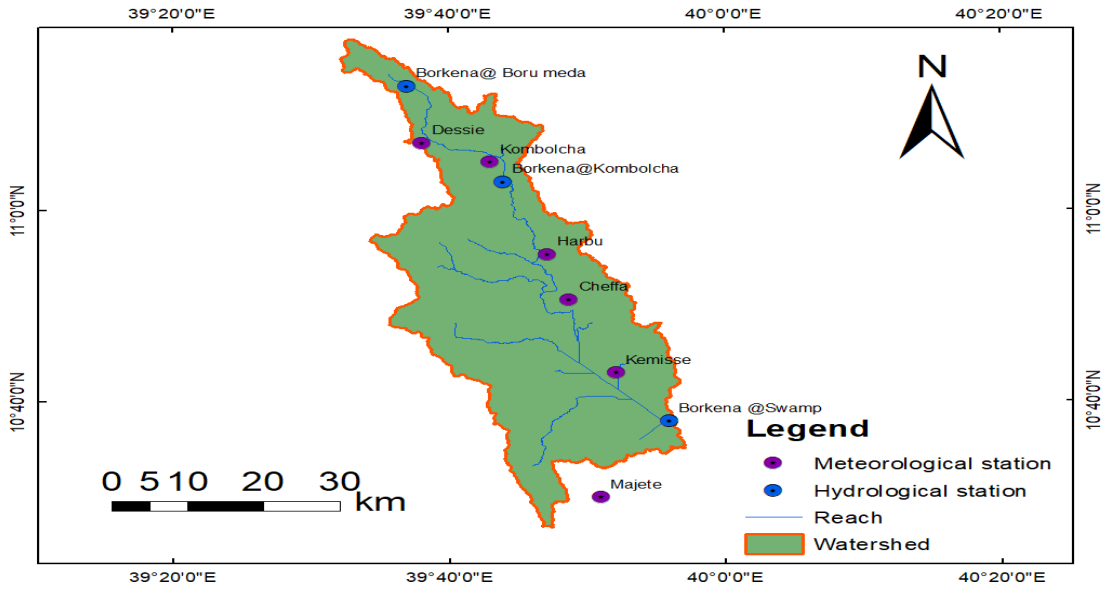

Figure 3-6.Selected Hydro-Metrological stations in Borkena watershed

3.2. Methodology

3.2.1. General methods of the study

The overall methodology of this study included four main approaches i) Data collection and quality analysis ii) Hydrological modeling of the watershed. iii) Selecting appropriate GCMs/RCMs based on the required criteria and downscaling to required station level using a bias correction method iv) Predicting the stream flow using the hydrological model to evaluate the potential impact of climate change on streamflow of Borkena River.

The daily climate projection data was generated by downscaling (bias correction technique) from the CORDEX- model output for the studied region. The projected climate change in the study area was investigated by comparing the projected climate data (precipitation and temperature) from the baseline period data. This was carried out by using the CORDEX- model output with two RCP scenarios (RCP4.5 and RCP8.5).

The climate change-induced streamflow changes by using baseline period and projected period climate data were evaluated, for the projection of two different scenarios of climate change for future time horizons: 2030s (2021-2040), 2050s (2041-2060), and 2070s (2061-2080) for CORDEX- model RCA4 (MPI, MIROC5, and IPSL).To simulate the stream flow for baseline and projected climate data physically-based semi-distributed Soil and Water Assessment Tool (SWAT) model was used.

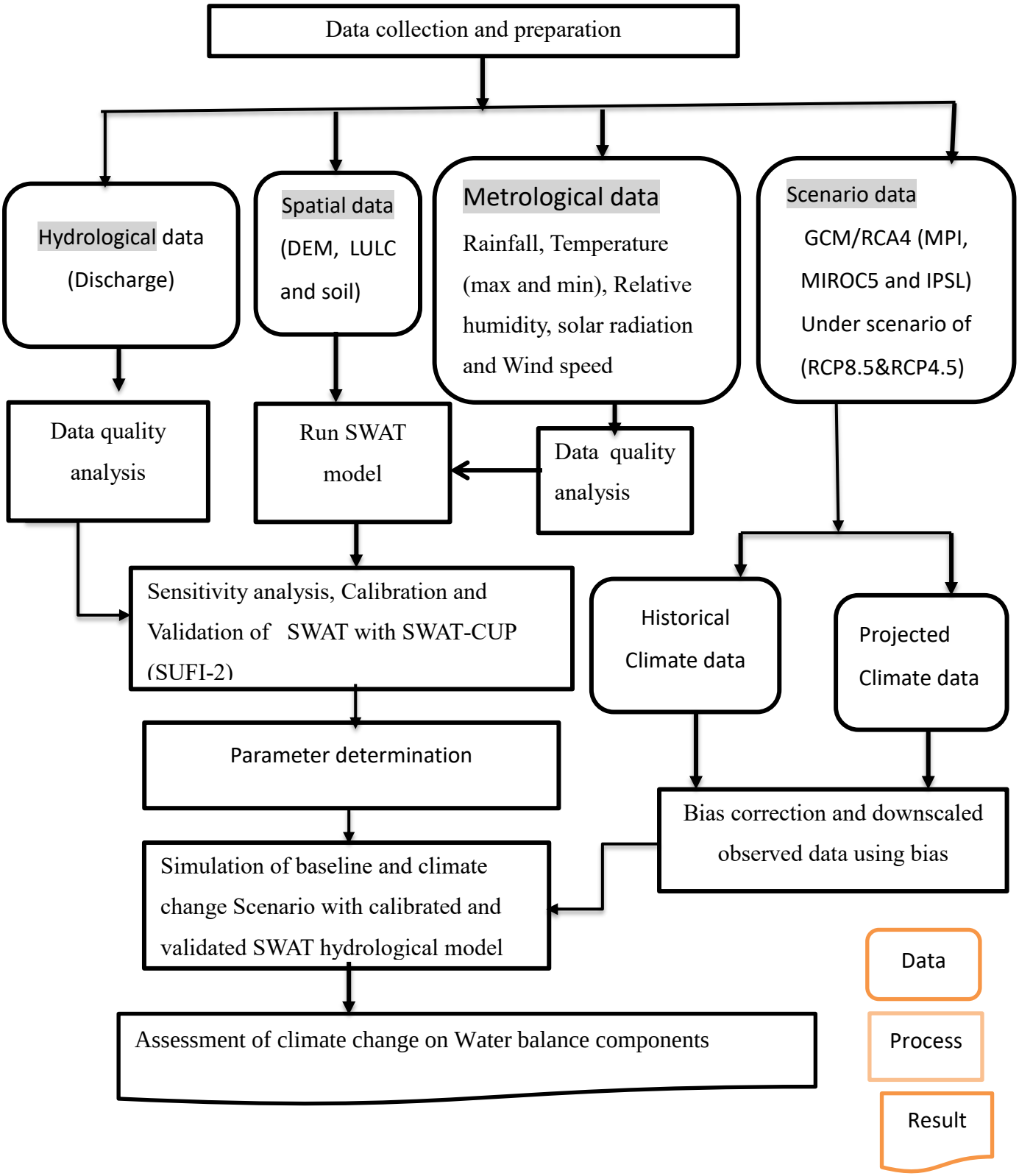

Figure 3-7.The general framework of this Research

3.3. Data types and Sources

3.3.1. Spatial data

Digital elevation model (DEM), land use/land cover, and soil are the three spatial data inputs required by the SWAT model. The topography is defined by a (DEM), which describes the elevation of any point in a given area at a specific spatial resolution as a digital file (Hirt, 2016). It is essential to delineate the watershed into sub-basins and to analyze the physical characteristics of the area such as the drainage pattern of the watershed, slope, stream length, width of the channel within the watershed. Therefore, the (DEM) with a resolution of 30*30 m was downloaded from the USGS data archive (https://www.earthexplorer.usgs.gov).

The land use/ Land Cover spatial dataset defines the densities and types of land use found within a given area. Therefore, Land use data was accessed from MERIS (Medium Resolution Imaging Spectrometer) based Glob-Cover 2009 land cover map. The soil data was also collected from the (MoWIE) Metadata section. To have the SWAT model inputs concerning catchment's soil physical and chemical properties, first, the shape file format of soil type distribution through the catchment was collected from Ethiopian MoWIE GIS department. Using this shape file, soil texture, available water content, hydraulic conductivity, bulk density and organic carbon content for different layers was extracted for each major soils types.

3.3.2. Meteorological data

The required Meteorological data for this study were rainfall, maximum and minimum temperature, wind speed, relative humidity, and solar radiation which are obtained from day time sunshine hour data. The data were collected from the Ethiopian National Metrological Agency (NMA).The collected Meteorological data were used for two purposes; hydrological model (SWAT) development and bias correction of the GCM /RCM data in the watershed. There are only a few meteorological stations that have 20 and more than 20 years record metrological values in the watershed. To alleviate such difficulty, data were collected from the surrounded stations of the catchment. The selection of the representative metrological stations depends on the availability of climatic variables, length of record period, the distance from the catchment, the selection of base period that used for the analysis of present and future climate characteristics,

Stations inside and surrounding the Borkena watershed are Kombolcha, Kemise, Harbu, Majtie, and Chefa. Twenty years of daily rainfall data (1986-2005) for all stations were obtained from the National Meteorological Agency of Ethiopia (NMA). But due to having a lot of missing data and haven't a long-time record of temperature data from the whole stations only one station namely Kombolcha meteorological station is the synoptic station that used to Prepare weather generators.

Table 3-1.Metrological Stations and data availability in Borkena Watershed

Station	Latitude (degree)	Longitude (degree)	Altitude (m.a.s.l.)	Rainfall(mm)	Temperature		Time-Step (Year)
					Max	Mm	
Kombolcha	11.08	39.72	1857	X	X	X	1986-2005
Kemisie	10.72	39.87	1435	X	X	X	1986 -2005
Dessie	11.12	39.64	2553	X	-	-	1986-2005
Harbu	10.92	39.79	1507	X	-	-	1986-2005
Chefa	10.84	39.81	1512	X	X	X	1986-2005
Majetie	10.5	39.88	2000	X	X	X	1986-2005

3.3.3. Hydrological data

Streamflow is an important water cycle variable since it combines all the processes occurring in a watershed and provides an output variable that can readily be determined besides serving as an indicator for climate change and variability by reflecting changes in rainfall and evapotranspiration (Sevruk, et, al., 2009). The Borkena watershed has an outlet river discharge gauging station, which is located at 10:38: 0 N and 39:56: 0 E Figure 3-1. In this study, Daily flow data for Borkena River for a period of ten-years from 1996-2005 recorded at Borkena swamp gauging station was collected from the hydrology department of MoWIE. These data were used for performing sensitivity analysis, calibration and validation of the model simulation using the SWAT_CUP software. The missing value of the data was filled using a long year average technique with the given gaging station data.

3.4. Data quality analysis of observed hydro metrological data

Initial data screening has been conducted by visually observing the data for outliers and missing values. Missed values and outstanding outliers at the initial screening were systematically ignored and refilled by the simple normal ratio (rainfall), arithmetic mean, and XLSTAT excel model (temperature, relative humidity, sunshine, etc).After

the initial screening was completed, all the meteorological data was subjected to detail screening to check the data quality against different indexes. In the principles of hydrology, data should be stationary, consistent, homogeneous, and free from trend when we use it for frequency analysis and hydrological modeling (Dahmen & Hall, 1990). For checking whether the data meet this measure or not the hydrologist needs a simple but efficient screening procedure of statistical variability. The quality of the data in this study was analyzed using the following procedures. i) Filling missing data ii) Homogeneity test iii) Consistency tests and IV) Test for absence of trend.

3.4.1. Estimation of Missing weather data

Before beginning any hydrological analysis, it is important to make sure that data are homogenous, correct, sufficient, and complete with no missing values. Errors resulting from the lack of appropriate data processing are serious because they lead to bias in the final answers,(Li et al., 2015). Generally, data should be appropriately adjusted for inconsistency, corrected for errors, extended for insufficient, and filled for missing using different techniques. The estimation of missing data is one of the most important tasks required in many hydrological modeling studies.

There are many methods and studies already developed to estimate the missing data, such as simple average (Station Average), linear or multiple regression, normal-ratio, coefficient of correlation, and inverse distance weighting method are commonly used to fill the missing records (Gómez et al, 2019). The method used to fill data gaps in this study was the normal ratio method. Recommended using this method only when the annual precipitation value at each of the neighboring gauges differs by greater than 10% from that for the gauge with missing data; hence, the normal ratio method is given by:

$$P_X = \frac{N_X}{n}\left(\frac{P_1}{N_1} + \frac{P_2}{N_2} + \frac{P_3}{N_3} + \ldots\ldots\ldots + \frac{P_n}{N_n}\right) \qquad (3\text{-}1)$$

Where: Px is the value of the missing data and Nx is the normal precipitation of the station in question, P1, P2, P3, and Pn are the recorded precipitation values of the nearest stations 1, 2, 3 and nth stations, respectively, for n observation stations; and N1, N2, N3, and N are the normal precipitation of 1, 2, 3 and nth stations, respectively.

3.4.2. Estimation of Missing Stream flow Data

The daily discharge of the study area is collected from the Ethiopian Ministry of Water, Irrigation, and Electricity (MoWIE). The daily discharge data has limited data composition for the considered stations to represent the study area. In this study, to fill missed data a simple arithmetic average method from its data set is applied. The filled stream flow data of Borkena River at the swamp gaging station (outlet) of the catchment was used for the analysis of this study.

3.4.3. Homogeneity test

One way of checking the reliability of the data series is to compare it with the surrounding stations. This is the idea behind all tests of the relative homogeneity. As non- homogeneous hydrological data are a poor source of information for hydrology research, hydrologists have often preferred to use double mass analysis to obtain information on the relative homogeneity of precipitation series (Dahmen & Hall, 1990).
The methods for testing the homogeneity of the series classified into two groups as an absolute method and relative method (Firat et al, 2010). In the relative method, the neighboring stations are used for the testing process. In this study, the graphical relative homogeneity (Non-dimensional plot) analysis was used. The results were indicated that the stations were homogenous and all meteorological stations were not overlapping each other rather the stations have similar patterns (Fig.3-11)

$$p_{i=}\left[\frac{P_i}{P_j}\right]*100 \qquad (3\text{-}2)$$

Where Pi is the non-dimensional value of rainfall for month i, Pi is over years -average monthly rainfall at station i and Pj is the over years - average yearly rainfall of the station

3.4.4. Consistency test

Estimating missing rainfall is one problem that hydrologists need to address. A second problem occurs when the catchment rainfall at rain gages is inconsistent over a period and adjustment of the measured data is necessary to provide a consistent record. A consistent record is the characteristics of the record have not changed with time. Adjusting for gauge consistency involves the estimation of an effect rather than a missing value. The time series of hydro-meteorological data should be consistent if the periodic data are proportional to an appropriate simultaneous time series (Zhang et al., 2011). To overcome the problem, which is inconsistency, a technique most widely

applied called a double mass curve is used. The double mass curve is used to check the consistency of many kinds of hydrologic data by comparing data for a single station with that of a pattern composed of the data from several other stations (Dahmen & Hall, 1990). Consistency of precipitation data from individual stations used in this study was checked using a double mass analysis and any of the stations used in this study and that has undergone a significant change during the baseline period (1986-2005) of the study was corrected by the equation:

$$P_{CX} = P_X - \left[\frac{M_C}{M_a}\right] \tag{3-3}$$

Where Pcx is corrected precipitation at any time T1 at station x, PX originally recorded precipitation at time T1 at station x, Mc is corrected slope of the double mass curve and Ma is original slope of the double mass curve. Where Pcx is corrected precipitation at any time T1 at station x, Px is original

3.4.5. Absence of trend Test

In hydrological studies on time series data, must be free from the trend. The plotting a time series, one must be sure that there is no correlation between the order in which the data have been collected and the increase (or decrease) in the magnitude of those data. The absence of trend was checked by applying the spearman correlation test which is distribution-free and powerful for both linear and nonlinear trends.

$$R_{sp} = 1 - \frac{6\sum_1^n (D_i * D_i)}{n * (n * n - 1)} \tag{3-4}$$

Where n is the total number of sample data, D is the difference and Rsp is spearman Correlation coefficient

$$D_i = K_{xi} * K_{yi} \tag{3-5}$$

Where Kxi is the rank of the variable and k is chronological transformed series for observation y. The Null hypothesis is finally checked for the acceptance with t-test statics which is described by

$$t_t = R_{sp}\left[\frac{n-2}{1 - R_{sp} * R_{sp}}\right] * 0.5 \tag{3-6}$$

With t as student t distribution having the degree of freedom (v) as n-2 and bounded at two-tailed 5% level of significance in between: $(-\infty, (v, 2.5\%))\ U\ (t\ (v, 97.5\%)), +\infty)$ With the bounded region of the null hypothesis, the time series has to be said "No Trend" if it satisfies and fall for t_t in between: $((v, 2.5\%)) < tt < (t\ (v, 97.5\%))$

3.4.6. Trend Analysis of hydro-meteorological data

The application of the Mann-Kendall non-parametric trend test is recommended by the World Meteorological Organization to detect statistically significant tendencies in environmental datasets (Irannezhad et al., 2015). Mann Kendall test is a statistical test widely used for the analysis of the trend in climatologic and in hydrologic time series. There are two advantages of using this test. First, it is a non-parametric test and does not require the data to be normally distributed. Second, the test has low sensitivity to abrupt breaks due to inhomogeneous time series (Tabari et al., 2011). Any data reported as non-detects are included by assigning them a common value that is smaller than the smallest measured value in the data set. According to this test, the null hypothesis H0 assumes that there is no trend (the data is independent and randomly ordered) and this is tested against the alternative hypothesis H1, which assumes that there is a trend.

The computational procedure for the Mann Kendall test considers the time series of n data points and Ti and Tj as two subsets of data where i = 1,2, 3, n-1 and j = i+1, i+2, i+3, …, n...The data values are evaluated as an ordered time series. Each data value is compared with all subsequent data values. If a data value from a later time period is higher than a data value from an earlier period, the statistic *S* is incremented by 1. On the other hand, if the data value from a later period is lower than a data value sampled earlier, *S* is decremented by 1. The net result of all such increments and decrements yields the final value of S. The Mann-Kendall S Statistic is computed as follows:

$$S = \sum_{i=1}^{n-1} \sum_{j=i+1}^{n} Sign(T_j - T_i) \qquad (3\text{-}7)$$

$$\text{Sign}\ (T_j - T_i) = \begin{cases} 1\ if\ T_j - T_i > 1 \\ 0\ \ if\ T_j - T_i = 1 \\ -1\ if\ T_j - T_i < 1 \end{cases} \qquad (3\text{-}8)$$

Where Tj and Ti are the annual values in years j and i, j > i, r spectively.If n < 10, the value of |S| is compared directly to the theoretical distribution of S derived by Mann and Kendall that is the two-tailed test. At certain probability level H0 is rejected in favor of H1 if the absolute value of S equals or exceeds a specified value Sα/2, where Sα/2 is the smallest S which has the probability less than α/2 to appear in case of no trend. A positive (negative) value of S indicates an upward (downward) trend (Drápela & Drápelová, 2011). For n ≥ 10, the statistic *S* is approximately normally distributed with the mean and variance as follows:

$$E(S) = 0 \qquad (3\text{-}9)$$

The variance (σ2) for the S-statistic is defined by:

$$(\sigma^2) = \frac{n(n-1)(2n+5) - \sum_{i=1}^{m} ti(i)(i-1)(2i+5)}{18} \qquad (3\text{-}10)$$

In which t_i denotes the number of ties to an extent i.The summation term in the numerator is used only if the data series contains tied values. The standard test statistic Zs is calculated as follows:

$$Zs = \begin{cases} \frac{S-1}{\delta} \; for s > 1 \\ 0 \; for S = 1 \\ \frac{S+1}{\delta} \; for \; S < 0 \end{cases} \qquad (3\text{-}11)$$

The test statistic Zs has used a measure of the significance of the trend. This test statistic is used to test the null hypothesis, H0. If | Zs| is greater than Zα/2, where α represents the chosen significance level (eg: 5% with Z 0.025 = 1.96) then the null hypothesis is invalid implying that the trend is significant (Motiee & McBean, 2009).

Another statistic obtained on running the Mann-Kendall test is Kendall's tau, which is a measure of correlation and therefore measures the strength of the relationship between the two variables. Kendall's tau, like Spearman's rank correlation, is carried out on the ranks of the data. That is, for each variable separately, the values are put in order and numbered, 1 for the lowest value, 2 for the next lowest, and so on. In common with other measures of correlation, Kendall's tau will take values between ±1 and +1, with a positive correlation indicating that the ranks of both variables increase together whilst a negative correlation indicates that as the rank of one variable increases, the other decreases .

In time series analysis it is essential to consider autocorrelation or serial correlation, defined as the correlation of a variable with itself over successive time intervals, before testing for trends. Autocorrelation increases the chances of detecting significant trends even if they are absent and vice versa. To consider the effect of autocorrelation, (Zafar et al., 2016) suggest a modified Mann-Kendall test, which calculates the autocorrelation between the ranks of the data after removing the apparent trend. The adjusted variance is given by:

$$Var(s) = \frac{1}{18}[N(N-1)(2N+5)]\frac{N}{N^*_S} \qquad (3\text{-}12)$$

where

$$\frac{N}{N_S} = 1 + \frac{2}{N(N-1)(N-2)}\sum_{i=1}^{p}(N-I)\,(N-i-1)(N--2)P_S(i) \qquad (3\text{-}13)$$

N is the number of observations in the sample, N_s* is the effective number of observations to account for autocorrelation in the data, Ps (i) is the autocorrelation between ranks of the observations for lag i, and p is the maximum time lag under consideration. (Sinha & Cherkauer, 2008) In this study Software used for performing the statistical Mann-Kendall test is Addinsoft's XLSTAT2014. The null hypothesis is tested at 95% confidence level for both, temperature and precipitation data for all gaging stations. Besides, to compare the results obtained from the Mann-Kendall test, linear trend lines are plotted for each station using Microsoft Excel 2010.

Table 3-2.Summary of hydro-meteorological data quality analysis

Test type	Methods of analysis
Test of homogeneity	Relative method (Non-dimensional plot)
Consistency test	Double mass curve
Absence of rend test	Spearman's correlation
Trend Analysis	Mann-Kendall non-parametric trend test

3.5. General Circulation Models (GCMs)

Global circulation models (GCMs) simulate the Earth's climate via mathematical equations that describe atmospheric, oceanic,biotic processes, interactions and feedback.

They are primary tools that provide reasonably accurate global, hemispheric, and continental-scale climate information and are used to understand present climate and future climate scenarios under increased greenhouse gas concentration (Wang, et al 2011).The spatial resolution of GCMs is generally quite coarse, with a grid size of about 100–500 kilometers. Each modeled grid cell is homogenous, (i.e., within the cell there is one value for a given variable).Moreover, they are usually dependable at temporal scales of monthly means and longer. GCMs provide quantitative estimates of future climate change that are valid at the global and continental scale.

Climate change scenarios developed from Global Climate Models (GCMs) are the initial source of information for estimating a plausible future climate. These models are limited by complexity and uncertainty as well as non-linear interactions among atmospheric and oceanic processes(Rosenzweig & Hillel, 2008).

3.6. Regional climate model (RCM) data

For the prediction of streamflow for future time horizon, the future precipitation and temperature (maximum and minimum) data should be required. In this study future climate projection data were obtained from the Coordinated Regional Downscaling Experiment (CORDEX) dataset from Earth System Grid Federation (ESGF) website https://esg-dn1.nsc.liu.se.CORDEX is regionally downscaled climate models established by the World Climate Research Program (WCRP).

The CORDEX-Africa project provides 10 GCMs under SMHI with downscaled climate data for the Africa region (Kim et al., 2014).The choice of GCM/RCM for the study region can have an impact on future projections. In this study, the selection of the RCM/GCMs were based on how well models represent the past and the present climate (precipitation, maximum and minimum temperature), their resolution, and other studies related to the impact of climate change on Awash River Basin and other adjacent Basins.

The representative concentration pathways (RCPs) chosen for this study were RCP4.5 and RCP8.5. And this study used three individual driving GCMs chosen from the CORDEX database. Each of the GCMs was downscaled using the RCA4 model developed by the Swedish metrological and hydrological Institute. Because in recent year the mostly widely used institute is SMHI because of the availability of more options over the requirement (Chokkavarapu and Mandla, 2019).

Table 3-3.Details of regional climate models considered in this study

S/NO	Institute	RCM	Acronym	Spatial resolution
1	SMHI	RCA4(SPL-IPSL-CM5A-MR)	IPSL	0.45°×0.45°
2	SMHI	RCA4(MIROC-MIROC5)	MIROC5	0.45°×0.45°
3	SMHI	RCA4(MPI-M-MPI-ESM-LR)	MPI	0.45°×0.45°

3.6.1. Downscaling

GCMs are used to generate large scale climate scenarios. When performing an impact assessment on a smaller region, it is necessary to downscale the outputs from the GCMs. This is due to scale related sensitivities. GCMs that are not downscaled do not accurately capture weather events on a regional scale. Downscaling is a technique that allows fine-scale information to be derived from GCM (RCMs) output and smaller-scale climate results from an interaction between global climate and local physiographic details (Sun et al., 2016). The regional model group outputs were employed to predict the past and the future climatic conditions of the specific region. Hence RCPs are required for planning the adaptation and mitigation option for the response of river flow by changing climate outputs of coupled climate models.

Three driving GCMs were employed over Borkena watershed, the daily precipitation, maximum and minimum temperature from 1986 to 2080, was mined from grid cells covering Borkena Catchment. The period from 1986 to 2005, was defined as the baseline period. While the future periods that are covered by this study are 2021-2040, 2041–2060, and 2061–2080, denoted by the (2030s, 2050s, and 2070s, respectively relative to the baseline period (1986–2005). Correction of Basis using the dynamical downscaling technique was carried out By (SMHI) to compensate for any tendency to over or underestimate the mean of conditional processes for the considered GCMs.

In the downscaling process, the data produces a fine resolution dataset that is similar to the observed data, but it may have a slightly different distribution, mean, or standard deviation. The reasons for some of these differences may come from biases that will be found in the GCMs or RCM that will use to produce the dataset. So, even if the driving GCM/RCM) models were dynamically downscaled the data (precipitation and

temperature) that derived from those GCMs should be appropriately downscaled (correlated) with the observed data at the watershed scale.

In this regard, the downscaling (bias correction) of precipitation data has employed a nonlinear (power transformation) method that corrects coefficient of variation (CV), and the meanwhile temperature correction is done by using variance scaling for this study on the Borkena watershed. The reasons why power transformation and variance scaling used were due to their ease of implementation, low computational requirements, their suitability for bias correction daily and widely

3.6.2. Grid points selection for downscaling

The outputs of the CORDEX data that are precipitation and Temperatures (maximum and minimum temperature) with a grid resolution of 50 km (0.44.latitude by 0.44 longitude grid size) have been further downscaled into station level by using bias correction method with both baseline and CORDEX model climate data. Closer observed stations for RCM grids were selected by overlaying both coordinates in the study area using ArcGIS10.3 and choosing the closest grid to the station having long year recorded data. The climate data were downloaded after inserting the coordinates of the study area in the box provided for the time required. The RCMs grid output that corresponds to the study area indicated with the spatial resolution of 0.44° of the location of all grid points within the catchment for this study. The grid point was selected depending on the distance and the availability of long year recorded data with gaging station. The grid point closest to the gaging station was selected Fig 3.8.

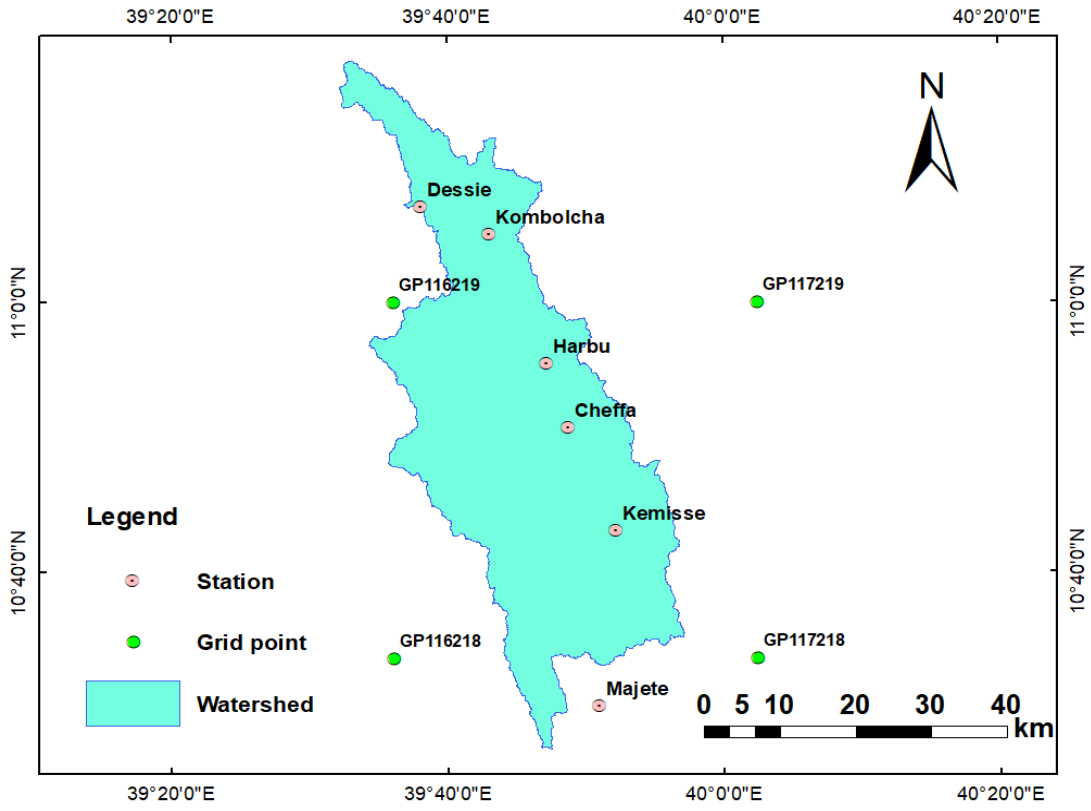

Figure 3-8.Locations of regional climate grid points and weather stations of Borkena watershed

3.6.3. Bias correction

CORDEX formed high resolution downscaled historic and upcoming climate data based on the new CMIP5 simulations used for impact and adaptation studies after applying on an ensemble RCMs for multiple GCMs (Hempel et al., 2013). However, it may not be directly used in the hydrological model for impact assessment studies in watershed-scale due to some systematic errors. If the realistic results required in different impact studies those biases shall be corrected by using different bias correction methods such as power transformation and variance of scaling. In this study, power transformation and variance of scaling, bias correction methods ware used to correct ranges of systematic errors to meteorological station data which will inherit in raw CORDEX-Africa under RCP4.5 and RCP8.5 climate scenarios of precipitation and rainfall data. The bias-corrected data was cross-checked with observed data obtained from Kombolcha station. The outputs of these scenarios were used to forecast changes in precipitation and temperature as well as inputs to the SWAT model.

3.6.3.1. Power Transformation for Precipitation

While the linear scaling and local intensity scaling account for the bias in the mean precipitation, it does not correct biases in the variance. The PT method uses an exponential form to further adjust the standard deviation of precipitation series.. Linear bias correction methods correct mean but do not consider variance. The precipitation is usually varied spatially and highly nonlinear (Watanabe et al., 2012). In this study Power transformation, a nonlinear method is used to correct both the mean and variance of precipitation. Power transformation can be employed as:

$$P^* = a * P^b \tag{3-14}$$

Where P* is corrected precipitation, P is simulated precipitation, a & b are constants and 'a' and 'b' are the parameters obtained from calibration in the baseline period and subsequently applied to the projection period. They are determined by matching the mean and coefficient of variation (CV) of simulated data with that of observed data.

3.6.3.2. Variance Scaling of Temperature

The PT method is an effective method to correct both the mean and variance of precipitation, but it cannot be used to correct temperature time series, as the temperature is known to be approximately normally distributed (Mamalakis et., al, 2017). The variance scaling method was developed to correct both the mean and variance of normally distributed variables such as temperature (Argüeso et al., 2013). In this study temperature was normally corrected using the VARI method that corrects not only the mean values but also the temporal variability of the model output by the observations (Navarro-Racines & Tarapues, 2015)

$$T_{cor} = \overline{T}obs + \frac{\sigma_{obs}}{\sigma_{sim}} * \left(Trcm - \overline{T}rcm\right) \tag{3-15}$$

Where; Tcor is bias-corrected future temperature, $\overline{T}obs$ is mean of observed temperature in the base period, $\overline{T}rcm$ is mean of RCPs temperature in the base period. And $Trcm$ is RCPs temperature of base period σ_{obs}, and σ_{sim} represents the standard deviation of the daily RCPs output and observations in the reference period respectively.

3.7. Hydrological modeling using SWAT

SWAT is the abbreviation for Soil and Water Assessment Tool, a river basin scale, continuous-time, spatially distributed model developed to predict the impact of land management practices on water, sediment and agricultural chemical yields in large complex watersheds with varying soils, land use, and management conditions over long periods (Neitsch et al., 2001).It was developed by Jeff G. Arnold for (USDA) United States Department of Agriculture –ARS (Agricultural Research Service) at Grassland, Soil and Water Research Laboratory in Temple, Texas, USA.SWAT model also has been used for evaluating the water balance of the catchment due to climate change and it is Process-based and semi-distributed parameters, which has been developed to predict the effect of land-use changes, climate change and management practices in the large and complicated basins as well as smaller catchments (Musau et al, 2015).

SWAT model is a semi-distributed process model, and uses specific information about climatology, soil, topography, vegetation and land cover in the catchment instead of using the equations to describe the relationships between input and output. Sub catchments are divided into hydrological response units (HRUs). Runoff in the SWAT Model is predicted separately for each HRU and routed to obtain the total runoff for the watershed(Arnold et al., 2012).

The SWAT model requires calibration and validation on the study catchment to ensure that the model parameters represent the study area. In this study SWAT2012 interface which is compatible with GIS (Arc Map10.3) software was used. The SWAT model differs from the rest of the hydrological models: in case of SWAT is an open-source model developed to predict the effects of land management and climate change on water, sediment, nutrients, and agricultural chemicals in small to large complex basins.

This model is semi-distributed with a physically based structure and can separate the basins into sub-basins and also as Hydrological Response Units (HRUs).The model requires specific information about climate, land use, soil properties, topography, and land management practices occurring in the watershed. The climate parameters generated from RCM are easily handled by SWAT to assess the climate change impact. The other uniqueness of the model was its availability, readily available inputs, and computation efficient, for long-term impacts change impact assessment worldwide.

3.7.1. SWAT model input and Setup

3.7.1.1. Model inputs

The SWAT model required the following input parameters to set up and run:

- Digital elevation model (DEM) of the watershed.
- Land use data
- Soil data
- Meteorological data.

3.7.2. SWAT Model Set up

The model setup involved data preparation, Watershed delineation, HRU definition, Parameter sensitivity analysis, calibration and validation. Based on the DEM, the area was divided into 25 sub-watersheds using the swamp River gauging station as the main outlet. Based on land use, soil type, and slope, the sub-watersheds were further divided into a total of 390 hydrologic response units (HRUs).The modified Soil Conservation Service (SCS) curve number method was used to estimate surface runoff from precipitation summed across all the HRUs in a sub-watershed based on soil, land use, and the Penman-Monteith method was used for estimating potential evapotranspiration, while channel runoff routing was simulated using the Muskingum method. Finally, the model was run for the year 1986 to 2005 by fixing the warm up period of three years.

3.7.2.1. Watershed Delineation

The watershed delineation was carried out based on an automatic delineation procedure based on digital elevation model (DEM). Default threshold sub-watershed area that is suggested by the model was used to define the minimum drainage area to form the origin of a stream. The watershed is divided into 25 sub-basins and 390 Hydrologic Response Units (HRUs).The total area of the delineated watershed is reported by the delineator as 165500.04ha. The delineated watershed and its twenty -five sub-basins are represented in Figure 3-9.

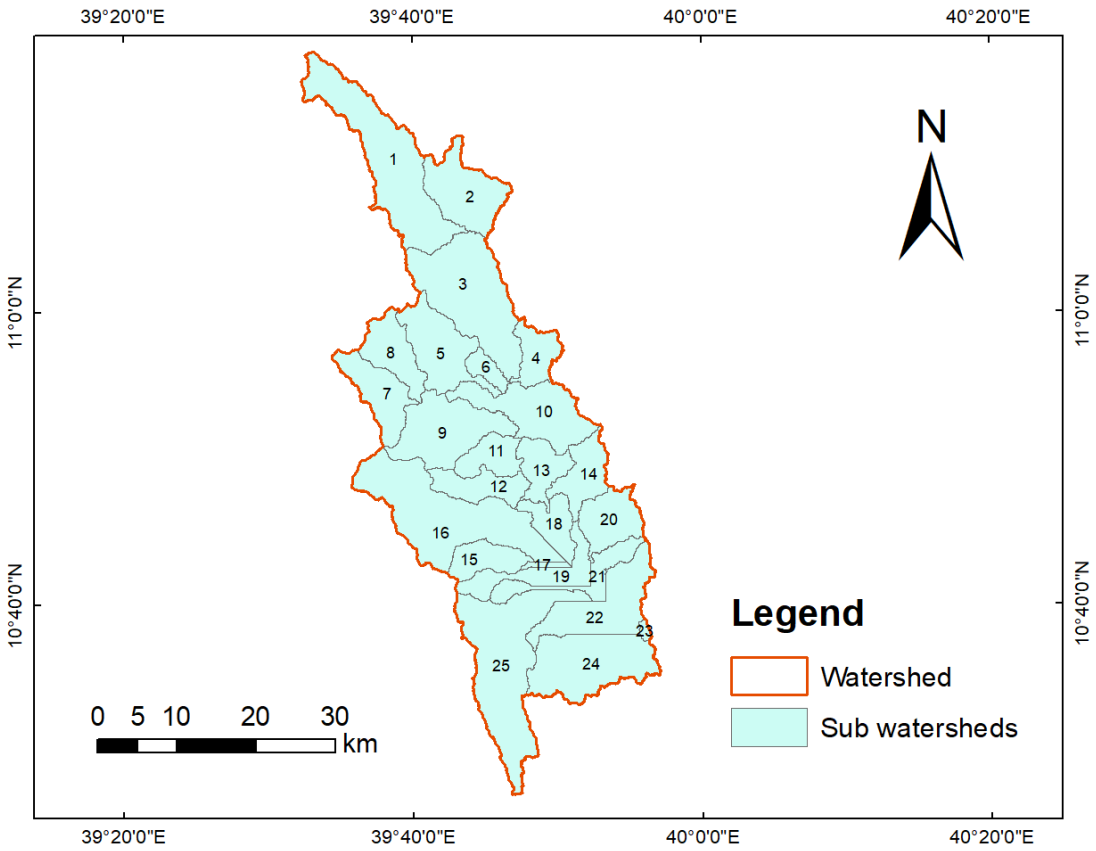

Figure 3-9.Delineated watershed and its 25 sub watersheds

3.7.2.2. Land use and land cover mapping of Borkena watershed

In the Borkena watershed, due to the rapid growth of population, the demand for cultivation area is growing and even steeply sloped areas are currently under cultivation (Sahele, 2001).Also, the use of woods for fuel consumption and as a construction material are influencing the land use land cover pattern of the area. As a result, the catchment is getting degraded from time to time (Sahele, 2001). Hence, based on the land use data that have been collected from MERIS (Medium Resolution Imaging Spectrometer) based Glob-Cover 2009 land cover map, ten different types of land use and land cover have been identified for the Borkena watershed. The land use map of Borkena watershed initially extracted from MERIS, 2009 to produce the land use map of the study area. MERIS land use data were prepared as per requirement of SWAT model and reclassified using SWAT2012 land use database Table 3-5 and Figure 3-10.

Table 3-4.Land use and land covers of the study area as re defined with SWAT code

Land use	SWAT redefined Land use	SWAT code
Rain fed croplands	Agricultural Land Generic	AGRL
Mosaic cropland (50-70%) / vegetation (grassland/shrub land/forest) (20-50%)	Agricultural Land-Close-grown	AGRC
Mosaic vegetation (grassland/shrub land/forest)(50-70%) / cropland (20-50%)	Forest-Deciduous	FRSD
Closed to open (>15%) broadleaved evergreen or semi-deciduous forest (>5m)	Forest-Mixed	FRST
Open (15-40%) broadleaved deciduous forest/woodland (>5m)	Forest-Evergreen	FRSE
Mosaic forest or shrub land (50-70%) / grassland (20-50%)	Smooth Brome grass	BROS
Mosaic grassland (50-70%) / forest or shrub land (20-50%)	Range-Brush	RNGB
Closed to open (>15%) (broadleaved or needle leaved, evergreen or deciduous) shrub land (<5m)	Range-Grasses	RNGE
Bare Areas	Barren	BARR
Water bodies	Water	WATR

Table 3-5.Land uses of the study area with their percentage of aerial coverage

SWAT RE DEFINED	SWAT CODE	Area (km2)	Area (%)
Agricultural Land Generic	AGRL	66.5	4.02
Agricultural Land-Close-grown	AGRC	929.6	56.17
Forest-Deciduous	FRSD	39.9	2.41
Forest-Mixed	FRST	5.0	0.3
Forest-Evergreen	FRSE	77.4	4.68
Smooth Brome grass	BROS	100.1	6.05
Range-Brush	RNGB	25.5	1.53
Range-Grasses	RNGE	410.1	24.78
Barren	BARR	0.3	0.02
Water	WATR	0.6	0.04

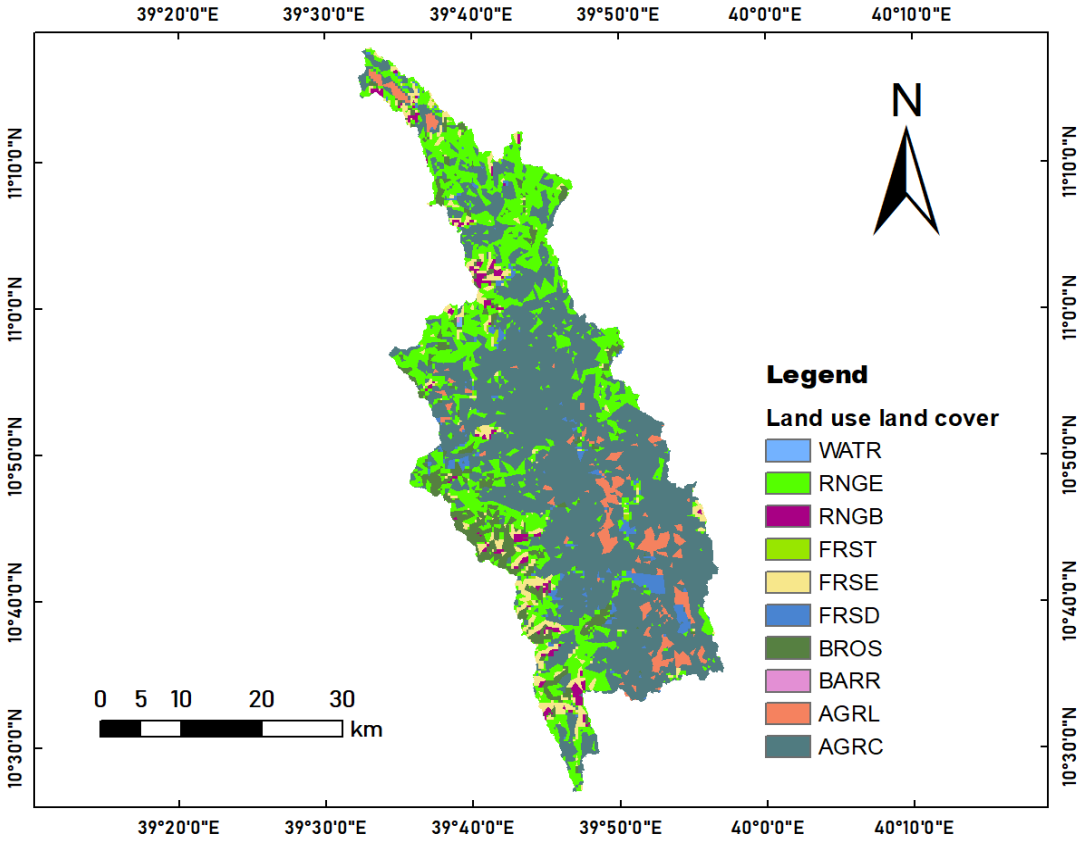

Figure 3-10.Land use and Land cover of the watershed as redefined by SWAT Code.

3.7.2.3. Soil

SWAT model basically needs the soil data to define HRUs. To integrate the soil map within the SWAT model; it was necessary to make a user soil database. Due to that different major soil groups that characterized the Borkena watershed were identified. As per the variety of landforms within the watershed, the soil characteristics are different for most of the mapping units. There are eighteen different soil types. The Dominant soil is Leithic Leptosols (44.4%) followed by Eutric regosols (15. 54%). For this study, the soil data of major soil groups of the watershed were collected from the MoWIE GIS department Table 3-6 and Fig 3-11.

Table 3-6 Classes of major soils and aerial coverage in Borkena watershed

S\NO	User-Defined soil Database	Area(km^2)	Area (%)
1	Chromic Vertisols	244.0	14.74
2	Dystic Leptosols	9.7	0.59
3	Eutric Cambisols	33.0	2
4	Eutric Leptosols	0.8	0.05
5	Eutric Regosols	257.3	15.54
6	Fluvic Cambisols	70.0	4.23
7	Gleyic Phaeozems	0.4	0.03
8	Haplic Luvisols	70.6	4.27
9	Hypereutric Fluvisols	4.6	0.27
10	Hypereutric Regosols	47.4	2.86
11	Hypo calcic Vertisols	98.4	5.95
12	Lepth Cambisols	2.8	0.17
13	Lithic Leptosols	734.7	44.4
14	Rhodic Nitosols	2.2	0.13
15	Vertic Fluvisols	8.1	0.49
16	Vertic Regosols	65.9	3.96
17	Vertic Vertisols	4.6	0.28
18	Waterbody	0.6	0.04
Total	----------	1655.0	100

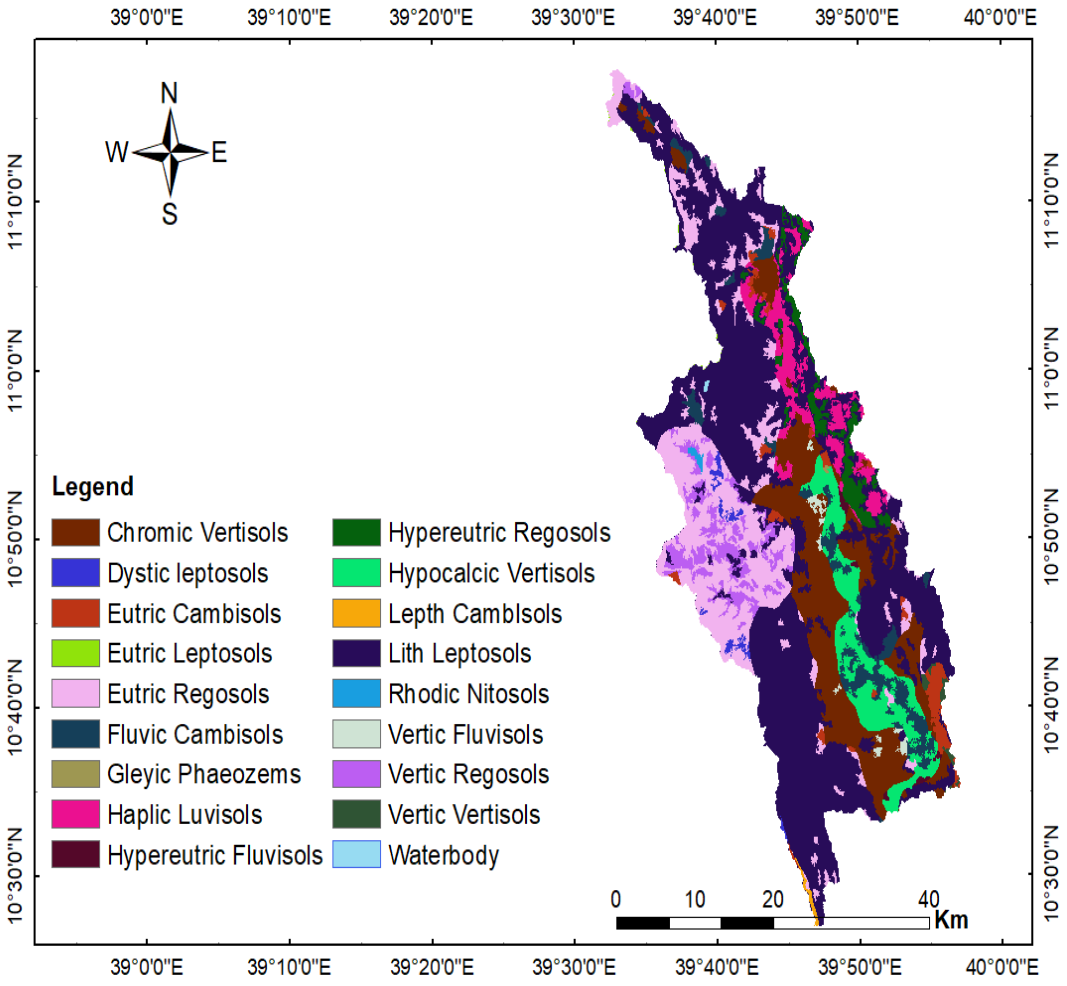

Figure 3-11 Soil Map of Borkena River watershed

3.7.2.4. Slope and HRU Definition

Based on the information found when delineating the watershed using the SWAT interface from the ArcGIS10.3 version through classifying the slope from the HRU definition step, the Borkena watershed has various slope features. Based on the suggested min, max, mean and median slope statistics of the watershed on the manual of Amhara national regional state bureau of water, irrigation and energy(2016) and as the area has lots of ranged topography, we considered five classes of slope, 0-3%, 3-8%, 8-15% ,15-30 and ≥30% in Figure 4.12.

Especially the mountainous part is very steep with different slope ranges. The dominant slope class is very steep (Mountainous) (>30%) which covers 35.11% of the total area followed by undulating slope (15-30) which covers 25.04% and the moderately steep slope (8-15) which covers 18.9%, gently sloping (3-8) covers 16.63%., and flat or

almost flat 0-3% accounts about 4.25% respectively. Based on the soil, land cover and slope data the definition of HRU was performed that assigns a unique value for each unit in the sub basin. The multiple HRU definition criteria were then performed for most applications. The default settings for land use threshold (20%) and soil threshold (20%) and slope threshold (10%) for slope of individual sub watershed area were used. Overall, there were 390 HRUs defined in the entire watershed within 25 sub watersheds.

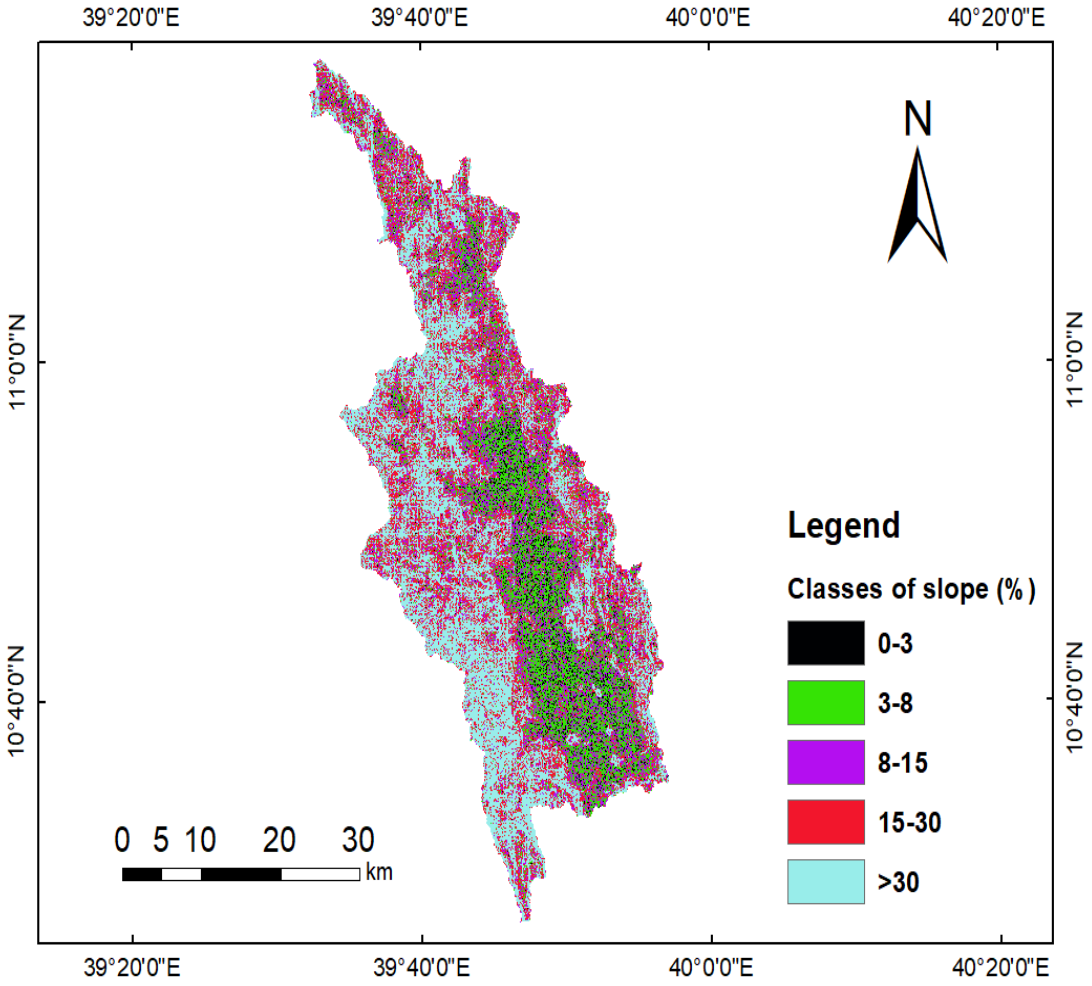

Figure 3-12.Slope map of Borkena watershed

3.7.2.5. Parameter Sensitivity Analysis

Selecting of sensitive parameters is the prerequisite for calibration and validation of the model. It is the technique of identifying the responsiveness of different parameters involving in the simulation of a hydrological model. Sensitivity analysis was carried out to determine the number of optimized parameters to obtain a good fit between the simulated and measured data due to having a lot of parameters. It helps to determine the relative ranking of which parameters most affect the output variance due to input

variability (van Griensven et al., 2006). It reduces the uncertainty of the outputs of the model and provides parameter estimation guidance for the calibration and validation step of the model. Sensitivity analysis was undertaken by using a built-in tool in SWAT-CUP that uses the global sensitivity design method. SWAT-CUP uses a t-test to rank the most sensitive parameter that corresponds to greater change in output response. A t-test result provides a table of output having columns of t-stat and p-values. A t-stat provides a measure of sensitivity (larger in absolute values are more sensitive) and p-values determined the significance of the sensitivity. A value close to zero has more significance in p-value. To improve simulation result and thus understand the behavior of the hydrological system in Borkena watershed, sensitivity analyses were conducted using the 23 streamflow parameters which are selected from previous research papers that are conducted in Awash River basin.

3.7.2.6. Model calibration and validation

Model calibration is the modification of input parameters and comparison of predicted output with observed values until a defined objective function is achieved (James & Burges, 1982).In this study, the measured streamflow data at the swamp gaging station was used to calibrate the model by SWAT-CUP using the Sequential Uncertainty Fitting version-2 (SUFI-2) algorithm. In SUFI-2, parameter uncertainty accounts for all sources of uncertainties such as uncertainty in driving variables (e.g., rainfall), conceptual model, parameters, and measured data (Abbaspour, 2011).

In this research, the SUFI-2 algorithm was selected from the other two algorithms (ParaSol and GLUE) because SUFI-2 is a widely used tool for combined calibration and uncertainty analysis of the SWAT model and it requires fewer simulations compared to the Generalized Likelihood. Uncertainty Estimation (GLUE), and Parameter Solution (ParaSol) to achieve a similar level of performance (Yang et al., 2008). The periods from (1996-2001) were used for calibration and the rest from 2002 to 2005 were used for validation. Because in this latter period (1996–2005) both the meteorological and stream flow records were complete and they presented both low and high flow conditions. For this study, both manual and automatic calibration methods have been applied.

3.7.3. Performance evaluation of soil and water assessment tool (SWAT)

The performance of SWAT was evaluated by using statistical measures to determine the quality and reliability of prediction when compared to observed values. In this study, the goodness of fit was quantified by three model evaluation statistics including Nash-Sutcliffe efficiency (NSE), Bias (PBIAS), and coefficient of determination (R^2).

3.7.3.1. Nash-Sutcliffe (NSE) efficiency criterion

The model efficiency measure NS proposed by Nash and Sutcliffe (1970) measures the normalized statistic that indicates how well a plot of observed with simulated data fits the 1: 1 line and determines the relative magnitude of the residual variance compared to the measured data variance (Harmel et al, 2010). And the Nash–Sutcliffe efficiency coefficient (NSE) is calculated by (Eqe3-16).

$$NSE\_1 - \frac{\sum_{i=1}^{n}(Q_o - Q_s)2}{\sum_{i=1}^{n}(Q_o - \bar{Q}_{o)})2} \quad (3\text{-}16)$$

Where Qs is the simulated flow, Qo observed flow and $\bar{Q}_o$ is the long term average of the observed flow.

3.7.3.2. Coefficient of Determination (R^2)

The coefficient of determination (R^2) is also another model performance evaluation criterion. It is used to evaluate the goodness of fit of the relations by examining the degree of linear association between the observed and simulated flows over a specified period and for a specified time step. The R^2 coefficient for n time steps is calculated as

$$R^2 = \frac{[\sum_{i=1}^{n}(Q_o - \bar{Q}_o)(Q_S - \bar{Q}_S)]^2}{\sum_{i=1}^{n}(Q_o - \bar{Q}_o)^2 \sum_{i=1}^{n}(Q_S - \bar{Q}_S)^2} \quad (3\text{-}17)$$

In which Q_o is the measured discharge, Q_s is the simulated Stream, $\bar{Q}_o$ is the average measured discharge and Q_s is the average simulated discharge.

3.7.3.3. Percent Bias (PBIAS)

Percent Bias (PBIAS) measures the average tendency of the simulated data to be larger or smaller than their observed counterparts, In other words, it characterizes the percent mean deviation between observed and simulated flows. PBIAS can be positive or

negative; positive means underestimation and negative means overestimation (Santhi et al., 2001). PBIAS is calculated as:

$$\text{PBIAS} = \left[\frac{\sum_{i=1}^{n}(Q_o - Q_S)}{\sum_{i=1}^{n} Q_o}\right] * 100 \quad (3\text{-}18)$$

Where Q_O and Qs are observed and simulated discharge respectively

Table 3-7 General performance ratings for recommended statistics in SWAT

Performance	NSE	PBIAS	R2
Very good	0.75<NSE≤1.0	PBIAS ≤±10	0.75< R^2≤1.0
Good	0.60<NSE≤0.75	±10≤PBIAS <±15	0.60< R^2≤0.75
Satisfactory	0.36<NSE≤0.60	±15≤PBIAS<±25	0.36< R^2<0.60
Bad	0.00<NSE≤0.36	± 25 < PBIAS ≤ ± 50	0.25 < R^2 ≤ 0.50
In appropriate	NSE<0.00	±50 ≤PBIAS	R^2<0.00

Source: Adapted from Moriasi et al. (2007), Van Liew et al. (2003) and Fernandez et al. (2005).

3.8. Impact of Climate Change on Stream flow

After finalizing the calibration and validation process for the observed climate data, the model was simulated for baseline (1986–2005) and climate change scenarios (the 2030s, 2050s, and 2070s). The simulation process was done by applying the Soil Conservation Service (SCS) curve number procedure to estimate surface runoff. The potential evapotranspiration was estimated by the Penman-Monteith method, whereas the channel routing was performed using the Muskingum method. The percentage change in annual and monthly water balance components under the climate change scenario was calculated.

In simulating the future flow other climate variables such as wind speed, solar radiation, and relative humidity were assumed to be constant throughout the future simulation periods. Even though it is definite that in the future land-use changes will also take place, this was also assumed to be constant as the objective of this study is only to get indicative results concerning the change in the climate variables (Rainfall and Temperature) keeping all other factors constant. Finally, the impact of climate change on the average flows of monthly, seasonal, and annual stream flow and Maximum and minimum annual flow was analyzed relative to base period flow based on the simulated water balance components under baseline and climate change scenario.

3.8.1. Extreme flow analysis

The analyses of the impacts of climate change on stream flow extreme (high or low) events are important for the reduction of risk. It is expected that climate change will have significant impacts on the regime of flow extremes. As a consequence, the design and management of water resource systems will have to adapt to the changing flow extremes. Analyzing the future low flow condition is important for drought studies, design of water supply systems. It will also help the estimation of safe water withdrawal and Classification of stream potential regulating waste disposal to streams (Riggs, 1985). In this study two directories were selected to describe the characteristics of the extreme stream flow including both low flow and high flow. For both low and high flow the flow duration curve, while for maximum flow, annual maximum flow method, and flow duration curve were used.

3.8.2. Flow Duration Curve (FDC) for stream flow analyses

Flow duration curve (FDC) is the relationship between any given discharge and the percentage of time that the discharge is equal or exceeded. A flow duration curve is one of the most informative means of displaying the complete range of river discharges, from low flows to flood events (Smakhtin, 2001).Using average discharge data, flow duration curves are cumulative frequency distributions that show the percent of the time that a specified discharge is equaled or exceeded during a period of interest (daily, monthly, annual, or the entire period of record).The classification includes; i) high-flow segment (0-20%)flow exceedance probability; characterizing watershed response to large precipitation events; ii) mid-segment(20-70%) flow exceedance probability; representing flows controlled by moderate precipitation events coupled to medium-term base flow; and iii) a low flow-segment (70-100%) exceedance probability; representing a catchment response dominated by long-term base flow during the extended dry periods (Yılmaz, 2008)

3.9. Performance Measures of CORDEX climate data Simulations

The ability of RCMs to simulate climate conditions at a particular location can be evaluated using a variety of techniques. However, no individual evaluation technique or performance measure is considered superior; rather, it is combined use of many techniques and measures that provide a comprehensive overview of model performance (Flato et al., 2013)

In this study, outputs from RCMs are evaluated against observations using some of the statistical measures recommended by the World Meteorological Organization (WMO) as reported by(Gordon &Shaykewich, 2000).These statistics include bias, root mean square error and Pearson correlation coefficient given in equations 3-19, 3-20 and 3-21 respectively.

The Bias is a percentage measure of whether RCMs overall underestimate or overestimate a particular climate variable. Positive bias values indicate overestimation while negative values indicate underestimation by the climate model. On the other hand, the RMSE is a measure of the absolute error of the climate model in simulating certain climate variables. Such that the smaller the RMSE the better the model and vice versa.

The Pearson correlation coefficient is a measure of the strength of the relationship between model simulations and observations and has the limits of 1 and –1. A Pearson correlation coefficient of 1 indicates a perfect positive correlation between model and observed data, while –1 indicates a perfect negative correlation between the two (Boberg & Christensen, 2012). All statistics are calculated based on observed average annual cycles over the base period of (1986–2005) from Kombolcha station and compared with the output from the RCMs. with equations presented as:

$$BIAS(\%) = 100\left(\frac{R_{CM} - R_G}{R_G}\right) \qquad (3\text{-}19)$$

$$RMSE = \sqrt{\sum_{i}^{N} \frac{(R_{RCM} - R_G)^2}{N}} \qquad (3\text{-}20)$$

$$r = \frac{\sum_i^N (R_{CM} - \bar{R}_{CM})(R_G - \bar{R}_G)}{\sqrt{\sum_i^N \left(R_{CM,} - \bar{R}_{CM}\right)^2 \sum_1^N (R_G - \bar{R}_G)^2}} \qquad (3\text{-}21)$$

Where the R_G denotes the mean gage statistical rainfall over the analysis period (1986–2005); the analysis period (N) covers 20 years; R denotes catchment rainfall amount on a certain year (t); subscripts RCM and G indicate catchment rainfall amounts obtained from either RCM simulations or the reference gauge respectively.

3.10. Materials used and their function to conduct the research

To accomplish this research work various materials, programming and software were used Table 3-8.

Table 3-8.Tools and software used for this study

Materials	Purpose
ArcGIS 10.3	Geo-referencing, and other various spatial analysis
ArcSWAT2012	SWAT model development, run execution, present results using reports and maps
XLSTAT 2014	For data quality testing (Homogeneity test and trend analysis) of meteorological and flow data
Google Earth Pro.	Helps to cross-check the recorded coordinates of the metrological and gauge stations, to cross-check the land-use features
PcpSTATA	Used to prepare weather generator, SWAT database input data
DEWPOINT02	To prepare weather generator input data
SWAT_CUP2019	Used for model calibration and validation
Minitab 18.1	used to stack the weather and flow data as a SWAT input format
UTM Converter	used to convert the coordinates of the stations and gauge station from geographic to UTM and UTM to geographic
Data-Toll	Used to plot Cumulative distribution graphs (CDF)
EndNote	To write references with an appropriate format

4. RESULTS AND DISCUSSION

4.1. Data quality analysis Results

4.1.1. Homogeneity test

The homogeneity of the annual total rainfall time series of the watersheds was tested by graphical relative homogeneity (Non-dimensional plot) analysis. While average annual maximum and minimum temperature was tested by Pettitt for a significance level of 95% using XLSTAT software. As a result of the test, the annual total rainfall and average annual maximum and minimum temperature values for each station of the watershed were homogeneous.

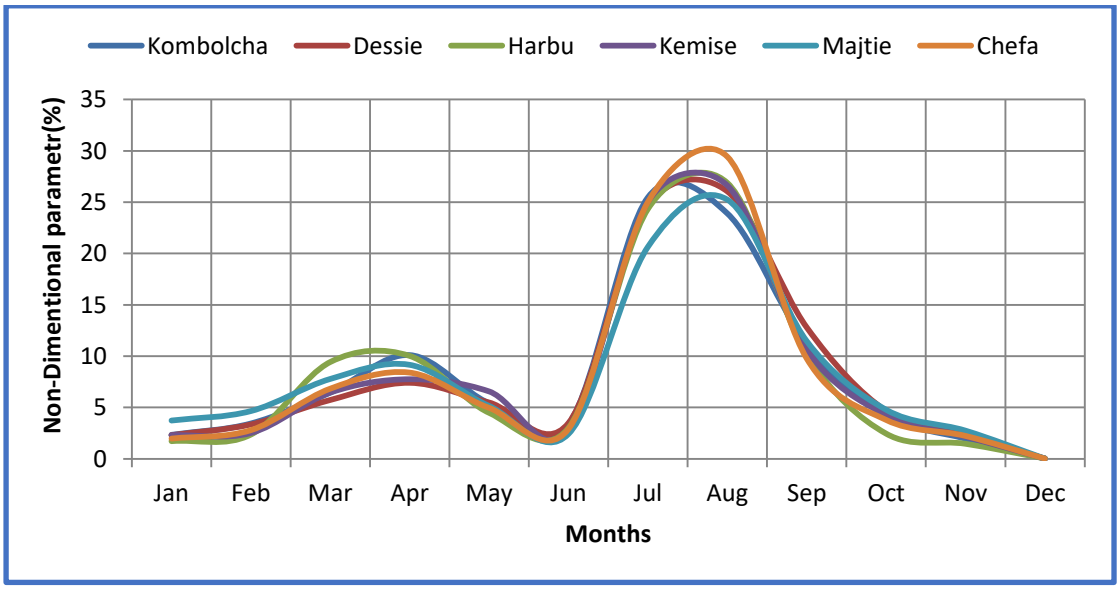

Figure 4-1.Homogeneity tests for rainfall stations in Borkena watershed

4.1.2. Consistency test

The consistency of the rainfall observed data from each station were checked by using the double mass curve. The double mass curve technique was used to adjust rainfall records to take account of non-representative factors such as change in location or exposure of rain gauge. The accumulated totals of the gauge are compared with the corresponding totals for a representative group of nearby gauges. The observed periodic data are proportional to an appropriate simultaneous period. The plot of the double mass curve indicates reasonable degree of consistency, with no discernible change of slop for any of sites.

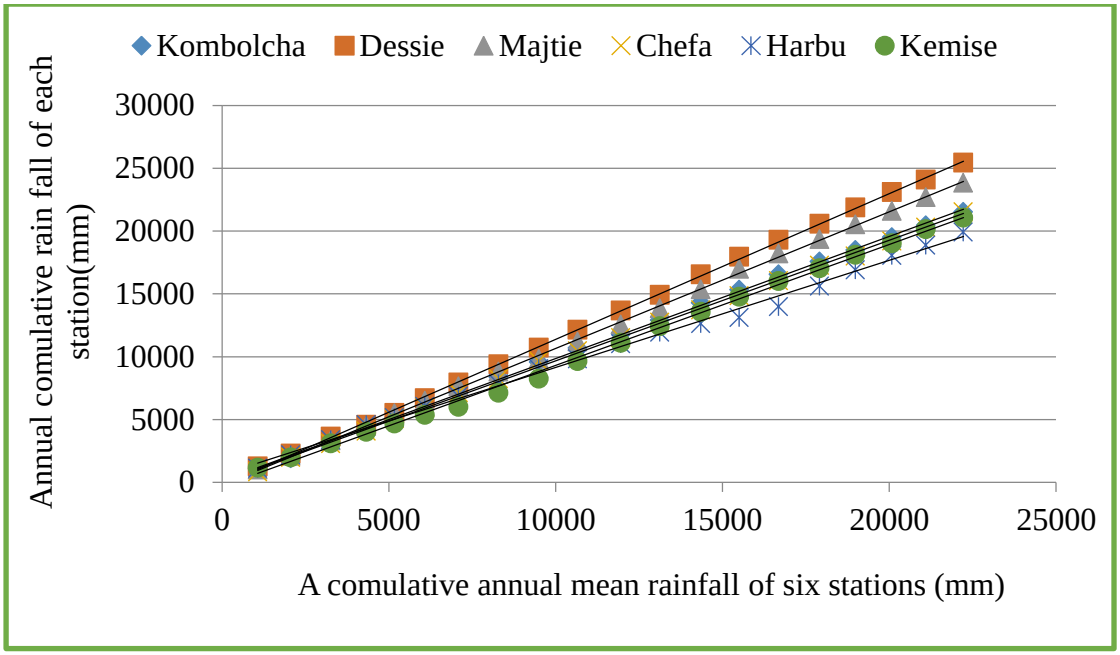

Figure 4-2.Consistency test graph for all the stations in the study area

4.1.3. Trend Test of observed Climate data

4.1.3.1. Observed rainfall trend test

The trend analysis of the observed rainfall for Borkena watershed stations from (1986-2005) was evaluated by using Mann-Kendall trend test and it was noted that there has been increasing trend of annual rainfall at all weather stations in the watershed. To determine the significance of trends of rainfall at the six meteorological stations Mann-Kendall statistic was used. Results for the test of significance in trend using Mann-Kendall showed that the computed p-value was greater than the significance level a=0.05, and therefore the null hypothesis was not rejected Table 4-1. It was thus concluded that although there was a trend in rainfall in the study area it was not significant. However small changes in rainfall can bring about significant changes in the river runoff in the watershed.

Table 4-1.Results for the test of significance of annual rainfall trends using Mann Kendall at Borkena watershed

Stations	Kombolcha	Dessie	Kemise	Majtie	Harbu	Chefa
Kendall's tau	-0.04	0.15	0.05	0.19	-0.02	0.20
S	13.00	28.00	10.00	36.00	24.00	38.00
Var(S)	0.00	0.00	0.00	0.00	0.00	0.00
p-value	0.61	0.19	0.39	0.13	0.56	0.12
alpha	0.05	0.05	0.05	0.05	0.05	0.05

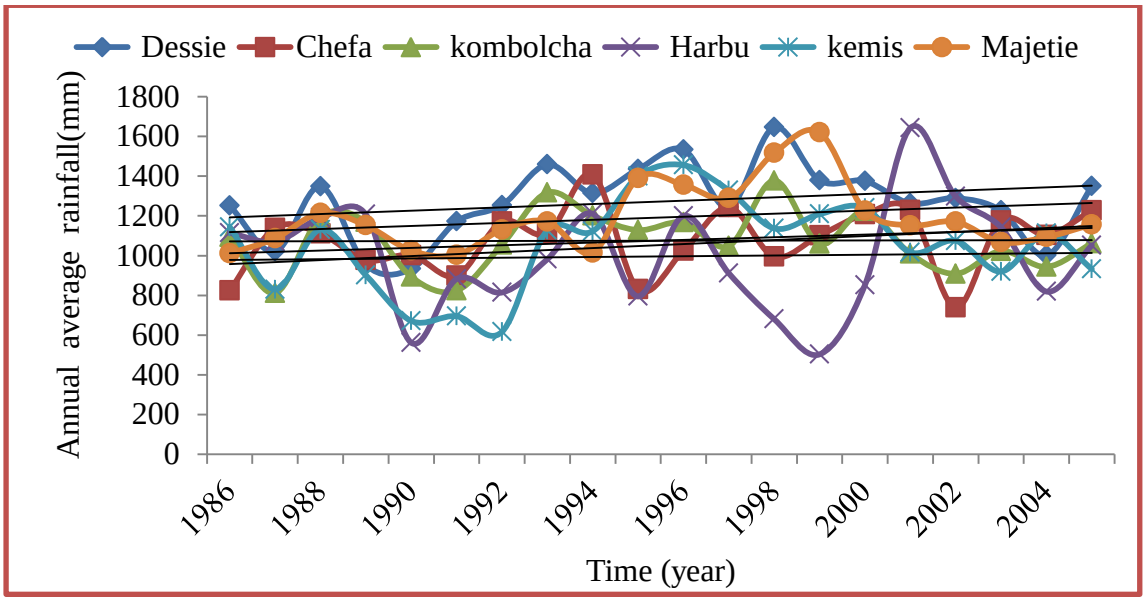

Figure 4-3.Trend test for observed rainfall for all metrological station in Borkena watershed

4.1.3.2. Observed temperature trend analysis

For observed maximum and minimum temperature, the Mann-Kendal trend tests were carried out in the past two decades (Table4-2) for the stations of Kombolcha, Kemise, Majtie and Chefa. The results indicated that the annual maximum and minimum temperature on the selected watershed show a significant increasing trend.

Table 4-2.Observed mean annual maximum and minimum temperature statistics Mann-Kendall trend test in Borkena watershed.

Weather. Stations	Kombolcha		Kemise		Majtie		Chefa	
Temperature	T-Max	T-Min	T-Max	T-Min	T-max	T-Min	T-Max	T-Min
Kendall's tau	0.52	-0.45	0.63	0.34	0.63	0.41	0.62	0.19
S	98.00	-86.00	120.00	64.00	120.00	78.00	118.00	36.00
Var(S)	0.00	0.00	0.00	0.00	0.00	0.00	0.00	0.00
p-value	0.00	0.01	<0.0001	0.02	<0.0001	0.01	<0.0001	0.13
alpha	0.05	0.05	0.05	0.05	0.05	0.05	0.05	0.05

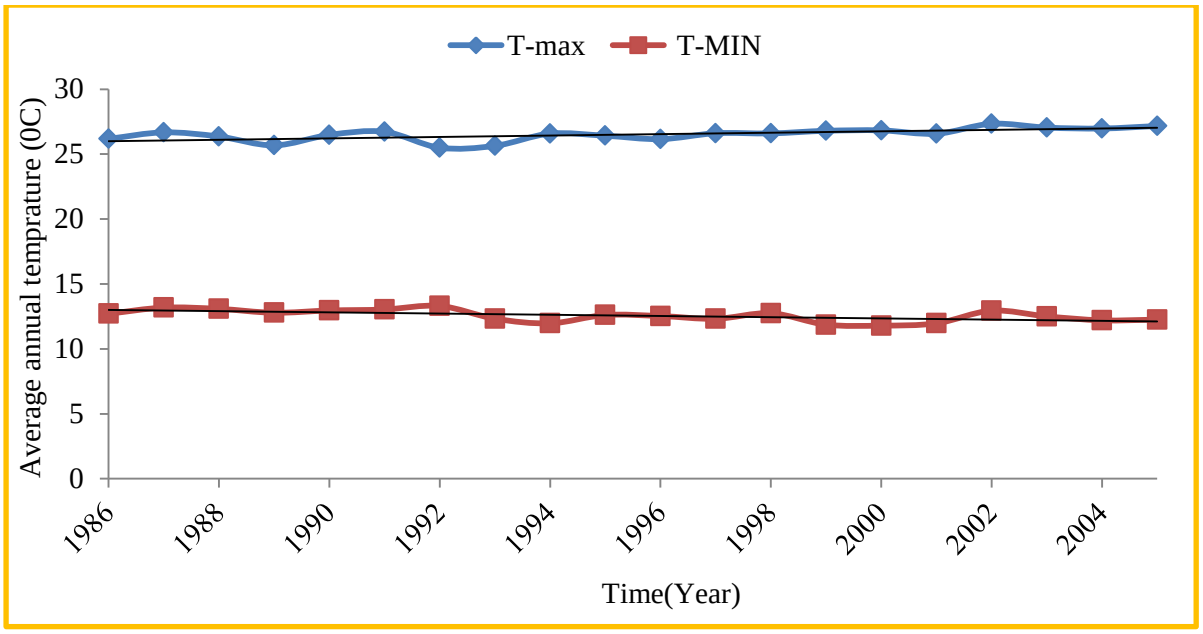

Figure 4-4.The trend test for observed maximum and minimum temperatures in Borkena watershed (Kombolcha weather station)

4.1.4. Trend Test of projected Climate data

4.1.4.1. Projected rainfall trend analysis

After bias correction, the projected future rainfall for the 2030s, 2050s, and 2070s-time horizons was analyzed by using the Mann-Kendall trend test. In the near term (2030s), the projected annual rainfall at Borkena watershed shows an increasing trend in both

RCP4.5 and RCP8.5 scenarios under all RCMs which are considered in this study excluding RCP8.5 under IPSL whereas in the mid-term (2041-2060) the rainfall shows an increasing trend for both scenarios except RCP4.5 and RCP8.5 under MIROC5 and MPI respectively. Correspondingly the trend shows an increasing trend in the late-term (2061-2080) but not for RCP8.5 under IPSL and MPI. So in most cases the mean annual rainfall for future periods in Borkena watershed shows a non-significant increasing trend for all RCMs in both scenarios Table4-3.

Table 4-3.Projected mean annual rainfall statistics resulted in Mann-Kendall trend test

Period	RCM	Scenario	Mann-Kendall trend test parameters				
			Kendall's tau	S	Var(S)	p-value	Alpha
2030s	MIROC-5	RCP4.5	0.04	8	0	0.82	0.05
		RCP8.5	0.09	18	0	0.59	0.05
	MPI	RCP4.5	0.08	16	0	0.63	0.05
		RCP8.5	0.03	6	0	0.87	0.05
	IPSL	RCP4.5	0.27	52	0	0.10	0.05
		RCP8.5	-0.07	-14	0	0.68	0.05
2050s	MIROC-5	RCP4.5	-0.33	-62	0	0.15	0.05
		RCP8.5	0.12	22	0	0.50	0.05
	MPI	RCP4.5	0.08	16	0	0.63	0.05
		RCP8.5	-0.06	-12	0	0.72	0.05
	IPSL	RCP4.5	0.19	36	0	0.26	0.05
		RCP8.5	0.08	16	0	0.63	0.05
2070s	MIROC-5	RCP4.5	0.22	42	0	0.19	0.05
		RCP8.5	0.12	22	0	0.50	0.05
	MPI	RCPs4.5	0.00	0	0	0.97	0.05
		RCP8.5	-0.01	-2	0	0.97	0.05
	IPSL	RCP4.5	0.11	20	0	0.54	0.05
		RCP8.5	-0.13	-24	0	0.46	0.05

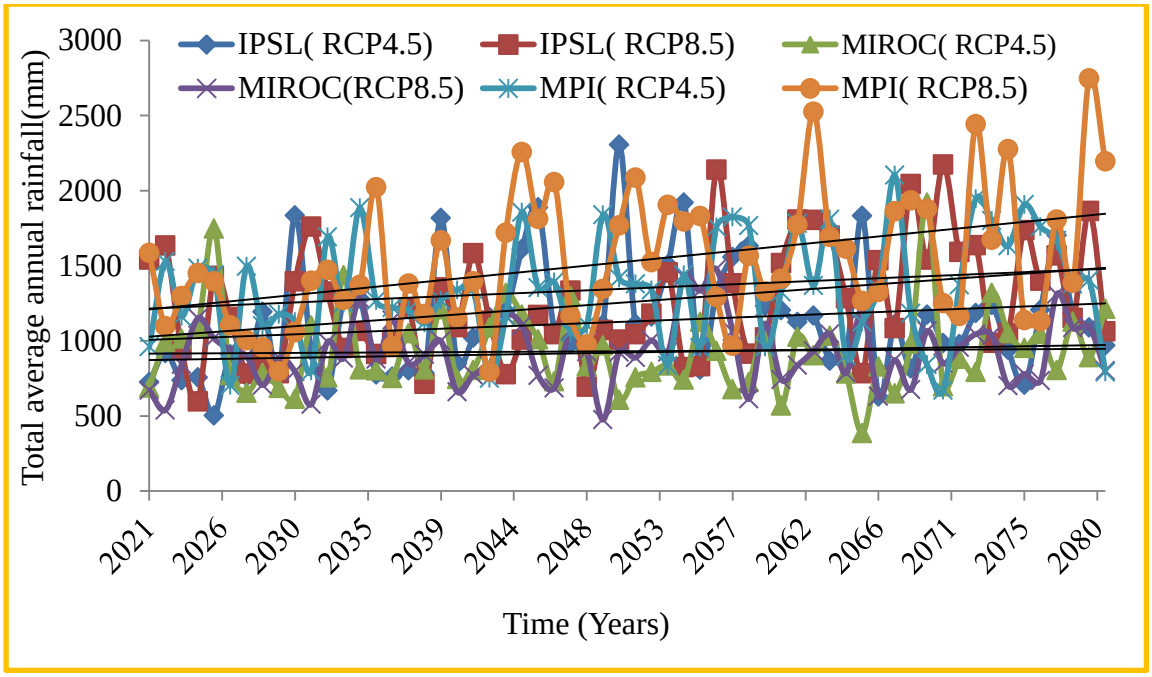

Figure 4-5.Trends for projected rainfall in Borkena watershed in the future (2021-2080)

4.1.4.2. Projected maximum future Temperature trend analysis

The projected future maximum temperature in near (2030s), mid (2050s) and late (2070s) terms was analyzed by using the Mann-Kendall trend test. The decadal projected maximum temperature shows a positive (increasing) trend for all RCMs under RCP4.5 and RCP8.5.The projected annual maximum temperature trend for all future periods indicated that there is statistically significant positive trend at 95 % confidence level Table 4-4.In general, the decadal projected maximum temperature shows an increasing trend for all RCMs under both RCP4.5 and RCP8.5 Scenarios.

Table 4-4.Mann-Kendall trend test in projected mean annual maximum temperature

Period	RCM	Scenario	Mann-Kendall trend test parameter				
			Kendall's tau	S	Var(S)	p-value	alpha
2030s	MIROC-5	RCPs4.5	0.25	48	0	0.04	0.05
		RCPs8.5	0.35	66	0	0.03	0.05
	MPI	RCPs4.5	0.54	102	0	0.00	0.05
		RCPs8.5	0.05	10	0	0.01	0.05
	IPSL	RCPs4.5	0.25	48	0	0.03	0.05
		RCPs8.5	0.62	118	0	< 0.0001	0.05

2050s	MIROC-5	RCPs4.5	0.15	28	0	0.02	0.05
		RCPs8.5	0.42	80	0	0.01	0.05
	MPI	RCPs4.5	0.41	78	0	0.01	0.05
		RCPs8.5	0.47	90	0	0.00	0.05
	IPSL	RCPs4.5	0.32	60	0	0.00	0.05
		RCPs8.5	0.63	120	0	< 0.0001	0.05
2070s	MIROC-5	RCPs4.5	0.14	26	0	0.04	0.05
		RCPs8.5	0.28	54	0	0.01	0.05
	MPI	RCPs4.5	-0.09	-18	0	< 0.0001	0.05
		RCPs8.5	0.49	94	0	0.00	0.05
	IPSL	RCPs4.5	0.34	64	0	0.04	0.05
		RCPs8.5	0.71	134	0	< 0.0001	0.05

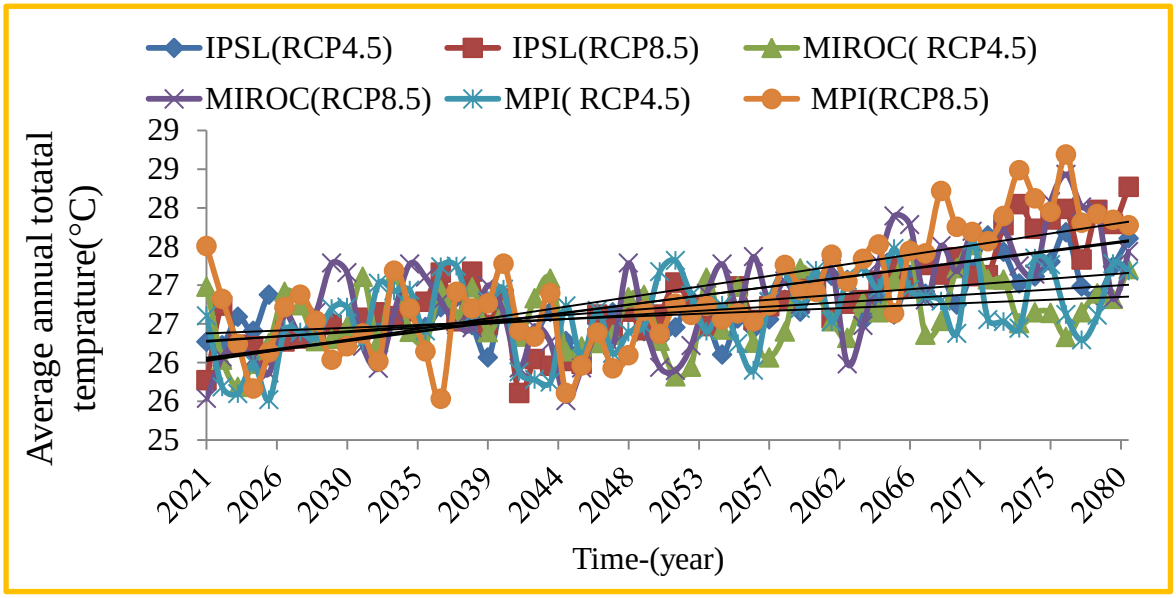

Figure 4-6.Trends for projected maximum temperature in Borkena watershed in the future (2021-2080)

4.1.4.3. Projected minimum future temperature trend analysis

The trend for projected future minimum temperature in near (2030s), mid (2050s) and late (2070s) periods was analyzed by using the Mann-Kendall trend test. The test has resulted in a clear increment of minimum temperature at a 95 % confidence limit in both

RCP scenarios for all Regional climate models that considered in this study. And the decadal projected minimum temperature shows an increasing trend for RCMs in RCP4.5 and RCP8.5.Trends in minimum temperature at Borkena watershed were tested for significance against the hypothesis that they are not significantly different from zero by use of Mann-Kendall statistic at a=0.05 level of significance. The results show that the computed p-value was lower than the significance level (0.05) for minimum temperature in the watershed and since the trend in temperature is statistically significant, the null hypothesis was rejected and alternative hypothesis accepted Table 4-5.

Table 4-5.Mann-Kendall trend test in projected mean annual minimum temperature

Period	RCM	Scenario	Mann-Kendall trend test parameter				
			Kendall's tau	S	Var(S)	p-value	alpha
2030s	MIROC-5	RCPs4.5	0.18	34	0	0.029	0.05
		RCPs8.5	0.29	56	0	0.01	0.05
	MPI	RCPs4.5	0.52	98	0	0.00	0.05
		RCPs8.5	0.09	18	0	0.00	0.05
	IPSL	RCPs4.5	0.40	76	0	0.01	0.05
2050s		RCPs8.5	0.52	98	0	0.00	0.05
	MIROC-5	RCPs4.5	0.12	22	0	0.02	0.05
		RCPs8.5	0.54	102	0	0.00	0.05
	MPI	RCPs4.5	0.19	36	0	0.01	0.05
		RCPs8.5	0.39	74	0	0.02	0.05
	IPSL	RCPs4.5	0.31	58	0	0.01	0.05
		RCPs8.5	0.57	108	0	0.00	0.05
2070s	MIROC-5	RCPs4.5	0.18	34	0	0.02	0.05
		RCPs8.5	0.42	80	0	0.01	0.05
	MPI	RCPs4.5	0.18	34	0	0.29	0.05
		RCPs8.5	0.38	72	0	0.02	0.05
	PSL	RCPs4.5	0.40	76	0	0.01	0.05
		RCPs8.5	0.62	118	0	< 0.0001	0.05

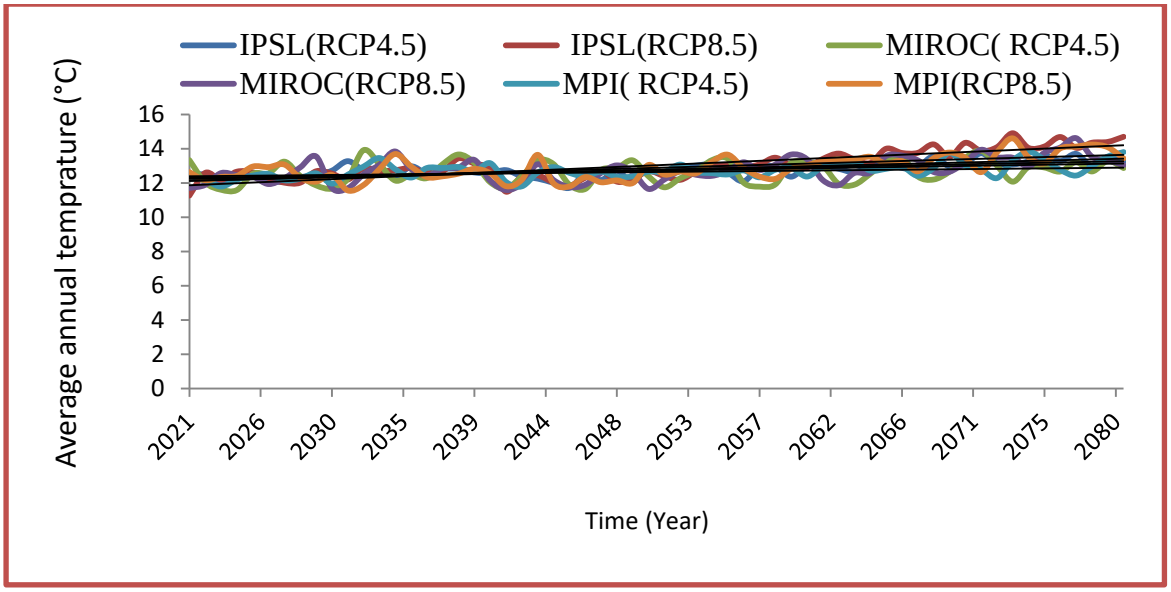

Figure 4-7.Trends for projected minimum temperature in Borkena watershed for the period of (2021-2080)

4.2. Performance evaluation of regional climate model simulation

In this study, the performance of CORDEX regional climate models in simulating the rainfall characteristics over the Borkena River catchment in the base period (1986-2005) is presented. The evaluation is based on determining how well the CORDEX RCMs reproduce mean annual cycles, in the rainfall as reproduced by the observed one at gaging station. Considering RMSE value as comparison criterion, the IPSL mean like most of RCMs exhibits the smallest value of RMSE and IPSL reproduces better the magnitude of rainfall compared with the other two models Table 4-6. In the same way when the correlation coefficient between rainfall data from the observed and simulated rainfall from the RCMs, considered the MPI performed better in simulating rainfall over the Borkena river catchment compare to the other two RCMs. All the RCMs are purely correlated with rainfall from the observed. Additionally, distribution parameters for the mean annual are compared and it is clear that the IPSL performs better compared to the other RCMs due to its mean and standard deviation are close to the observed mean annual rainfall. Similarly, the MPI and MIROC overestimate the observed mean data values. Generally, even if the CORDEX RCMs reproduce the annual cycles of rainfall, the models' surfer to reproduce correctly the magnitudes of rainfall. The intention of this study was also mainly concerned for assessment of climate change impact on stream flow and catchment water balance sensitivity to climate change for the Borkena River

catchment in Awash Basin; therefore, it is recommended that the bias correction is essential to be performed to correct the RCMs for this study.

Table 4-6.Statistical parameters of simulated rainfall from corresponding regional climate models before bias corrected

	RCMs			
Statics	Observed	MIROC5	MPI	IPSL
Mean	1075.5	2726.97	2688.07	945.1
Bias (%)	-----	153.6	149.9	-12.1
RMSE (mm/Year)	-----	1742.97	1766.27	338.4
Correlation	------	-0.33	0.09	-0.3

4.2.1. Bias correction of regional climate models (RCMs) simulations

The grid-based RCM simulation was downscaled to weather station scale using bias correction techniques that are illustrated in the previous section. The daily bias corrections between the observed and simulated variables during the control period (1986-2005) for each RCM models were applied. The bias correction was done on RCM-simulated rainfall, maximum and minimum temperature. Each RCMs rainfall and maximum and minimum temperature was bias-corrected using the power transformation and variance scaling approaches respectively for the extracted nearby grids and results show that for rainfall, the PT method expressively corrects the biased raw RCM. Likewise similar results were obtained for maximum and minimum temperature, for those extracted grids. Then the corrected meteorological data were compared to the observations in the baseline (1986-2005).Consequently each RCMs output graphically represented for Borkena watershed at Kombolcha station, the station used to downscale the RCMs independently (Figure 4-8-Figure 4-12).These station-based meteorological data were then up scaled to watershed scale with the rainfall and temperature under each representative concentration scenarios (RCP4.5 and RCP8.5) before they were used to drive the hydrological model. Finally, the simulated stream flow driven by the corrected and observed meteorological data was compared to each other.

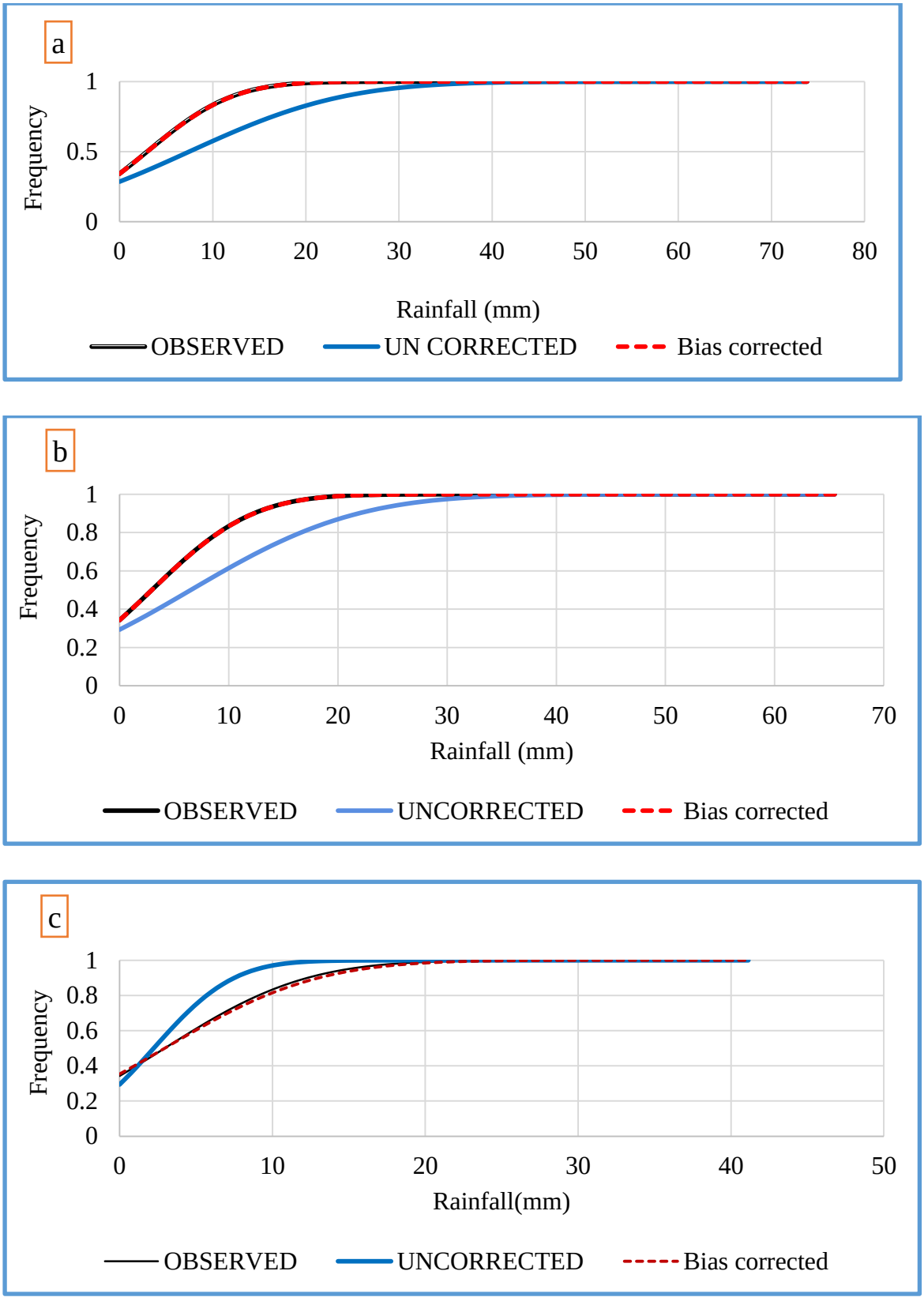

Figure 4-8.Rainfall cumulative distribution function mapping results for both bias corrected and uncorrected for (a)MIROC5,(b)MPI and (c)IPSL model out puts at Kombolcha weather station.

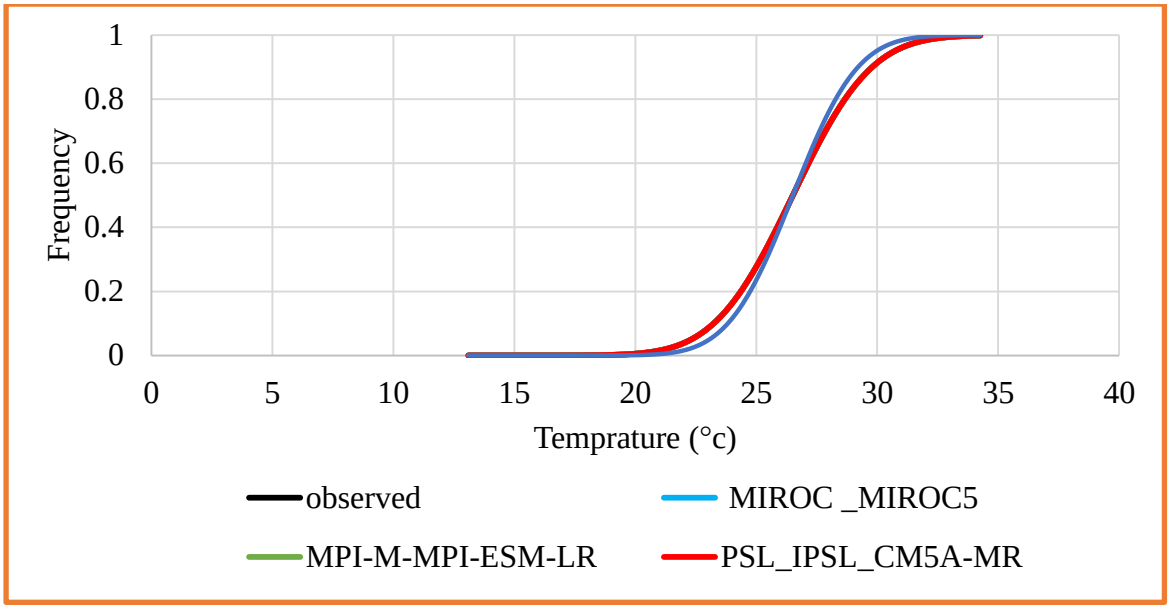

Figure 4-9.Maximum temperature cumulative distribution function mapping results after bias correction of each regional climate models

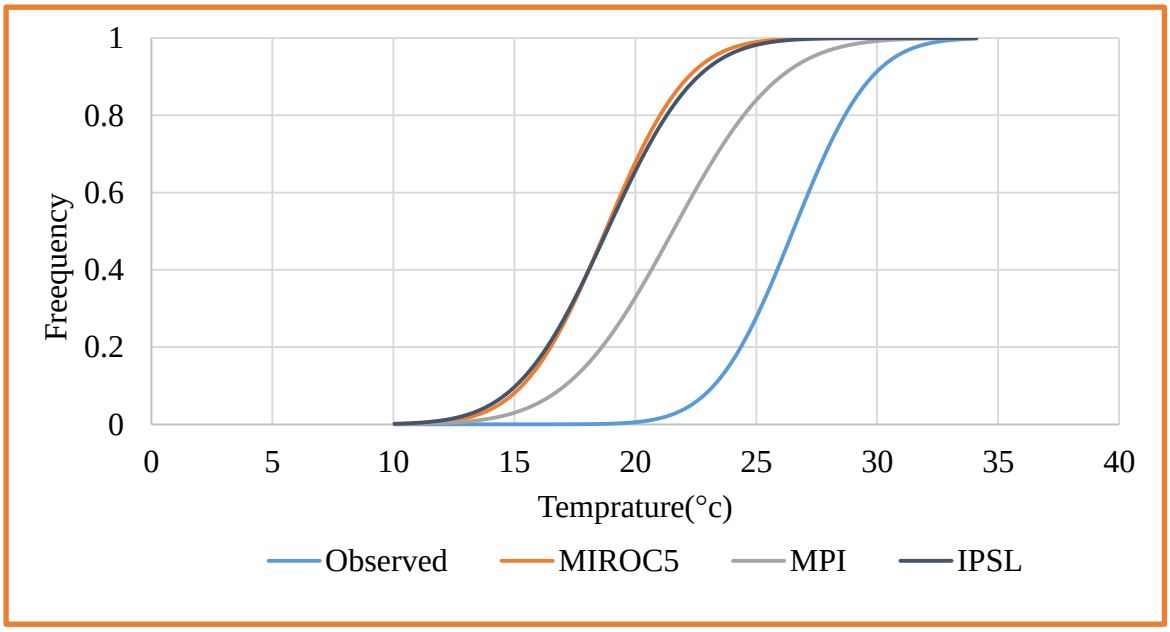

Figure 4-10.Maximum temperature Cumulative Distribution Function mapping results before bias correction of Each Regional climate models.

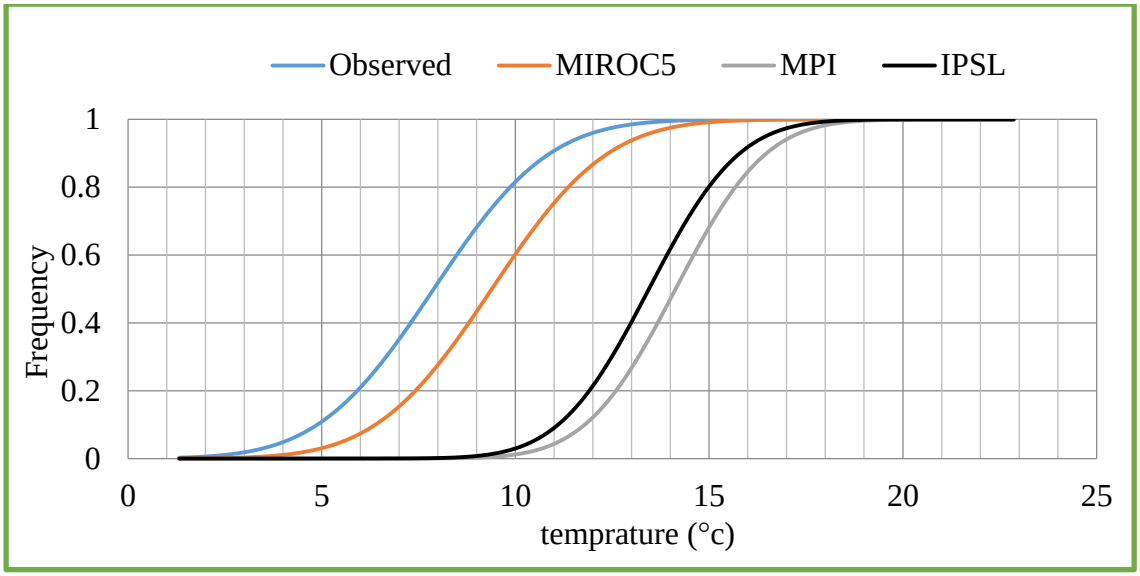

Figure 4-11.Minimum temperature cumulative distribution function mapping results for Kombolcha weather station before bias-corrected regional climate model (RCM) data at the watershed scale.

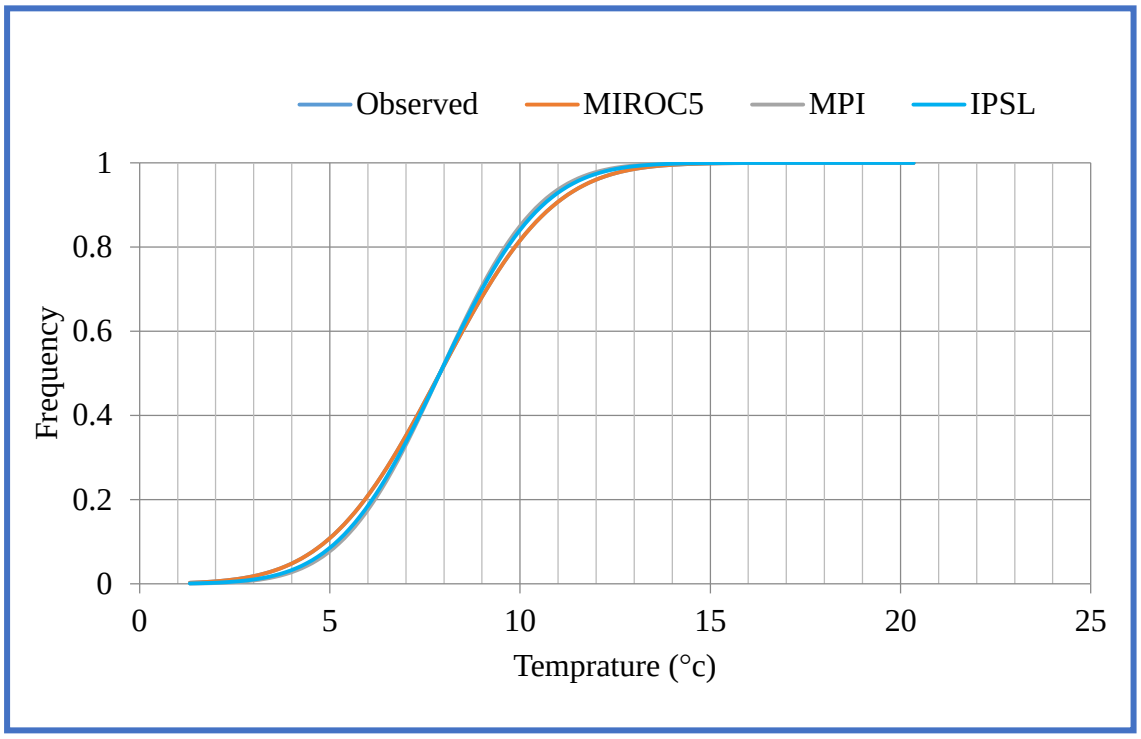

Figure 4-12.Minimum temperature cumulative distribution function mapping results for the station after bias-corrected regional climate model (RCM) data at the watershed scale.

4.2.2. Assessment of corrected and uncorrected RCM rainfall simulation

Plots of average daily precipitation and temperature of the model- uncorrected and corrected data were made at one of the stations of the catchment (Kombolcha) and compared with plots of the observed data to assess the superiority of the corrected data over the uncorrected. The comparison was also to establish the importance of bias correction in this study. The assessment was done by comparing the annual mean values, and standard deviations of the model-uncorrected and corrected mean annual rainfall to the observed data Table 4-7. Besides, plots of daily rainfall and daily mean temperature, the probability of exceedance of defined stream flow classes were made to assess the accuracy with which the model uncorrected and corrected data against the observed.

Table 4-7.Basic statistics of annual uncorrected and bias-corrected (MIROC5, MPI and IPSL) model simulations (rainfall) of historical (1986-2005) rainfall at Kombolcha

	Before Corrected				After Corrected		
RCMs	Observed	MIROC5	MPI	IPSL	MIROC5	MPI	IPSL
Mean	1075.5	2726.9	2688.0	945.1	1077.4	1074.3	1068.5
Bias (%)	-----	153.6	149.9	-12.1	0.18	-0.10	-0.65
RMSE (mm/Year)	-----	1742.9	1766.2	338.4	330.90	476.35	351.04
Correlation	-------	-0.33	0.09	-0.30	-0.11	0.05	-0.20

4.2.3. Evaluation of daily corrected and uncorrected RCM simulation

The daily bias corrections between the observed and simulated variables during the control period (1986-2005) for each RCM models were applied. The bias correction was done on RCM-simulated rainfall, max/min temperature, using the PT and VARI methods respectively. Results show that the power transformation method significantly corrects the biased raw RCM for rainfall and similar results were obtained for minimum and maximum temperature, and when the frequency-based statistics of observed (obs), raw RCM-simulated (raw) and corrected rainfall and temperature data compared to the observation, the raw RCM simulation departs significantly from observation, with over and underestimation of all the statistics (Mean & Stdev). The bias correction methods improve the raw RCM-simulated precipitation and temperature Table 4-8. It can be noticed that the Mean and Standard deviation for rainfall and temperature was improved

and nearly the same as observation data, this proves the methods (PT&VRI) used for bias correction can reproduce the observed data long term mean and variance. Hence, the models capture the observation after correction than the raw RCMs. Thus, the bias correction methods improve the raw RCM-simulated precipitation and temperature.

Table 4-8.Basic statistics of daily uncorrected and bias-corrected RCA4 (MIROC, MPI and IPSL) model simulations of historical (1986-2005) rainfall and temperature at Kombolcha weather station

		Before corrected				After corrected		
climate variable	Statistics	Observed	MIROC5	MPI	IPSL	MIROC	MPI	IPSL
Rainfall	Average	2.94	7.47	7.36	2.59	2.95	2.94	2.93
	Stdev	7.28	13.22	13.61	7.66	7.39	7.27	7.83
Maximum temperature	Average	26.52	18.83	18.76	21.55	26.52	26.52	26.52
	Stdev	2.56	2.94	2.69	3.48	2.56	2.56	2.56
Minimum temperature	Average	12.55	8.49	7.54	9.46	12.55	12.55	12.55
	Stdev	3.18	4.11	4.33	4.64	3.18	3.18	3.18

4.2.3.1. Validation of bias correction according to the hydrological performance

The calibrated and validated SWAT model for the Borkena river catchment is used to simulate the surface runoff corresponding to each of the RCMs, which were considered in this study, for the historical period. The surface runoff generated for each of these RCMs was compared with the observed runoff by computing different model performance indicators. This was done by forcing the SWAT model with each possible combination of raw/corrected RCM-simulated precipitation and temperature. For each SWAT run, we calculated the performance of the models efficiency for long-term monthly mean values of stream flow simulations. All the simulations were conducted at swamp hydrological station where the model calibrated parameters were obtained. A strong outline for all three stream flow characteristics can be seen with R^2, NS and PBIAS value on Table 4-9: with increasing quality of the bias-corrected RCM climate variables, the values in R^2, NS and PBIAS increase as well; this indicates a better model performance, whereas using raw data resulted in the poorest performance. The above

evaluation clearly illustrates that performance indicators behave differently for different RCMs before and after bias correction.

Table 4-9.Validation of bias correction with corresponding regional climate models

	Un-corrected			Corrected		
RCM	R2	NSE	PBIAS	R2	NSE	PBIAS
MIROC5	0.33	-0.12	-93.6	0.71	0.64	5.81
MPI	0.27	0.12	-48	0.62	0.51	11.43
IPSL	0.42	-0.42	-62	0.7	0.6	18.23

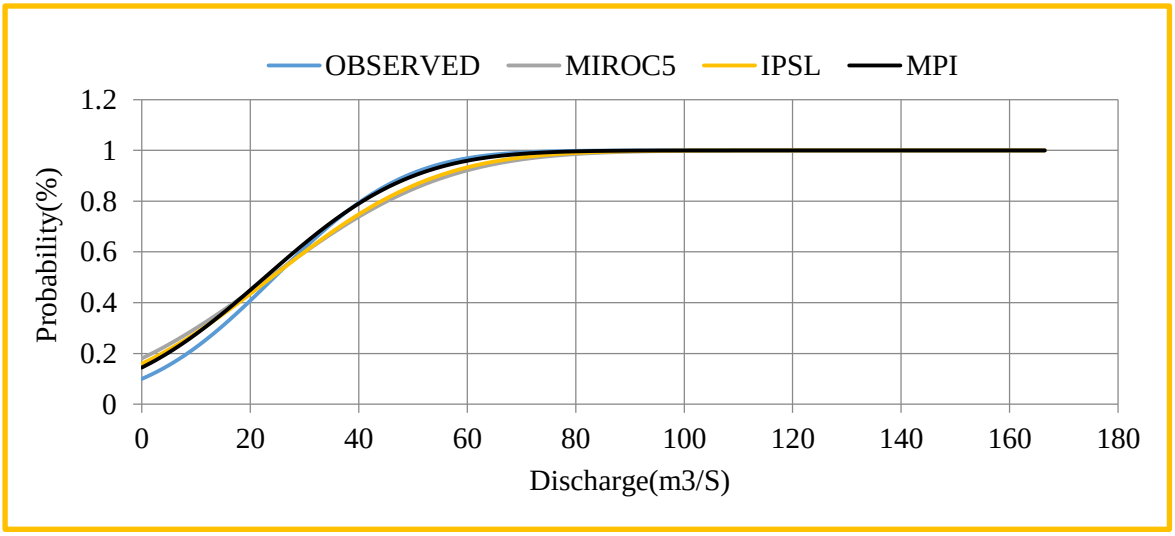

Figure 4-13.Discharge cumulative distribution function mapping results for base period simulation of all three RCMs at swamp hydrological gaging station (outlet)

1.1.1 Validation of bias correction using flow duration curve (FDC)

Further, the performance of the selected RCMs was evaluated by its, ability to capture the hydrologic characteristics of the catchment. Since the primary interest concerns for runoff generated, the emphasis is given on the analysis of surface runoff, which is intended to provide indications of the consistency of historical representation of the hydrologic-regime of the catchment when the regional climate models are used as inputs to the hydrological model.

Flow–duration curve is one of the most intuitive ways of studying the variability in stream flow through the graphical presentation of the distribution of the flow regime. An FDC was constructed by plotting surface runoff against various levels of dependability. Fig. 4-14 shows flow duration curves (FDCs) for all the selected RCMs against the

observed FDC.The comparison of observed and simulated flows for the three RCMs demonstrates that in almost all the locations RCM simulations match very well with the observed data. Consequently, Results demonstrate the accuracy of RCMs forcing to capture the basic hydrologic properties of the watershed in terms of surface runoff.

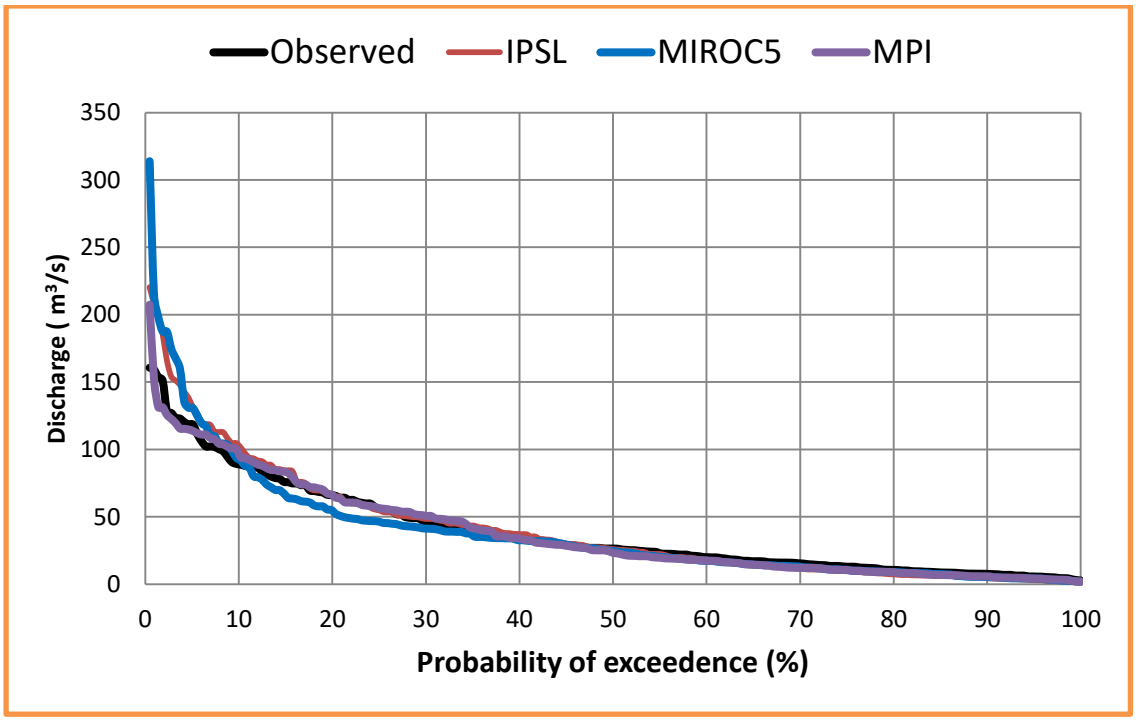

Figure 4-14.Performance Evaluation of selected models using Flow duration curve

4.3. Projected Change in Climate

In this study, the future climate was represented by rainfall and temperature (both maximum and minimum) and was projected under RCP4.5 (medium) and RCP8.5 (high) emission scenarios by correcting biases in three RCMs, such as MPI, MIROC5, and IPSL. Biases in baseline were first corrected using variance scaling and power transformation methods for temperature and precipitation respectively. And then (1) the three RCMs were used to project the rainfall scenarios for the baseline period (1986–2005) and future period (2021–2040), (2041-2060) and (2061-2080) in two RCP scenarios (RCP4.5,and RCP8.5).(2) Stream flow change evaluation due to climate change by simulating discharge using the baseline period and projected climate variables was carried out. Figure 4-15 (a, b and c) shows the projected changes in mean monthly rainfall over the Borkena watershed for specified periods of the 21st century. The variability is most pronounced during the wet season (June-September).

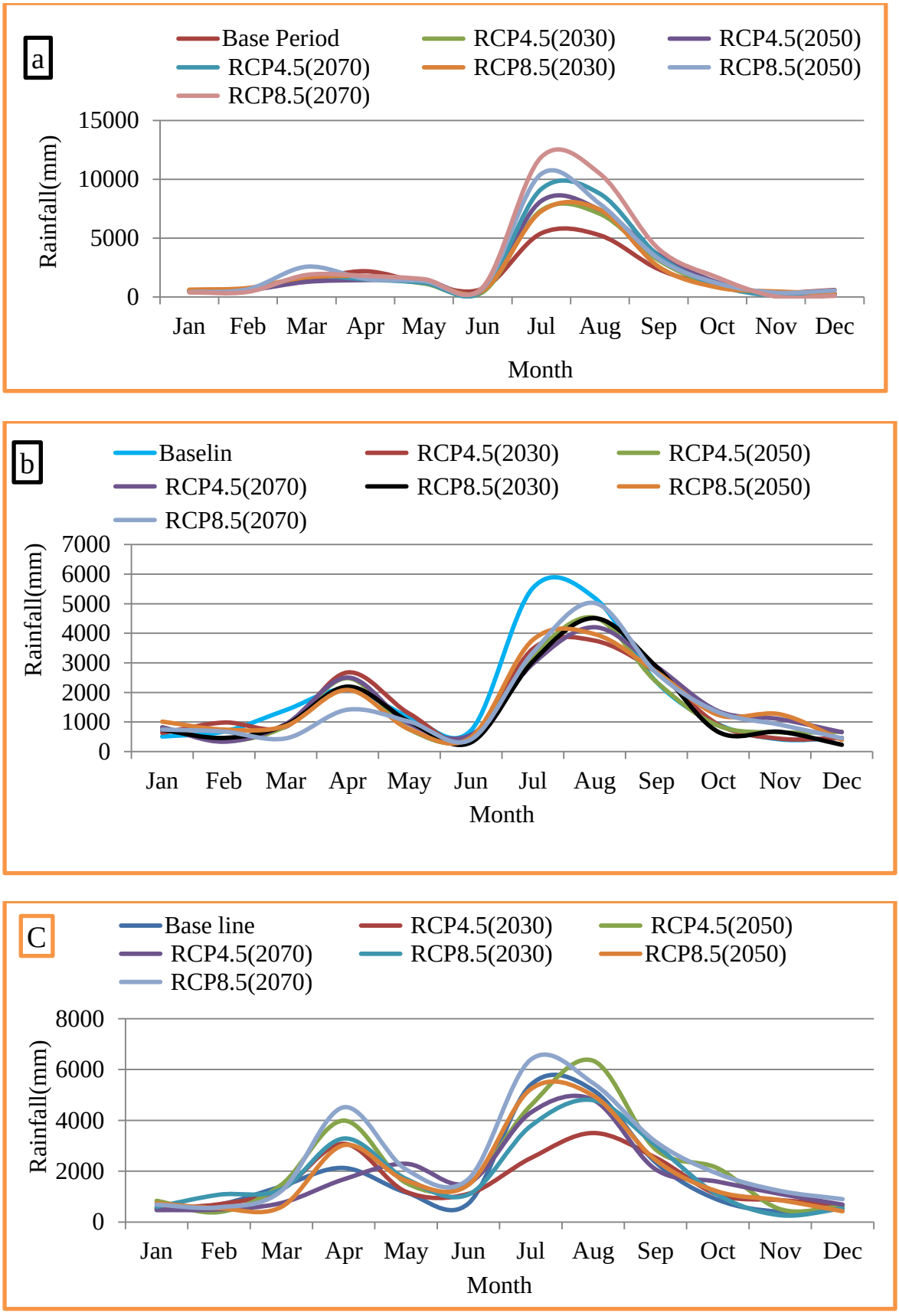

Figure 4-15.Projected monthly rainfall compared to the baseline a) MIROC5 b) MPI, c) IPSL

4.3.1. Monthly changes in projected rainfall

The analysis of average monthly rainfall over the catchment for the near, mid and late-century showed a high level of uncertainties, with mixed signals of increases and decreases in precipitation amounts across the models. Changes in rainfall between the baseline and future periods were considered to analyze the variation characteristics generated by RCM outputs, projected changes in future mean monthly rainfall in the Borkena watershed varied at different time horizons for each RCMs.

Changes in rainfall showed that both increasing and decreasing trend in all-time horizons in the future under both RCPs.The projected average monthly rainfall percentage change in both scenarios varied ranging from -80.9% to +42.8%, -47.7% to 44.8% and-53.4% to 114.1% under RCP4.5 and -47.9% to 41.4%, -50% to+61.8% and -30.0 %to 57.5% under RCP8.5 in near term (2021-2040) for MIROC5, IPSL and MPI respectively compared to the baseline period .Changes in rainfall projected by mid-term ranges from -48.1% to +52.3%, -47.0% to 61.1% and -42.5% to 141.4% under RCP4.5 and -29.3.% to 93.1%, -38.0% to+94.1% and -57.8 %to 13.8% under RCP8.5 in mid-term (2041-2060) for MIROC5,MPI and IPSL compared to the baseline(1986-2005) Similarly changes in rainfall projected by late term ranges from -65.3% to +69.4%, -50.6% to 65.3% and -46.7% to 110.7% under RCP4.5 and -90.3% to 119.8%, -68.1% to+120.2% and -15.0 %to 131.3% under RCP8.5 for MIROC,MPI and IPSL respectively compared to the baseline.

Changes in rainfall projected by MIROC5 projected to increase for the maximum number of months excluding March, July, August, and December which has a decreasing trend that ranges from (-80.9% to -0.2%) in late-term in the future projected period compared with the baseline under both RCP scenarios. Changes in rainfall projected by the other two RCMs (MPI and IPSL) at the same time horizons in different RCP scenarios showed similar patterns, the amplifications of which were mostly within (-90.3% to+141.3%) with valuation results. In the near period, the RCM projected to increase in monthly mean rainfall with the largest increase (114.1%) by IPSL under RCP4.5 and (61.8%) by MPI under RCP8.5 scenarios the month of April and November respectively. In the mid-term, the largest increase in projected rainfall under RCP4.5 is found in June (141.4% by IPSL.

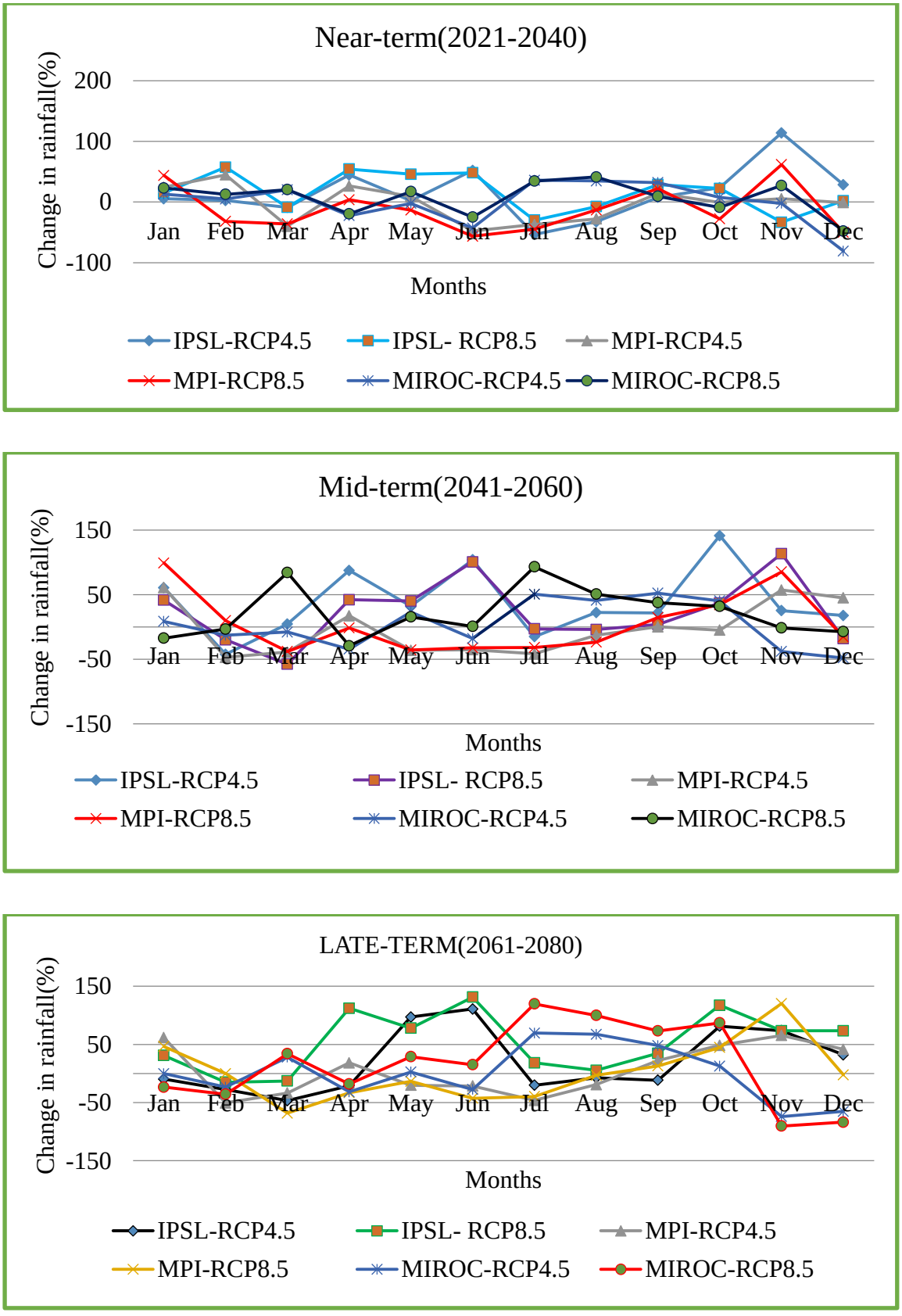

Figure4-16.Relative percentage change of average monthly rainfall for the period of (2021-2040), (2041-2060) and2061-2080)

4.3.2. Annual and seasonal changes in projected rainfall

The relative changes in rainfall for each of the RCPs were also analyzed based on the different seasons, such as -summer, (June -August), autumn (September to November), winter (December to February), and spring (March to May) as well as annually for all designated future periods. The projected rainfall shows there would be a anon significant increment of annual rainfall in all time horizons for both RCPs under all RCMs with a maximum increment of +26.09% in the late century (2061-2080) for IPSL under RCP8.5.Likewise, changes in autumn also show an increment trend with a maximum increment of +118%. More ever, the projected rainfall shows different trends for all RCMs during winter, summer, and spring seasons respectively under both RCPs in all time horizons.

Table 4-10.Percentage change of Mean annual and seasonal rainfall of Borkena River catchment for RCMs during future periods concerning the control period (1986-2005)

Time		**The 2030s**					
RCM		MIROC5		MPI		IPSL	
Scenario		RCPs4.5	RCPs8.5	RCPs4.5	RCPs8.5	RCPs4.5	RCPs8.5
	winter	-21	-4.1	22.8	-12.7	12.1	24.9
	Autumn	12.5	9.2	6.2	18.7	48.4	5.9
Season	summer	9.3	17	-37.5	-38.2	-11.3	3.5
	spring	-1.5	6.1	-1.5	-15.2	12.7	30.5
	Annual	11.32	4.59	13.90	18.11	17.23	19.16
Time		**The 2050s**					
RCM		MIROC5		MPI		IPSL	
scenario		RCPs4.5	RCPs8.5	RCPs4.5	RCPs8.5	RCPs4.5	RCPs8.5
	winter	-17.5	-9.3	19.7	31.2	12	1.2
	Autumn	18.2	22.7	17.5	84.8	62.8	51.4
Seasons	summer	24.6	48.2	-29.9	-29.2	37.1	31.1
	spring	-6.4	23.5	-19.3	-25.1	41.4	8.2
	Annual	24.35	7.56	16.09	10.27	14.84	4.08
Time		**The 2070s**					
RCM		MIROC5		MPI		IPSL	
Scenario		RCPs4.5	RCPs8.5	RCPs4.5	RCPs8.5	RCPs4.5	RCPs8.5
	winter	-29.6	-47.6	17.5	14.6	-1.6	29.7
	Autumn	-4.5	23.2	78.7	59.3	81.1	118.4
Seasons	summer	36.4	78.1	-28.9	-28.5	27.7	51.6
	spring	-0.3	14.9	-11.8	-38.2	9.8	59
	Annual	1.34	8.58	10.39	14.24	23.83	26.09

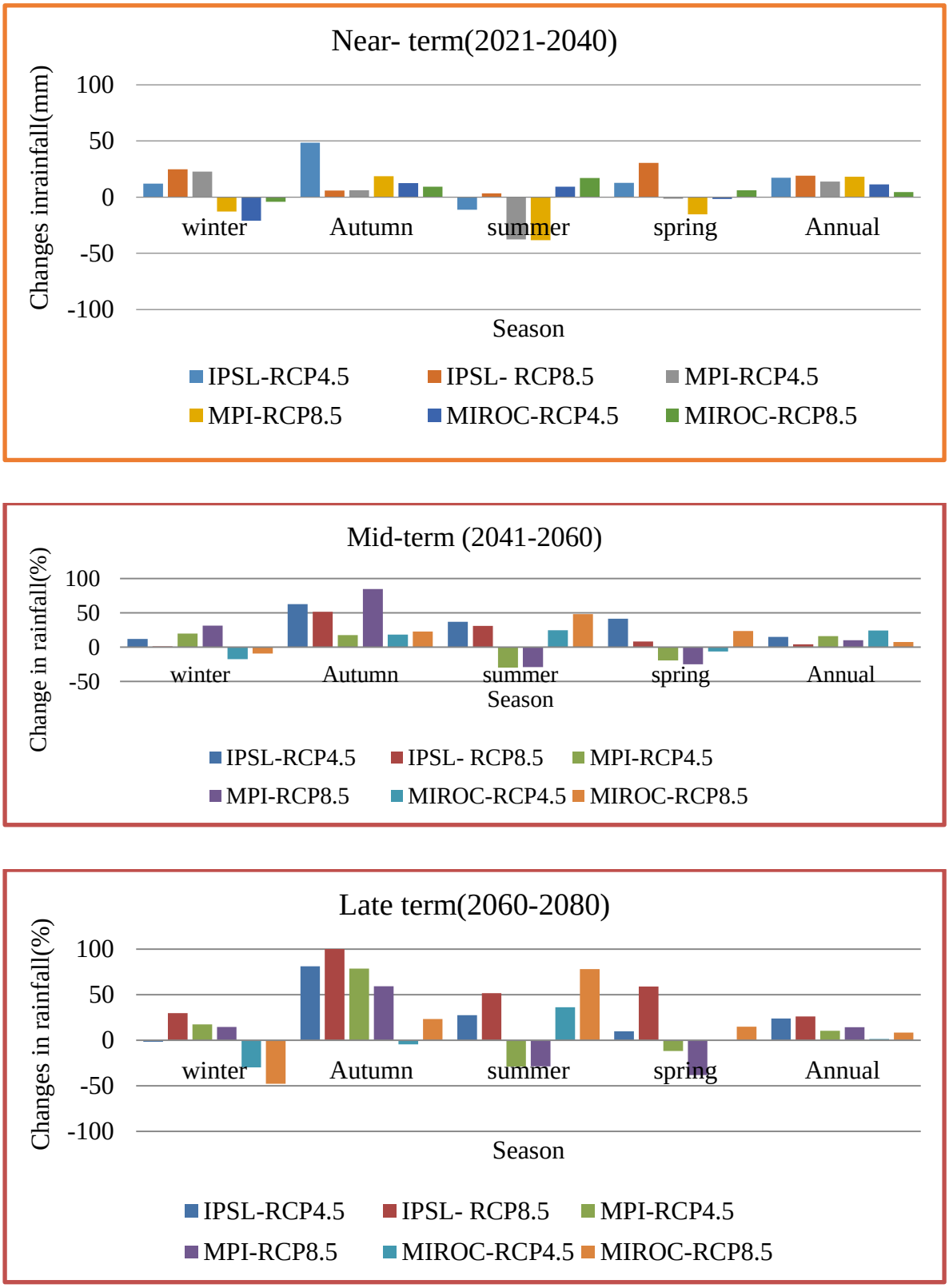

Figure 4-17.Seasonal Rainfall changes by the projected period of (2021-2040), (2041-2060) and (2061-2080) for all RCMs under both Scenarios (RCP4.5 and RCP8.5)

4.3.3. Monthly changes in projected maximum temperature

For the Borkena river catchment, the downscaled maximum temperature shows that both an increasing and decreasing trend for the months in all future time horizons for both RCPs4.5 and RCPs8.5 emission scenarios. The near and mid-century tended to decrease in temperature for all RCMs. The late-century experienced an overall decrease to the temperature at the beginning of the year (March &April) and an overall increase for the reaming months in the century. The percent change fluctuated between increasing and decreasing for all the climate models during the near and mid-century. The late-century experienced an average increase in temperature except for MIROC in March and April.

For IPSL the maximum change in maximum temperature was observed in August (+0.6 °c, +0.2°c, and +1.2°c) in the 2030s, 2050s, and 2070s under RCP4.5 respectively. Similarly, for RCP8.5 the maximum change was observed in August (+0.4.°c, +0.4°c, and +1.5°c) in the 2030s, 2050s, and 2070s respectively. For the MIROC5 RCM model the maximum change of maximum temperature was observed in July (2.1°c, 2.1°c, and 2.4°c) in the 2030s, 2050s, and 2070s for RCP4.5 respectively. For RCP8.5 the change was observed in July (+2.0°c, +1.7°c, and +2.6°c) in the 2030s, 2050s, and 2070s respectively.

For the MPI model the maximum change in maximum temperature was observed in April (+1.0°c,+1.2°c, and +1.7°c) in the 2030s, 2050s, and 2080s for RCP4.5 respectively. For RCP8.5 the change was observed in April (+1.1°c, +1.3°c, and +3.0°c) in the 2030s, 2050s, and 2080s respectively (Figure4.18). From the results, it is established that the uncertainty in the projections increases with increasing RCP forcing and increasing time frames.

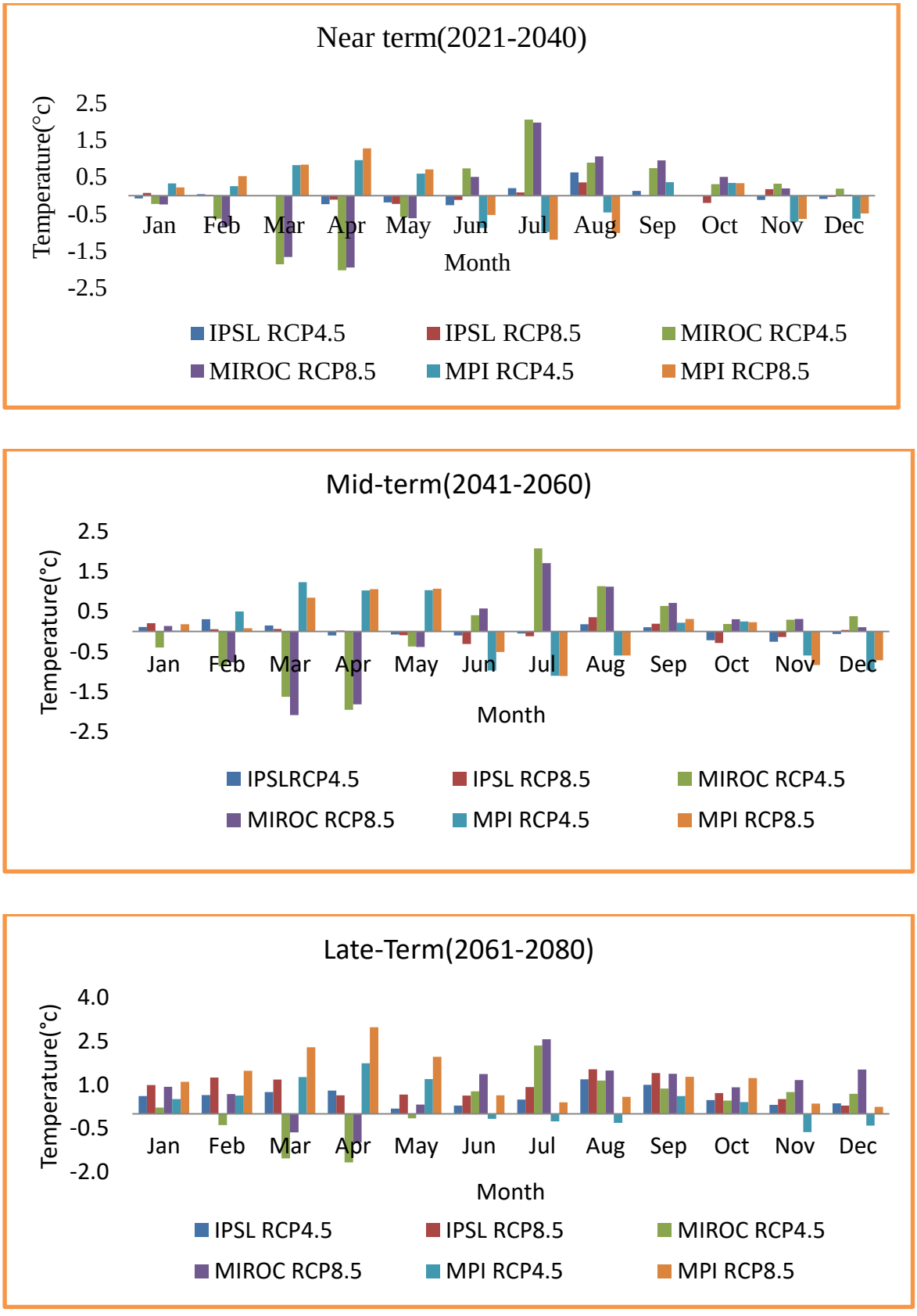

Figure 4-18.Monthly maximum temperature change in the period of (2021-2040) ,(2041-2060) (2061-2080) under all RCMs.

4.3.4. Annual and seasonal changes in projected maximum temperature

The results of temperature change varied annually and from season to season. The results varied depending on the RCM used. Typically, the three RCM outputs agreed on an overall increase or decrease in temperature. Changes in temperature projected to increase in three of the model outputs for all seasons in all the near, mid, and late-century under both RCPs. But there was a decrease in the overall temperature during the summer and spring period in the RCP 4.5 and RCP8.5 for MIROC5 and MPI in all projected time horizons.

Relative to the baseline, annual temperature for the near term (2021-2040) ranged between 0.17 °c and +0.88 °c, with a mean of +0.55 °c under the RCP4.5 scenario and between +0.12 °c and +0.87 °c, with a mean of +0.54 °c under the RCP8.5 scenario. Likewise the mid (2041-2060) of the 21st-century projection showed temperature changes of between +0.14 °c and +0.86 °c, with a mean of +0.53 °c under the RCP4.5 scenario. The high emission RCP8.5 scenario projects changes ranging between 0.16 °c and +0.84 °c, with a mean of 0.54 °c.

Similarly for the late (2061-2080) of century projection showed temperature changes of between +0.24°c and +0.83 °c, with a mean of +0.56 °c under the RCP4.5 scenario. The high emission RCP8.5 scenario projects changes ranging between 0.32°c and +0.7 °c, with a mean of 0.56 °c. Generally, the overall RCMs output indicated a progressive increasing maximum temperature change in all months for the future two periods.

Table 4-11.Percentage change of mean seasonal and annual maximum temperature during future periods of the 2030s, 2050s and 2070s

Time		**The 2030s**					
RCM		MIROC5		MPI		IPSL	
Scenario		RCPs4.5	RCPs8.5	RCPs4.5	RCPs8.5	RCPs4.5	RCPs8.5
	winter	-0.22	-0.35	-0.01	0.09	-0.04	0.02
	Autumn	0.46	0.55	0.00	-0.10	0.00	-0.01
Season	summer	1.23	1.18	-0.77	-0.91	0.19	0.11
	spring	-1.49	-1.41	0.79	0.94	-0.15	-0.12
	Annual	0.88	0.87	0.61	0.65	0.17	0.12
Time		**The 2050s**					
RCM		MIROC5		MPI		IPSL	
scenario		RCPs4.5	RCPs8.5	RCPs4.5	RCPs8.5	RCPs4.5	RCPs8.5
	winter	-0.29	-0.17	-0.15	-0.15	0.12	0.10
	Autumn	0.37	0.44	-0.04	-0.10	-0.12	-0.08
Seasons	summer	1.21	1.13	-0.89	-0.74	0.01	-0.02
	spring	-1.32	-1.43	1.10	0.99	-0.01	0.00
	Annual	0.86	0.84	0.71	0.63	0.14	0.16
Time		**The 2070s**					
RCM		MIROC5		MPI		IPSL	
Scenario		RCPs4.5	RCPs8.5	RCPs4.5	RCPs8.5	RCPs4.5	RCPs8.5
	winter	0.17	1.04	0.24	0.94	0.54	0.84
	Autumn	0.69	1.15	0.13	0.95	0.59	0.87
Seasons	summer	1.42	1.81	-0.25	0.54	0.65	1.03
	spring	-1.12	-0.43	1.40	2.41	0.57	0.83
	Annual	0.83	0.70	0.61	0.66	0.24	0.32

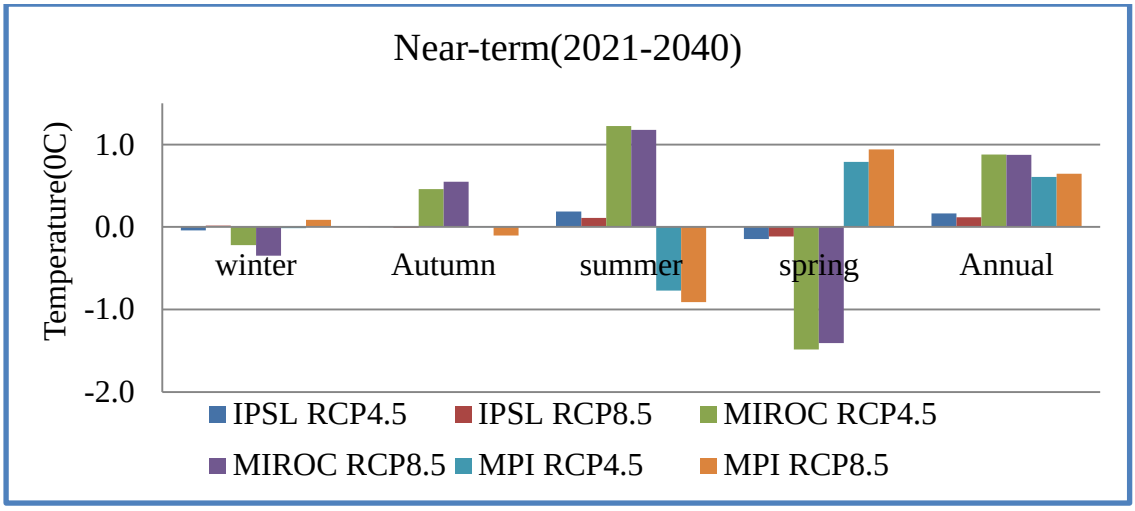

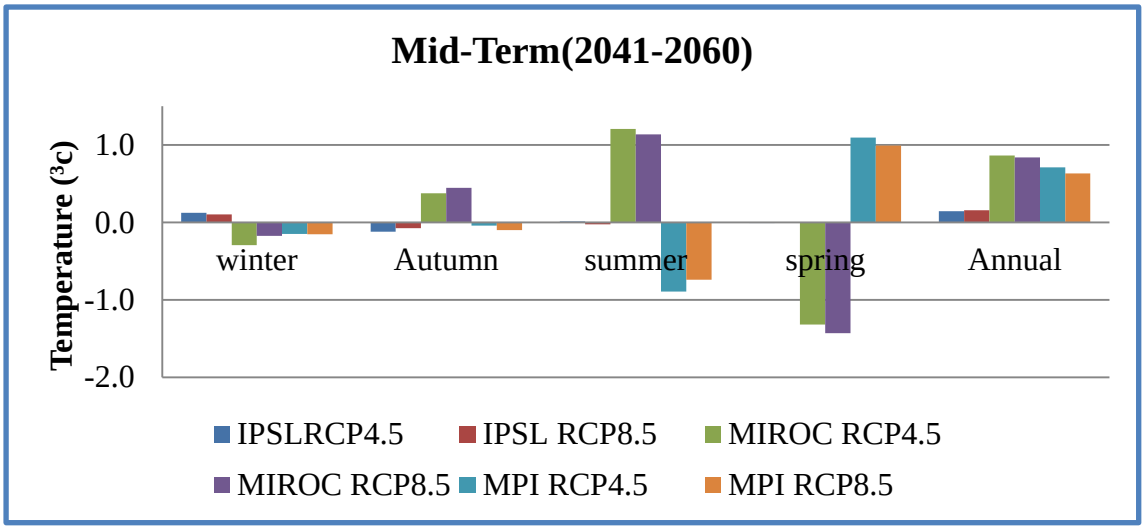

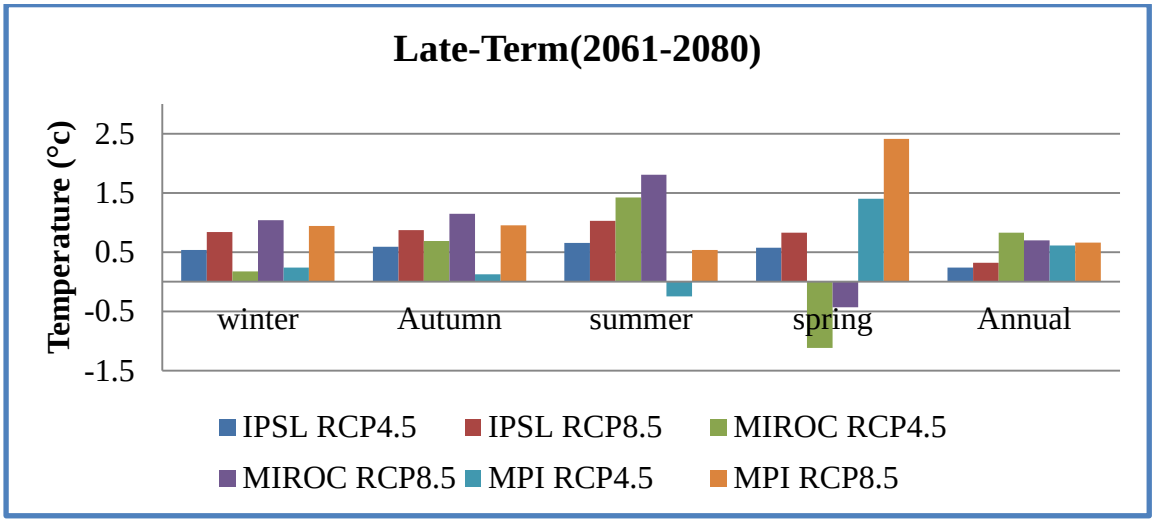

Figure 4-19.Changes in mean seasonal and annual Maximum temperature changes under models and scenarios, by near (2021-2040), mid-term (2041-2060), and late-term (2061-2080).

4.3.5. Monthly changes in projected Minimum temperature

The minimum temperature showed an increasing trend in all three of future time horizons from baseline for both RCPs4.5 and RCPs8.5 emission scenarios, except for January, February, March, April, and May in all-time horizons under RCP 4.5 and RCPs 8.5 for MIROC5, MPI and IPL, RCMS. For IPL, the maximum change in minimum temperature was observed in August for the near term and May for the mid and late-term (+0.4°c, +0.8°c and+1.1°c) in the 2030s, 2050s, and 2070s for RCP4.5 respectively. Similarly, for RCP8.5 the maximum change was observed in May (+0.4°c, +0.8°c, and+2.3°c) in the 2030s, 2050s, and 2070s respectively. For MIROC5 the maximum change of minimum temperature was observed in October (+0.5°c, +0.7°c, and +1.1°c) in the 2030s, 2050s, and 2070s for RCP4.5 respectively. For RCP8.5 the change was observed in October (+0.5°c, +0.7°c, and +2.4°c) in the 2030s, 2050s, and 2070s respectively. Likewise, the minimum change was observed in December in the 2030s, 2050s, and 2070s for both RCP4.5 and RCP8.5.

For MPI the maximum change of minimum temperature was observed in November and October (+0.3°c, +0.6°c, and +1.1°c) in the 2030s, 2050s, and 2070s for RCP4.5 respectively. For RCP8.5 the change was observed in January (+0.5°c, +0.6°c, and +1.8°c) in the 2030s, 2050s, and 2070s respectively. The minimum change was observed in December in the 2030s, 2050s and2070s for both RCP4.5and RCP8.5 (Figure4-20).

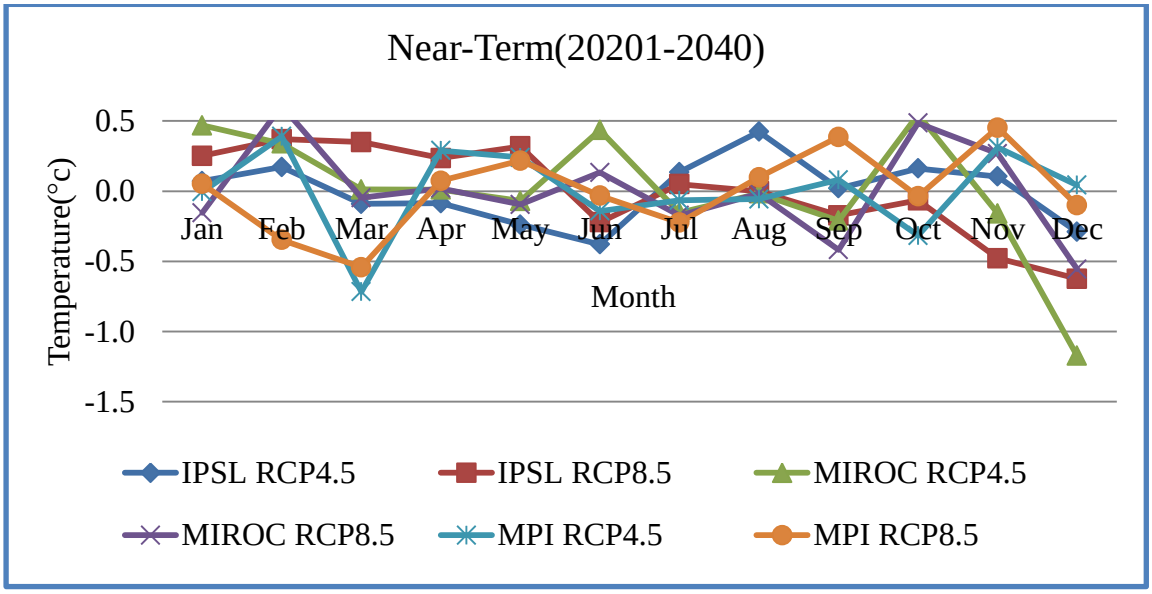

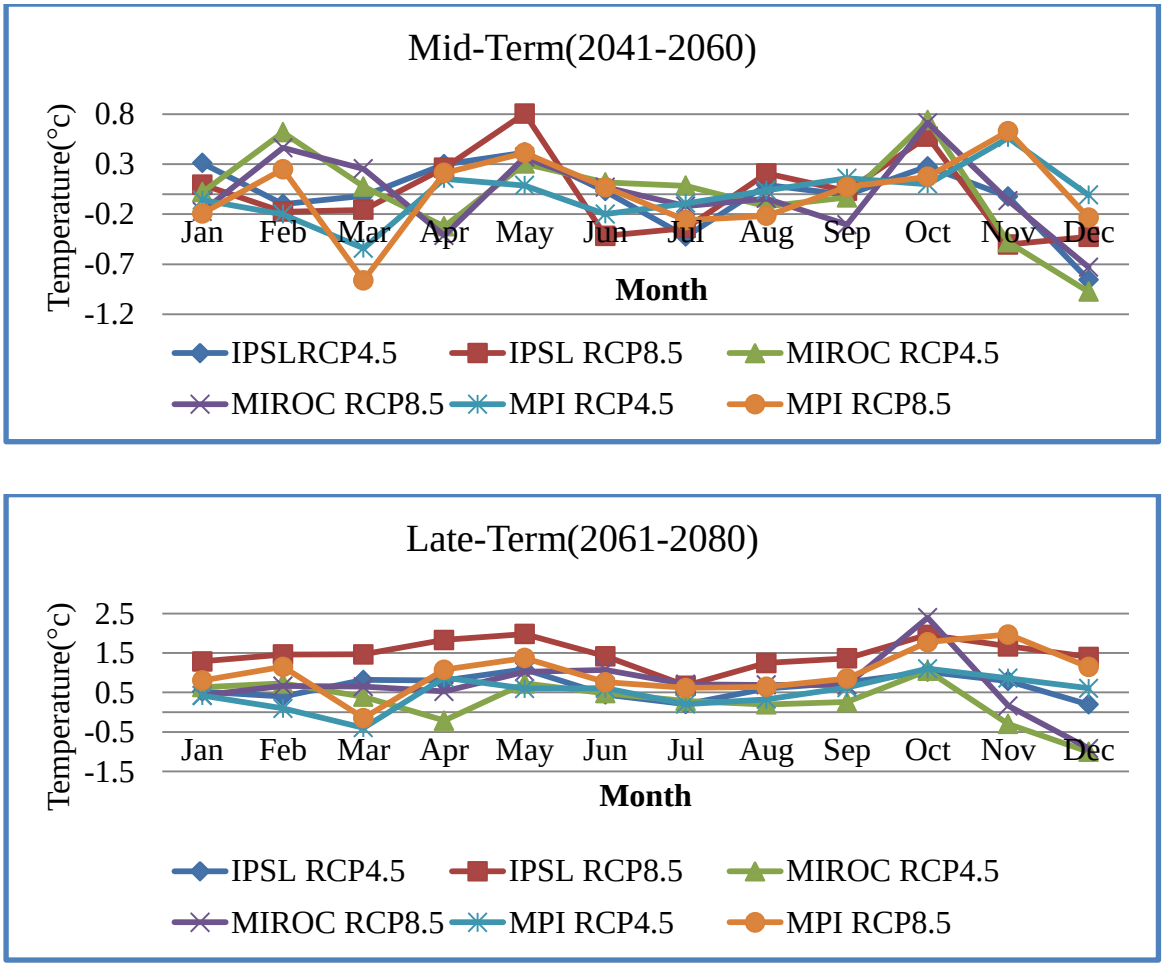

Figure4-20.Monthly minimum temperature change by the projected period (2021-2040), (2041-2060) and (2061-2080) under all RCMs

4.3.6. Annual and seasonal changes in projected minimum temperature

Likewise maximum temperature the results of minimum temperature change varied annually and from season to season. The results varied depending on the RCM used. Relative to the baseline, annual temperature for the near term (2021-2040) ranged between 0.18 °c and +0.3 °c, with a mean of +0.23 °c under the RCP4.5 scenario and between +0.21 °c and +0.26 °c, with a mean of +0.24 °c under the RCP8.5 scenario. Likewise the mid (2041-2060) of the 21st-century projection showed temperature changes of between +0.18 °c and +0.32 °c, with a mean of +0.25 °c under the RCP4.5 scenario. The high emission RCP8.5 scenario projects changes ranging between 0.3 °c and +0.33 °c, with a mean of 0.31 °c. Similarly for the late (2061-2080) of the 21st-century century, projection showed temperature changes of between +0.24 °c and +0.4 °c, with a mean of +0.31 °c under the RCP4.5 scenario. The high emission RCP8.5

scenario projects changes ranging between 0.25 °c and +0.42 °c, with a mean of 0.36 °c. Generally, the overall RCMs output indicated a progressive increasing minimum temperature change in all months for the future three periods. Finally during summer, spring, winter, and autumn under RCP4.5 and RCP8.5 scenarios, the MPI model is the warmest RCM in the near and midterm periods.

Table 4-12.Percentage change of mean seasonal and annual minimum temperature during future periods of the 2030s, 2050s and 2070s

Time		**The 2030s**					
RCM		MIROC5		MPI		IPSL	
Scenario		RCPs4.5	RCPs8.5	RCPs4.5	RCPs8.5	RCPs4.5	RCPs8.5
	winter	-0.12	-0.03	0.14	-0.13	-0.02	0.00
	Autumn	0.06	0.11	0.03	0.27	0.10	-0.24
Season	summer	0.09	-0.02	-0.09	-0.05	0.06	-0.06
	spring	-0.02	-0.04	-0.06	-0.08	-0.14	0.30
	Annual	0.30	0.25	0.22	0.21	0.18	0.26
Time		**The 2050s**					
RCM		MIROC5		MPI		IPSL	
scenario		RCPs4.5	RCPs8.5	RCPs4.5	RCPs8.5	RCPs4.5	RCPs8.5
	winter	-0.11	-0.15	-0.09	-0.06	-0.21	-0.17
	Autumn	0.08	0.11	0.27	0.29	0.08	0.04
Seasons	summer	0.03	-0.03	-0.08	-0.14	-0.10	-0.18
	spring	0.02	0.07	-0.10	-0.08	0.23	0.30
	Annual	0.32	0.31	0.18	0.30	0.24	0.33
Time		**The 2070s**					
RCM		MIROC5		MPI		IPSL	
Scenario		RCPs4.5	RCPs8.5	RCPs4.5	RCPs8.5	RCPs4.5	RCPs8.5
	winter	0.12	0.06	0.38	1.03	0.37	1.38
	Autumn	0.34	1.08	0.86	1.53	0.86	1.66
Seasons	summer	0.32	0.83	0.38	0.67	0.42	1.11
	spring	0.30	0.73	0.36	0.77	0.91	1.76
	Annual	0.40	0.42	0.30	0.41	0.24	0.25

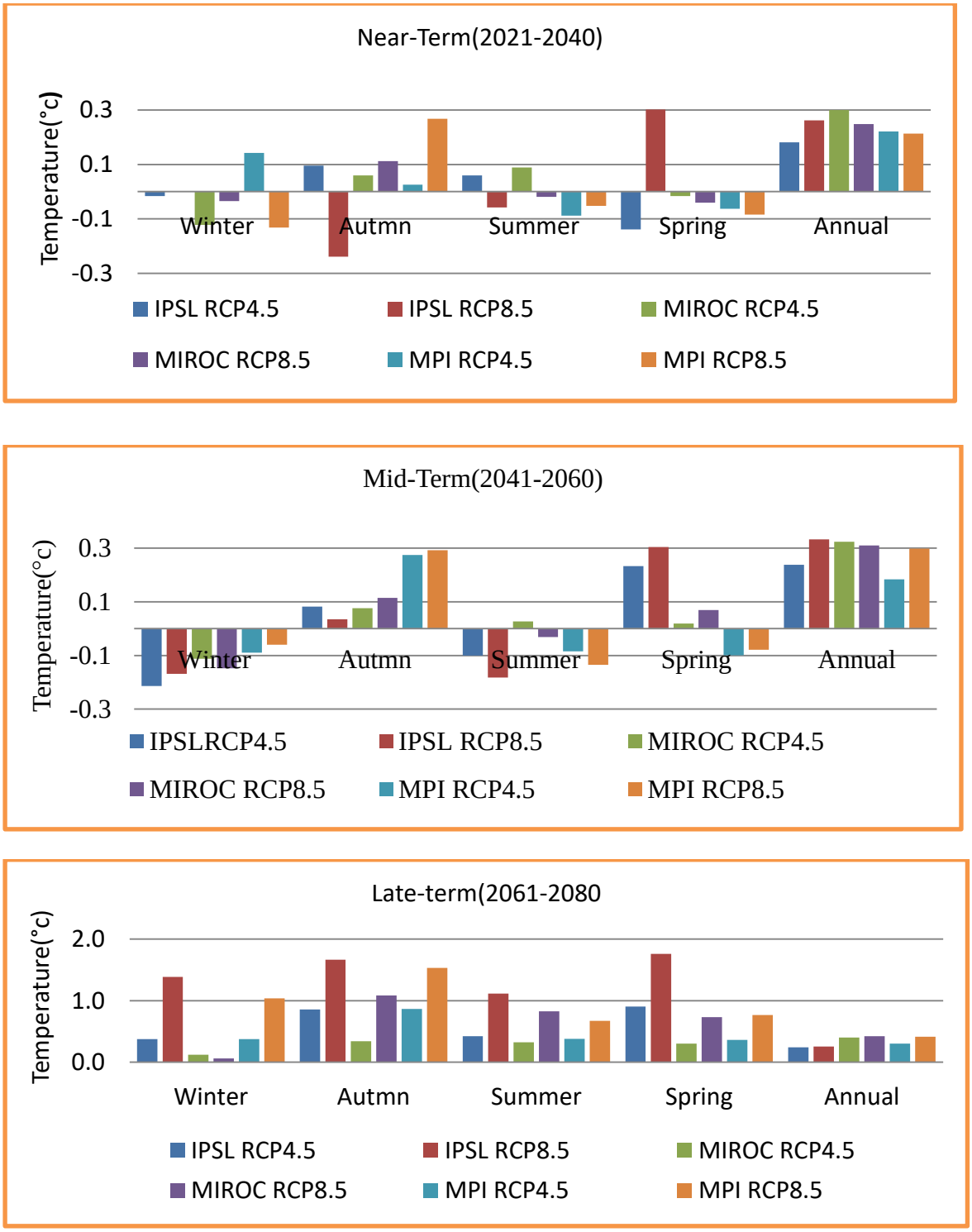

Figure 4-21.Changes in bias-corrected mean seasonal and annual Minimum temperature changes under models and scenarios, by near (2021-2040), mid-term (2041-2060) and late-term (2061-2080)

4.4. SWAT Model Results

4.4.1. Parameter's Sensitivity Analysis

Sensitivity analysis was carried out to find the order of sensitivity of stream flow to the input parameters. There are a few methods available in assessing the sensitivity of input parameters in hydrological models. In the SWAT model, input parameters can be either manually adjusted or can be accessed in the SWAT-CUP (Calibration and Uncertainty Programs(Arnold et al., 2012).

In this study, SUFI-2(Sequential Uncertainty Fitting) calibration and uncertainty algorism, which is linked with SWAT-CUP was used and twenty-two parameters that previously mentioned by other researchers in the study area were considered for the analysis of sensitivity. After setting up the SWAT-CUP using SWAT model outputs and incorporating all input parameters, simulations were carried out with SUFI-II by running 500 simulations and sensitivity analysis was run with monthly flow data from 1996-2001using global sensitivity analysis (Appendix C). In the global sensitivity analysis, the t-stat offers a measure of sensitivity, the largest absolute value represents higher sensitivity and p-value determined the significance of sensitivity, a value close to zero has more significance (Abbaspour, 2013).

By considering this, in global sensitivity analysis thirteen crucial parameters (SCS Curve Number II (CN2), Lateral flow travel time (LAT_TTIME), ground water delay (GW_DELAY), ground water"revap "coefficient (GW_REVAP), Manning's "n" value for overland flow (OV_N),base flow alpha factors (ALPHA_BF), soil evaporation compensation factor (ESCO), GWQMN, Base flow alpha factor for bank storage(ALPHA_BNK),Depth from soil surface to bottom of layer (SOL_Z), Manning's "n" value for the main channel (CH_N2.rte), Available water capacity of the soil layer (SOL_AWC) and Deep aquifer percolation fraction (RCHRG_DP) have been pointed out due to their control of the hydrological processes of the studied area. However, SCS Curve Number II (CN2) and Lateral flow travel time (LAT_TTIME) were found to be most crucial than other parameters for Borkena watershed.

Table 4 11.Flow-sensitive parameters and fitted values in ranked order

NO	Hydrological Parameters	min value	Max- value	Fitted- value
1	r__CN2.mgt	-0.25	0.25	0.01
2	v__ALPHA_BF.gw	0	1	0.06
3	v__GW_DELAY.gw	0	500	484.94
4	v__GWQMN.gw	0	2	0.33
5	v__GW_REVAP.gw	0.02	0.2	0.02
6	v__ALPHA_BNK.rte	0	1	0.57
7	v__RCHRG_DP.gw	0	1	0.1
8	v__LAT_TTIME.hru	0.25	120.3	13.66
9	v__ESCO.hru	0	1	0.32
10	r__CH_N2.rte	0	1	0.88
11	r__SOL_Z (..).sol	-0.25	0.25	0.05
12	r__SOL_AWC (..).sol	-0.25	0.25	0.17
13	r__OV_N.hru	0.01	30	23.22

Note (i). R-sensitive parameter shows multiply by 1+ the given fitted value. (ii).V-sensitive parameter shows replace the value by the given fitted value. (Iii).A: add Values to Initial Parameter.

4.4.2. Calibration of SWAT model

The simulation of the model with the default value of parameters in the Borkena River catchment showed relatively good matching between the simulated and observed stream flow hydrographs. Hence, calibration was done for sensitive flow parameters of SWAT with observed average monthly discharge data. First, some sensitivity flow parameters adjusted by manual calibration procedure based on the available information in some literatures that are conducted in the study area. In this procedure, the values of the parameters varied iteratively within the allowable ranges until the simulated flow as close as possible to observed stream flow. Then, auto-calibration carried out using sensitive parameters identified during sensitivity analysis. Calibration was done based on monthly time step to observe the performance of the model at selected hydro gauging station (swamp) of the Borkena river catchment for the year 1996-2001. The correlation coefficient (R^2) and Nash-Sutcliffe simulation efficiency (NSE) and percent of bias

(PBIAS) were used as the main objective functions for the model following the SUFI-2 approach between the observed and predicted stream flow. According to the model performance evaluation given by Moriasi et al.(2007), the calibration results of the SUFI-2 program summarized the values of correlation coefficient (R^2) and the Nash-Sutcliffe (1970) simulation efficiency (NS), percent of bias (PBIAS) as 0.79,0.78 and -19 Table4-13.

4.4.3. Validation of the SWAT model

Validation proves the performance of the model for simulated flows in periods different than the Calibration period without any further adjustment in the calibrated parameters. The validation was performed for four years period from January 1st, 2002 to December 31st, 2005. The validation statistics of the simulated flow indicate that R^2, ENS and PBIAS values were found as 0.76, 0.73 and -21 respectively. For Monthly simulations, in the validation period, this value shows a good agreement between predicted and measured stream flow. The calibration and validation result in Fig 4-22 and Fig 4.23 shows that SWAT could successfully simulate realistic stream flow in the Borkena watershed.

Table 4-13.Evaluation of SWAT model Performance during calibration and validation

Description			Model performance evaluation index		
Duration	Time step	Analysis	R2	ENS	PBIAS
1996-2001	Monthly	Calibration	0.79	0.78	-19
2001-2005	Monthly	Validation	0.76	0.73	-21

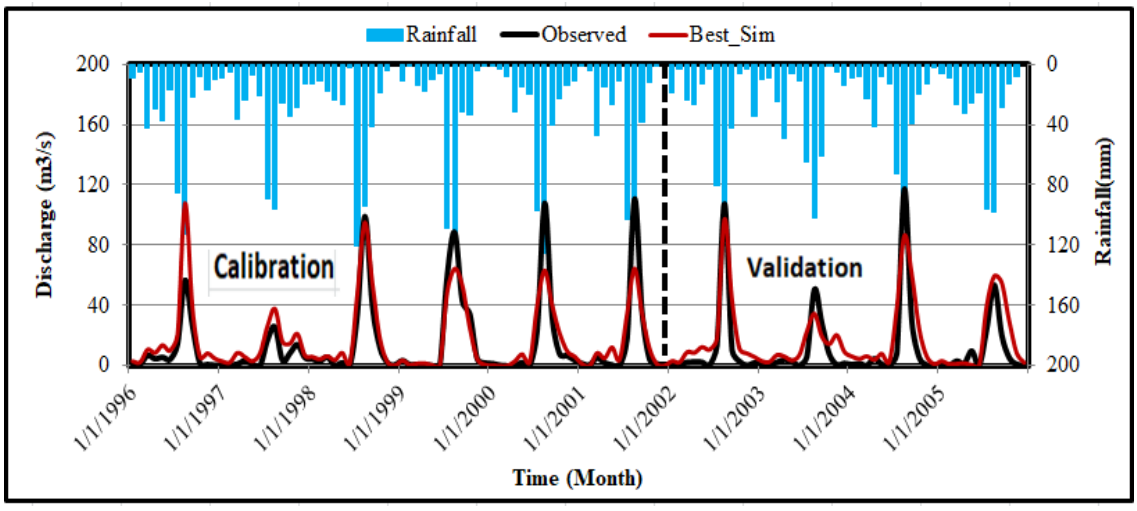

Figure 4-22.Calibration and validation result of monthly simulated and measured flow at the outlet of the Borkena watershed, where the gauging station is located.

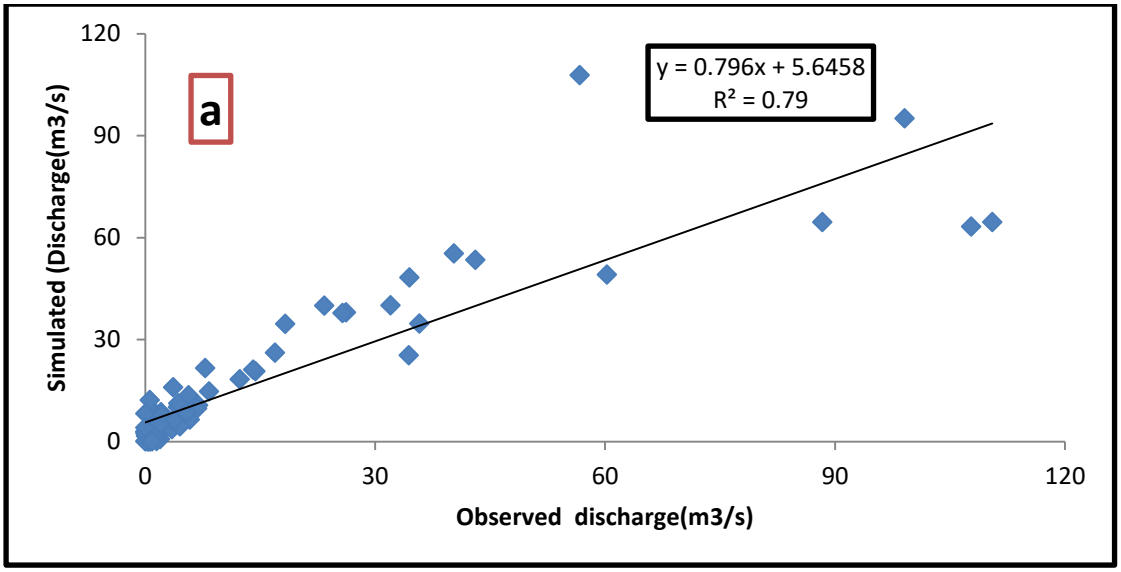

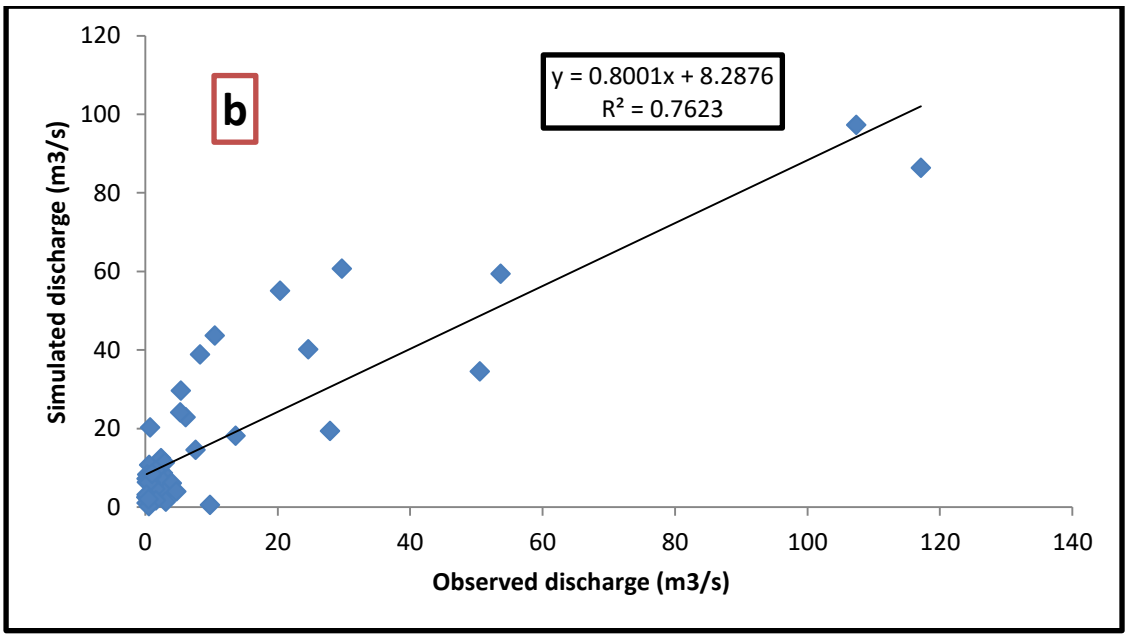

Figure 4-23.Regression coefficient of Monthly calibration (a) and validation (b) of discharge in the outlet of the Borkena watershed

4.5. Climate Change Impact on Streamflow of Borkena River catchment

4.5.1. Climate Change Impact on monthly Streamflow

After the SWAT model was calibrated and validated, the bias-corrected weather inputs for each RCM were imported into the model. And then the calibrated and validated SWAT model was employed to generate future projections of stream-flows using three selected RCMs (IPSL, MIROC and MPI), at swamp gauge site, for three twenty-year

time horizons, near- term (2021-2040), mid-term (2041 –2060) and (2061-2080) late-term.

The future projected alterations in precipitation are reflected by the changes between future and reference surface runoff derived from the simulations of the SWAT model forced by the bias-corrected future projections from the three RCMs. The runoff estimated for three well-performed RCMs suggest that the monthly mean surface runoff estimated by SWAT for March to May and September to November increases substantially in all-time horizons in the future whereas runoff for the reaming months of periods projected to decrease.

For RCA4 (IPSL) the maximum change of increment of Stream flow was observed in May (+57.0%), April (+82.8%), and June (+91.4 %,) in the 2030s, 2050s. and 2070s, respectively under RCP4.5.The maximum change of decrement was also observed in August (-48.0%), February (-10.0%), March (-48.0%) in the 2030s, 2060s, and 2090s respectively. Similarly, for RCP8.5, the maximum change was observed in May (74.4%, 93.8%) in the 2030s, and 2050s respectively. But In the 2070s the maximum change of increment of flow was observed in June (+132.2%). The maximum reduction was also observed in July, February, and March in the 2030s, 2050s, and 2070s respectively.

For MIROC5 the maximum change of increment was observed in July (+71.1%, +99.4%) in the 2030s and 2070s for RCP4.5.In the 2050s the change was observed in September (72.8 %,). Correspondingly for RCP8.5, the maximum change was observed in March (67.9%), August (103.2%), and July (76.6%) in the 2030s, 2060s, and 2090s respectively. The maximum reduction was observed in April (-23.2%, in the 2070s. For MPI, the maximum change of increment was observed in February (91.8%), January and (27.3%), and November (58.9%) in the 2030s and 2050s and 2070s for RCP4.5 respectively. Likewise, for RCP8.5 the maximum change was observed in February (+32.2%,+93%.4,+61.1%) in the 2030s,2050s, and 2070s. The maximum reduction was observed in July (+59.8%, 40m^3/s) in the 2030s.

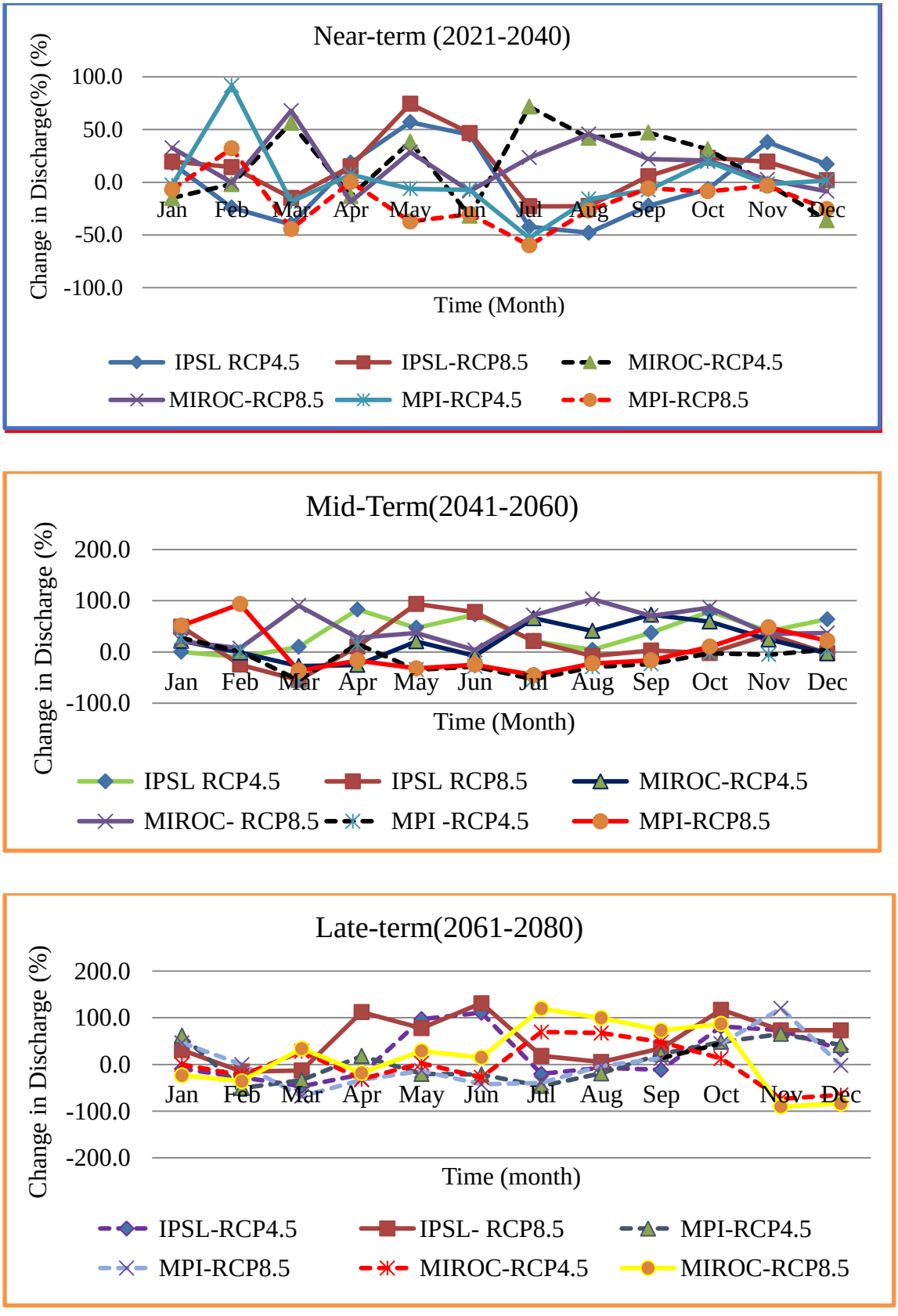

Figure 4-24.Relative changes in average monthly flow for each Representative Concentration Pathway (RCP) during late-century refer to (2021-2040)

4.5.2. Climate change impact on Seasonal and annual streamflow

In most cases decrement of flow on Borkena River was observed in most of seasons (summer, winter, spring and autumn) across all GCM groups. The maximum flow increment reaches 32.2% for the periods of near term (2021-2040) under RCP 4.5 for the MIROC5 model. A maximum flow Reduction was also observed during the autumn season on the MPI model under RCP 4.5 in the near term.Figure4.16.

The other maximum decrement also predicted during the 2050s and 2070s from all model outputs which are considered in this study under both concentration pathways (RCP 4.5 and RCP 8.5) scenarios during winter, summer, and autumn except summer and spring under both RCP4.5and RCP8.5 for regional climate models except MIROC5 in spring and summer. The average annual stream flow projected to decrease in the future time horizons under both RCPs for all three RCMs.

The average annual flow shows a maximum decrement of 32.8%, 39.1%, and 42.1% in the 2030s.2050s and 2070s respectively for MIROC5 under both RCPs4.5and RCPs8.5.Seasonal change in flow volume from Borkena River will imply both the negative and positive impact, which will greatly affect the watershed especially in the downstream. As this region is largely occupied by urban and rural settlers they are expected to experience major impacts on water availability and supply, food security. Therefore, the region requires integrated watershed- water management practice.

Table 4-14.Seasonal and annual Percentage change of streamflow for future periods in two scenarios as compared to the flow in the base period (1986-2005)

Time		**The 2030s**					
RCM		MIROC5		MPI		IPSL	
Scenario		RCPs4.5	RCPs8.5	RCPs4.5	RCPs8.5	RCPs4.5	RCPs8.5
	winter	-13.6	-17.9	-33.5	-10.1	-14.7	-10.0
	spring	-35.7	25.0	21.5	-12.9	8.1	6.2
Season	summer	17.3	23.2	-28.3	-24.9	-26.1	10.4
	Autumn	32.2	-36.1	-38.8	-23.1	-21.9	-28.3
	Annual	-32.8	-24.8	-10.5	-23.3	-16.2	1.7
Time		**The 2050s**					
RCM		MIROC5		MPI		IPSL	
scenario		RCPs4.5	RCPs8.5	RCPs4.5	RCPs8.5	RCPs4.5	RCPs8.5
	winter	20.0	-31.8	-13.0	-46.5	-28.0	-17.2
	spring	42.1	-44.2	-27.4	-24.0	34.4	23.5
Seasons	summer	32.2	-22.9	-20.1	-43.9	42.7	24.3
	Autumn	-20.8	41.8	-44.4	-18.4	-53.2	26.5
	Annual	-37.5	-39.1	-23.6	-14.0	-38.6	8.5
Time		**The 2070s**					
RCM		MIROC5		MPI		IPSL	
Scenario		RCPs4.5	RCPs8.5	RCPs4.5	RCPs8.5	RCPs4.5	RCPs8.5
	winter	-20.0	-35.9	-29.7	-43.3	-13.0	-37.2
	spring	25.2	-75.6	-38.3	-25.7	21.6	36.8
Seasons	summer	40.2	40.2	-43.1	-44.0	26.7	28.4
	Autumn	25.9	12.7	-36.1	-53.9	-12.6	-44.6
	Annual	-42.1	-30.4	-16.2	-20.6	-0.7	-40.7

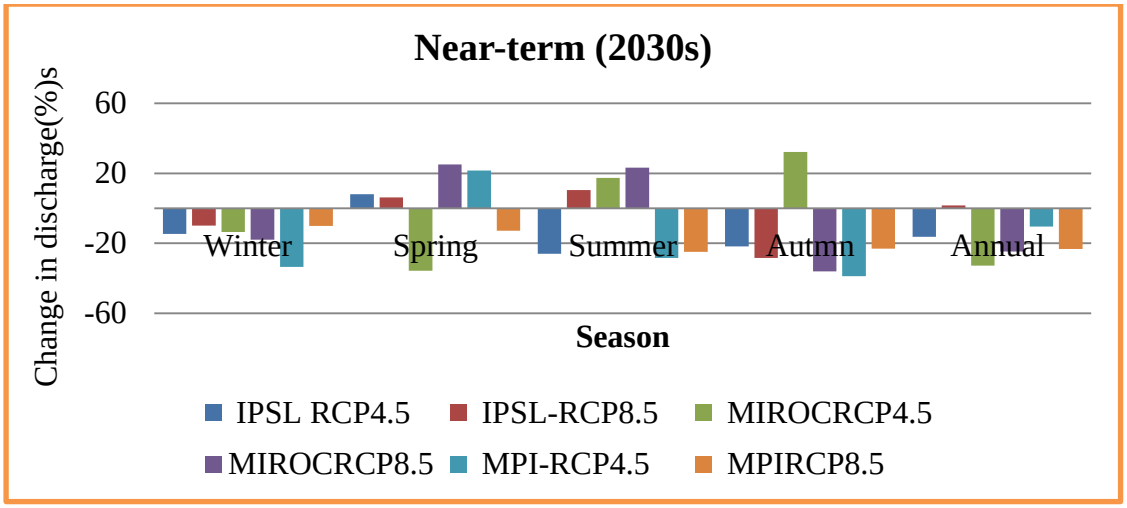

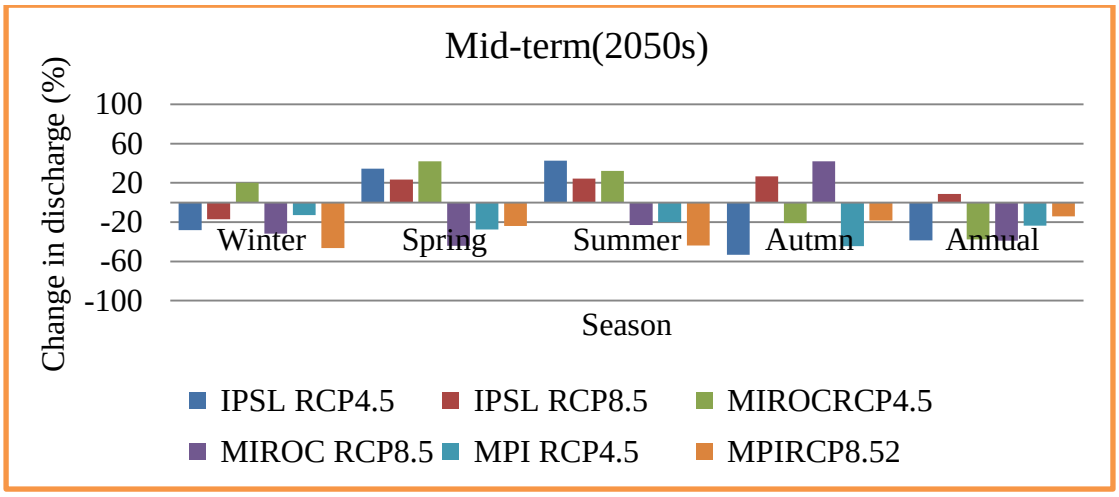

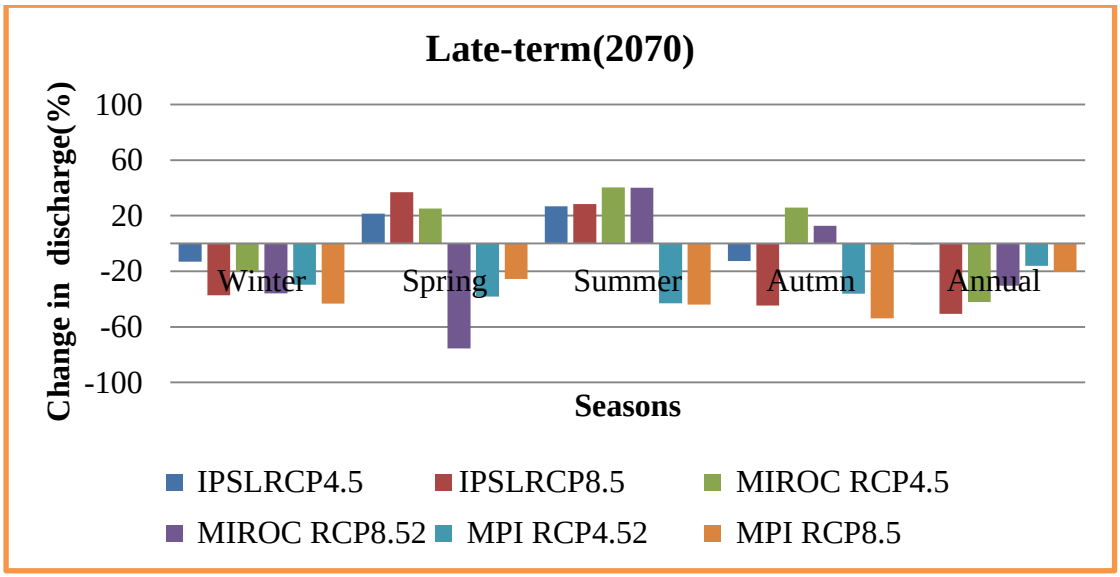

Figure 4-25.Seasonal and annual Percentage change of stream flow for future periods of (2021-2041), (2041-2060) and (2061-2080)

4.6. The impacts of climate change on extreme events

4.6.1. Maximum streamflow Analysis Using Annual maximum method

The maximum flow analysis was carried out using the annual maximum method. This method evaluates the maximum annual flow by selecting the maximum flow from the year that is considered in this study. The change of maximum annual flow for the first future time series (2030s) indicated a decreasing trend under both RCP4.5 and RCP8.5 for all RCMS scenarios for the Borkena River catchment concerning the base period maximum flow (1986-2005). However, the highest decrement was (42.5%) for IPSL under RCP8.5.

For the second future time horizon (2050s) the percentage change of maximum annual flow showed a decrement trend in both RCP scenarios. The maximum increment was (39.3%) for MPI under RCP4.5.For the third future time horizon (2070s) the percentage change of maximum annual flow also showed a decrement trend in both RCP scenarios with a maximum decrement of 45.0% for MIROC5 under RCP8.5.For this study, the change of maximum annual flow in the long -term future time horizon indicated a decreasing trend in the catchment under both RCPs (RCP4.5and RCP8.5) for all selected regional climate models. In general, the decreasing of high flow extremes in the future will not cause flooding and groundwater reduction.

Table 4-15.Percentage change of extreme stream flow for future periods in two scenarios as compared to the flow in the base period (1986-2005)

Projection period	Near -Term		Mid Term		Late-Term	
SCENARIO	RCPs4.5	RCPs8.5	RCPs4.5	RCPs8.5	RCPs4.5	RCPs8.5
MPI	-33.1	-36.3	-39.3	-27.0	-45.0	-12.7
IPSL	-15.1	-45.2	-7.4	-10.6	-17.5	-13.7
MIROC5	-7.0	-16.8	-22.4	-34.5	-34.2	-36.8

4.6.2. Maximum flow analysis using flow duration curve (FDC)

Flow duration curves show the percentage of time that certain values of discharge daily, monthly, or yearly were equaled or exceeded in the available number of years of record. The selection of the time interval depends on the purpose of the study. For stream flow for a particular river basin providing an estimate of the percentage of time for given

stream flow was equaled or exceeded over a future period (Vogel & Fennessey, 1994)). In this study, the impacts of climate change on extreme events of the study area have also been evaluated based on the flow duration curve. The flow duration curves (FDC) for swamp gauging station is drawn to compare the exceedance probability of monthly stream flow, between the baseline (1986–2005) and projected (2021–2080) climate to assess the flow patterns during 2021–2080 Figures 4-26, 4-27 and 4-28.

It is evident from the figures that under both emission scenarios for all RCMs considered the magnitude of stream flow decreases, and the curve becomes relatively flattered during Q30–Q70 (mid-flow). A flat curve generally indicates that groundwater contributions to the stream reach are significant which supports sustain the flow throughout the year (Chambers et al.2017). FDCs further show a considerable decreases in both high flows (5% exceedance) and low flows (95% exceedance) respectively from 2021–2080 concerning base period (1986–2005).

For five percent probability (Q_5) (high flow) of exceedance, the percentage change of maximum monthly flow in all-time horizons (the 2030s, 2050s, and 2070s) was decreasingly projected under both scenario (RCP4.5and RCP8.5) in the catchment in the near term concerning the base period flow (1986-2005).This comparison shows that the probability of occurrence of flow and magnitudes of flow could be lower in both future periods in the catchment under both scenarios. For the ninety-five percent of probability (Q95(low flow), the percentage change of flow projected to decrease under all considered RCMs (MPI, IPSL, and MIROC5) for both RCP4.5 and RCP8.5 in future time horizons.

Generally, the high flow (Q_5) changed in a wide range Table 4-16. Thus, it assets to note that the flow duration curve under future period changes in high flow (-43.1% to 14.7%, -38.3% to–22.2%, and -33.3% to -10.5 %,) under RCP4.5 and (-37.5% to 5.4, -30.6% to 2.3% and -49.4% –9.1%) under RCP8.5 in the 2030s, 2050s, and 2070s respectively. These changes show the frequency of the discharge and its magnitudes will decrease in all future periods. Therefore, proper utilization and management of the available discharge should be required to minimize the risk in the watershed as well as in the Basin.

Table 4-16.Percent future changes in high and low flows with respect to the baseline flow (1986–2005) under RCP 4.5 and RCP 8.5 scenarios in the Borkena watershed.

SCENARIO	RCM	Near –Term (2021-2040)		Mid Term (2041-2060)		Late Term (2061-2080)	
Probability		Q5	Q95	Q5	Q95	Q5	Q95
RCPs4.5	MPI	-43.1	-12.6	-34.7	-20.6	-33.3	-38.9
	IPSL	-24.9	-4.5	-22.2	-3.0	-10.5	-33.7
	MIROC5	14.7	-8.3	-38.3	+7.4	-28.7	-35.9
RCPs 8.5	MPI	-37.5	11.1	-14.2	-10.0	-14.7	-7.3
	IPSL	-36.6	-20.5	-38.6	-39.2	9.1	-13.6
	MIROC5	5.4	-35.0	+2.3	-8.7	-49.4	-36.3

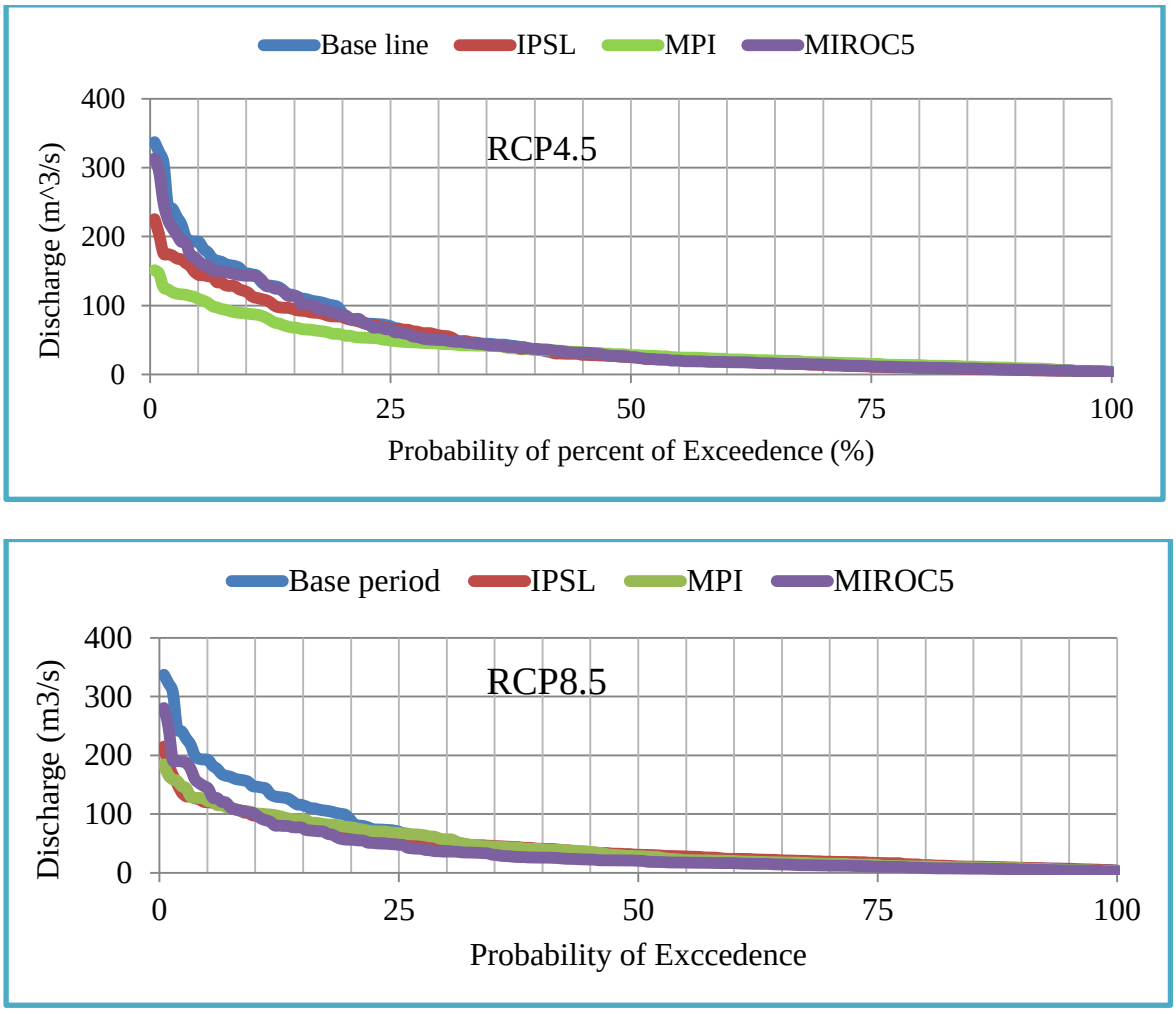

Figure 4-26.FDCs of the Borkena watershed for different climate models in the near term (2021-2041)

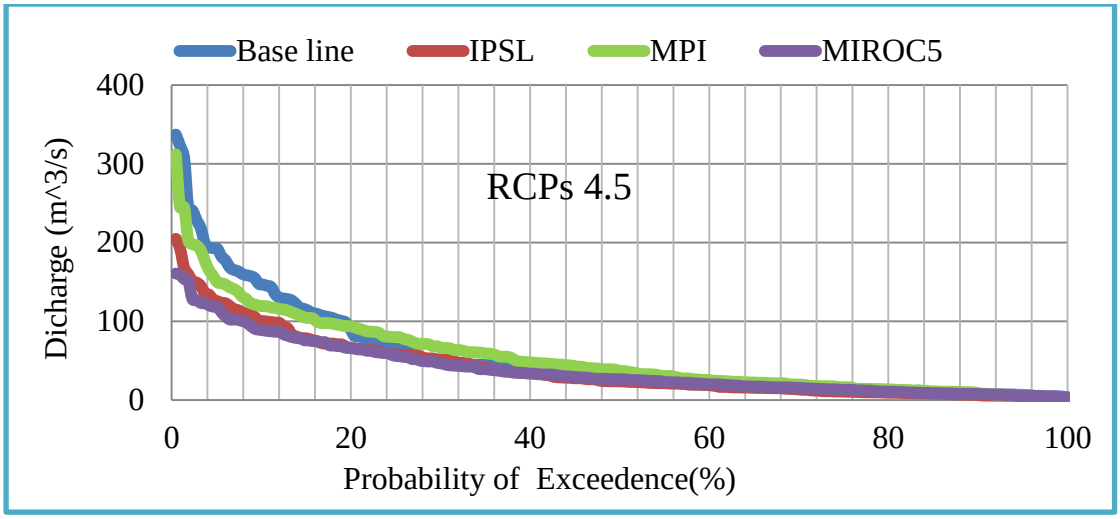

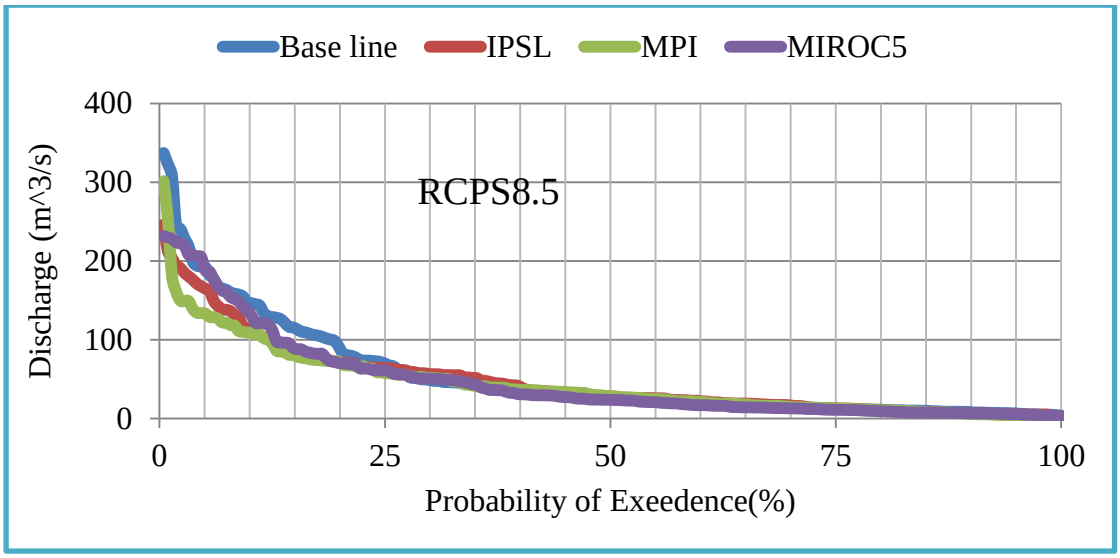

Figure 4-27.FDCs of the Borkena watershed for different climate models in the mid-term (2041-2060)

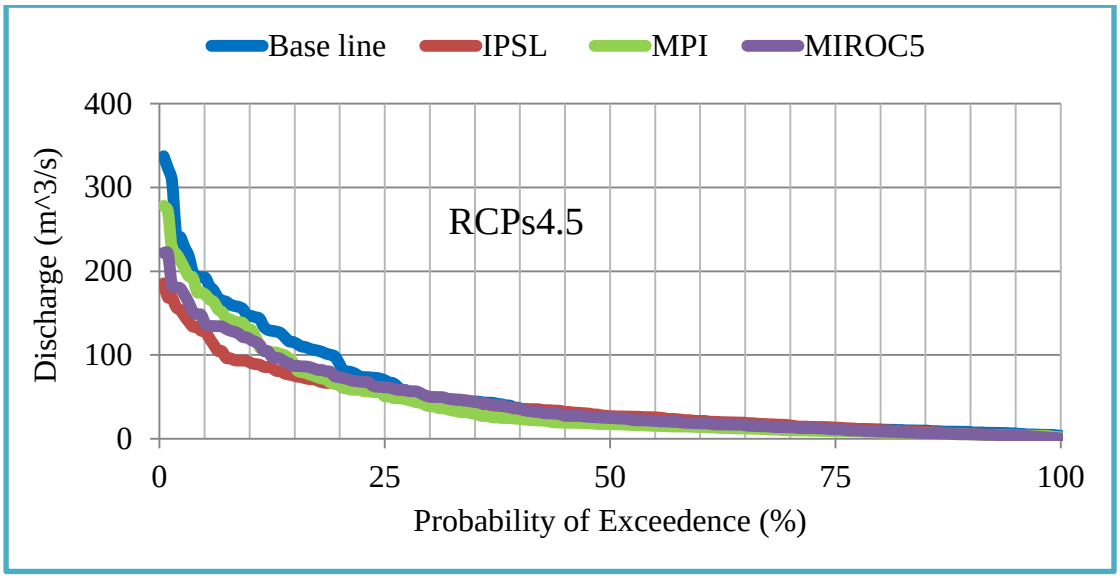

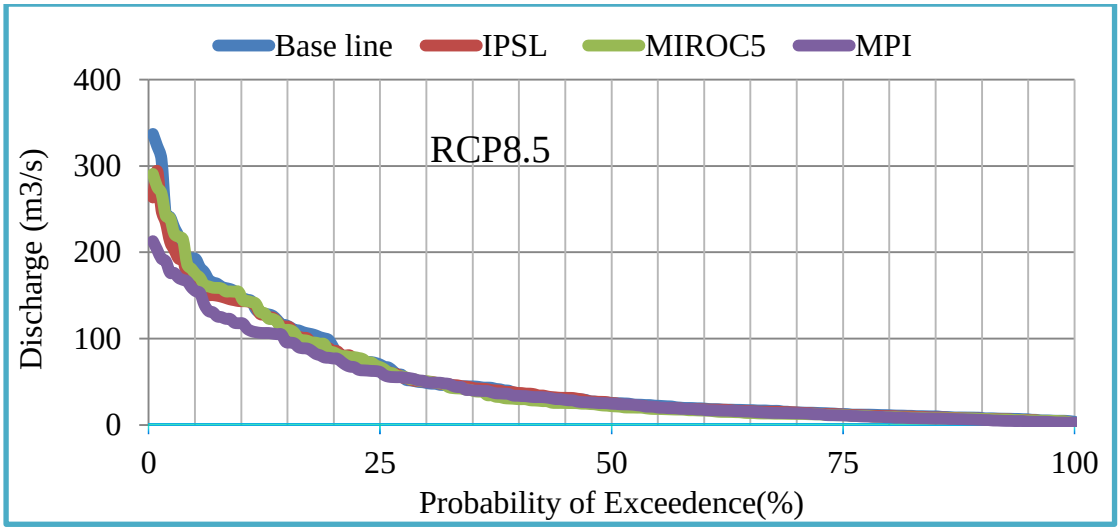

Figure 4-28.FDCs of the Borkena watershed for different climate models in the late-term (2061-2080)

4.7. Potential Evapotranspiration

The projected change in average monthly potential evapotranspiration indicated an increase for RCP4.5 and RCP8.5 for all RCMs except for some months in which the change slightly projected to decrease. For IPSL_RCM, the maximum change in potential evapotranspiration was observed in May (+7.2%, +8.1%, and +12.0%, in the 2030s, 2050s and 2070s for RCP8.5 respectively. Similarly, for RCP4.5 the change was observed in May (+4.2%, +8.2.3%, and +6.0%) in the 2030s, 2050s, and 2070s respectively.

The minimum evapotranspiration change was detected in December (-+1.2 %,), in 2030s, and in July (-0.8% and 2.8% in 2050s and 2070s for RCP8.5 respectively. In RCP4.5 the minimum change was observed in December (-1.3 %, and 0.8%) in 2050 and 2070s time horizons respectively. And the minimum change in 2030s was observed in July. Annually, the change of potential evapotranspiration increasingly projected to (1.8%, 2.1%, and 1.5%) in the 2030s, 2050s, and 2070s for RCP4.5. Similarly, for RCP8.5 the change was projected to (+1.9%, +1.7%, and +1.94 %.) in the 2030s, 2050s, and 2080s respectively.

For MIROC5_RCM, the maximum change in potential evapotranspiration was observed in June (1.4%, 0.5%, and 1.6%) in the 2030s, 2050s, and 2070s for RCP4.5 respectively. Similarly for RCP8.5 the change was observed in November (1.1%,) in the 2030s and (1.1%, and 0.8%) in 2050s and 2070s respectively. The minimum evapotranspiration

change was observed in April (-2.1%, 0.5%, and 0.0%) in 2030s, 2050s and 2070s for RCP4.5 respectively. In RCP8.5 the minimum change was observed in May in the near term in April for the other time windows. Annually, the change of potential evapotranspiration increasingly projected to (0.7%, 0.3%, and 0.4%) in 2030s, 2050s, and 2070s for RCP4.5. Similarly, for RCP8.5 the change was projected to (+0.3%, +0.4%, and +0.5 %.) in the 2030s, 2050s, and 2080s respectively

For MPI_RCM, the maximum change in potential evapotranspiration was observed in April (5.2%, 4.9%) in the 2030s, and 2050s respectively. And in October (2.0 %,) in the 2070s for RCP4.5.Similarly, for RCP8.5, the change was observed in June (2.7%, 3.0%) and in February (6.4%) in the 2030s, 2050s, and 2070s respectively. The minimum evapotranspiration change was observed in October (-1.2%, -0. 3.9%) in the 2030s and 2050s for RCP4.5 respectively.

In the 2070s the minimum change was observed in May (-5.3%) for RCP4.5. In RCP8.5 the minimum change was observed in October and May (-0.6%, -0.3%, and 2.2%) in the 2030s, 2050s, and 2070s respectively. Annually, the change of potential evapotranspiration increasingly projected to (1.2%, 1.1%, and 1.7%) in the 2030s, 2050s, and 2070s under RCP4.5. Likewise, under RCP8.5 the change was projected to (+0.8%, +1.1%, and +0.9 %.) in the 2030s, 2050s, and 2070s respectively. The projected average seasonal potential evapotranspiration also varies from season to season and it depends on the RCM concerned.

In most seasons the change was projected to increase under both emission scenarios. Generally, a positive and negative potential evaporation change was resulted in both seasonally and annually for all future time horizons as compared to the baseline period (Figure4.29). This was due to the uncertainty of temperature and rainfall such as increasing temperature and decreasing rainfall result the increase of evapotranspiration and vies versa. This also results in the uncertainty of runoff in the catchment.

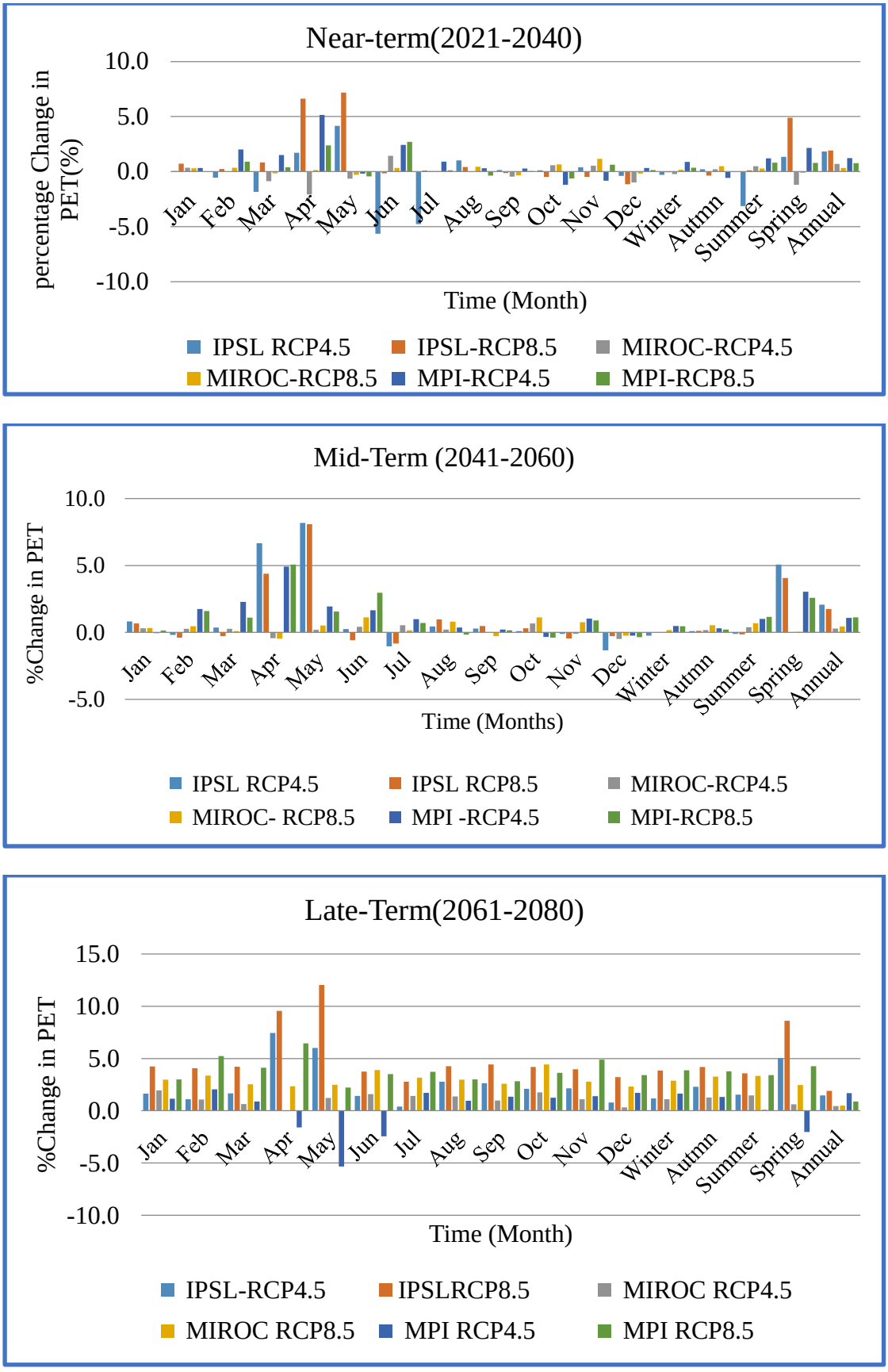

Figure 4-29.Percentage change in monthly and seasonal Potential Evapotranspiration

5. CONCLUSIONS AND RECOMMENDATIONS

5.1. Conclusions

This study evaluated the impacts of climate change on the extreme state of hydrology using the downscaled bias-corrected output of three regional climate models which were part of the Coupled Model Inter-comparison Project Phase 5 (CMIP5) with a physically based distributed hydrologic SWAT model.

Trend analysis of annual future rainfall pointed in positive directions. The trends were however statistically insignificant at the 5% level of significance. In this case the Mann Kendall test demonstrates that in the case of projected rainfall, no clear trend is noticeable and predictions of the three GCMs pointed out the temperature will increase while the change in rainfall is non-significant in the future.

We also evaluated the performance of dynamically downscaled regional climate models using a suite of performance measures such as Bias, RMSE, and correlation coefficient to assess performance of climate models to capture and represent in-situ based rainfall distributions in the watershed. The finding of the present study indicates that all the three (GCMs) show a good performance to capture rainfall and flow characteristics in the watershed as compared to the baseline .The result also suggests that climate change impact studies in Borkena watershed as well as Awash River Basin may profit from the use of simulated climate variables (rainfall and temperature) as obtained from such separate multiple climate models.

Climate change assessment in Borkena watershed showed a significant monthly and seasonal variation compared to annual changes against the base period. The results presented the fact that, climate change is highly uncertain as the results were varying widely with models, scenarios, and time frames. Almost consistent results were obtained on projected temperature changes with all GCMS. The maximum and minimum mean annual temperatures are projected to increase for all-time horizons with largest increments of 0.56°c and 0.31°c under RCP8.5 scenario respectively as compared to the base line period.

Therefore high temperatures may affect water availability and use in the watershed. This also indicates there would be higher demand of evapotranspiration in dry season which

additional water resource developments need to be planned for irrigation to sustain the already delicate food security of the country because of, the change in the mean annual rainfall is non-significant towards near, mid and late of the century. Similarly Seasonal and annual change in flow volume for Borkena River also expected in the coming decades. Likewise, the maximum flow reduction is also predicted during the near, mid and late century from all model outputs and approximately by 43.1% under RCP4.5 for MPI, 38.6% and 49.4% under RCP8.5 for IPSL and MIROC5 respectively.

Flow duration curves also showed that the probability of occurrence of high and low flows will be less in the future and are projected to decrease relative to the baseline flows. The overall conclusion of the study is that, the hydrologic component of the watershed is highly sensitive for both rainfall and temperature change such that the decrease the rainfall, warmer temperature and substantial reduction in volume of surface runoff and associated extreme peak flows over the coming decades. Hence the water resource management and planning in the Borkena watershed should address this phenomenon. Therefore, prevention and adaptation strategies in and around the watershed have to be developed so as to maintain sustainability of available water resources and to prevent extreme events.

5.2. Recommendations

From the results presented, the following recommendations are drawn

- The simulation results shown in this study are only acceptable under current land-use scenarios in the study region. Considering this, it is necessary to integrate the land cover change that is expected in the coming decades and thus associated impacts should be assessed and should be planned by taking different mitigation measurements and management practices.
- Even though the results presented in this work may change quantitatively, we do not expect them to change in the negative direction of this result. Therefore I recommend the incorporation of more RCMs (GCMs) and emission scenarios for the analyses of climate change impacts on Borkena watershed to improve confidence in the quantitative aspects as well.
- The bias correction technique and other GCM related uncertainty should be further examined. Hence, the results of this study should be taken with care and be considered as indicative of the likely future rather than accurate predictions.
- Sustainable and adaptive measures for future water resources management are required to ease tremendous pressure on the hydrological system of Borkena watershed due to increment of temperature and significant decrement in the hydrologic components, particularly the runoff and associated extreme peak flows over the coming decades.

6. REFERENCES

Abbaspour, Karim C. (2011). SWAT-CUP4:SWAT calibration and uncertainty programs–a user manual.Swiss Federal Institute of Aquatic Science and Technology, Eawag, 106.

Abbaspour, Karim C. (2013). SWAT-CUP 2012. SWAT Calibration and uncertainty program—a user manual.

Abtew, Wossenu, & Dessu, Shimelis Behailu. (2019). The Grand Ethiopian Renaissance Dam on the Blue Nile: Springer.

Ahmed, Syud Amer, Diffenbaugh, Noah S, Hertel, Thomas W, Lobell, David B, Ramankutty, Navin, Rios, Ana R, & Rowhani, Pedram. (2009). Climate volatility and poverty vulnerability in Tanzania: The World Bank.

Akhtar, Muhammad, Ahmad, Nasir, & Booij, Martijn J. (2008). The impact of climate change on the water resources of Hindukush–Karakorum–Himalaya region under different glacier coverage scenarios. Journal of hydrology, 355(1-4), 148-163.

Argüeso, D, Evans, JP, & Fita, L. (2013). Precipitation bias correction of very high resolution regional climate models. Hydrology and Earth System Sciences, 17(11), 4379.

Arnold, Jeffrey G, & Allen, P M. (1999). Automated methods for estimating baseflow and ground water recharge from streamflow records 1. JAWRA Journal of the American Water Resources Association, 35(2), 411-424.

Arnold, Jeffrey G, Moriasi, Daniel N, Gassman, Philip W, Abbaspour, Karim C, White, Michael J, Srinivasan, Raghavan, Van Liew, Michael W. (2012). SWAT: Model use, calibration, and validation. Transactions of the ASABE, 55(4), 1491-1508.

Balint Jr, Joseph P, & Hargreaves, Richard E. (1987). Protein A-silica immunoadsorbent and process for its production: Google Patents.

Barker, Terry, Davidson, Ogunlade, Davidson, William, Huq, Saleemul, Karoly, David, Kattsov, Vladimir, . . . Matsuno, Taroh. (2007). Climate change 2007: Synthesis report. Valencia; IPPC.

Barlow, Jay, Calambokidis, John, Falcone, Erin A, Baker, C Scott, Burdin, Alexander M, Clapham, Phillip J, Mattila, David K. (2011). Humpback whale abundance in the North Pacific estimated by photographic capture-recapture with bias correction from simulation studies. Marine Mammal Science, 27(4), 793-818.

Bekele, Daniel, Alamirew, Tena, Kebede, Asfaw, Zeleke, Gete, & Melesse, Assefa M. (2019). Modeling climate change impact on the Hydrology of Keleta watershed in the Awash River basin, Ethiopia. Environmental Modeling & Assessment, 24(1), 95-107.

Boberg, Fredrik, & Christensen, Jens H. (2012). Overestimation of Mediterranean summer temperature projections due to model deficiencies. Nature Climate Change, 2(6), 433-436.

Bogner, Jean, Pipatti, Riitta, Hashimoto, Seiji, Diaz, Cristobal, Mareckova, Katarina, Diaz, Luis, Research. (2008). Mitigation of global greenhouse gas emissions from waste: conclusions and strategies from the Intergovernmental Panel on Climate Change (IPCC) Fourth Assessment Report. Working Group III (Mitigation). 26(1), 11-32.

Bryan, E, Deressa, T, Gbetibouo, G, & Ringler, G. (2009). Adaptation to climate change in Ethiopia and South Africa: options and constraints, environmental science and policy.

Budinger, William D, & Jensen, Elmer W. (1990). Pad material for grinding, lapping and polishing: Google Patents.

Carter, T. R. (2007). General Guidelines on the use of scenario data for Climate Impact and Adaptation Assessment, Finnish Environmental Institute, Helsinki, Finland.

Chekol, Dilnesaw A, Tischbein, Bernhard, Eggers, Helmut, & Vlek, Paul. (2007). Application of SWAT for assessment of spatial distribution of water resources and analyzing impact of different land management practices on soil erosion in Upper Awash River Basin watershed. Catchment and Lake Research, 110-117.

Daba, Mekonnen H. (2018). Modelling the Impacts of Climate Change on Surface Runoff in Finchaa Sub-basin, Ethiopia. J. Sci. Food Agric, 2, 14-29.

Dahmen, ER, & Hall, Michael John. (1990). Screening of hydrological data: tests for stationarity and relative consistency: ILRI.

Data, Climate. (2009). Guidelines on analysis of extremes in a changing climate in support of informed decisions for adaptation. World Meteorological Organization.

Dile, Yihun Taddele, Berndtsson, Ronny, & Setegn, Shimelis G. (2013). Hydrological response to climate change for gilgel abay river, in the lake tana basin-upper blue Nile basin of Ethiopia. PloS one, 8(10).

Drápela, Karel, & Drápelová, Ida. (2011). Application of Mann-Kendall test and the Sen's slope estimates for trend detection in deposition data from Bílý Kříž (Beskydy Mts., the Czech Republic) 1997-2010. Beskydy, 4(2), 133-146.

Edossa, Desalegn Chemeda, Babel, Mukand Singh, & Gupta, Ashim Das. (2010). Drought analysis in the Awash River Basin, Ethiopia. Water resources management, 24(7), 1441-1460.

Ehret, Uwe, Zehe, Erwin, Wulfmeyer, V, Warrach-Sagi, K, & Liebert, J. (2012). HESS Opinions" Should we apply bias correction to global and regional climate model data?". Hydrology & Earth System Sciences Discussions, 9(4).

Feser, Frauke, Rockel, Burkhardt, von Storch, Hans, Winterfeldt, Jörg, & Zahn, Matthias. (2011). Regional climate models add value to global model data: a review and selected examples. Bulletin of the American Meteorological Society, 92(9), 1181-1192.

Firat, Mahmut, Dikbas, Fatih, Koç, A Cem, & Gungor, Mahmud. (2010). Missing data analysis and homogeneity test for Turkish precipitation series. Sadhana, 35(6), 707.

Flato, Gregory, Marotzke, Jochem, Abiodun, B, Braconnot, P, Chou, SC, Collins, W, Eyring, V. (2013). Climate change 2013: the physical science basis. Contribution of Working Group I to the Fifth Assessment Report of the Intergovernmental Panel on Climate Change. Evaluation of Climate Models, eds TF Stocker, D. Qin, G.-K. Plattner, M. Tignor, SK Allen, J. Boschung, et al.(Cambridge: Cambridge University Press).

Gassman, Philip W, Reyes, Manuel R, Green, Colleen H, & Arnold, Jeffrey G. (2007). The soil and water assessment tool: historical development, applications, and future research directions. Transactions of the ASABE, 50(4), 1211-1250.

Getahun, Yitea Seneshaw, & Lanen, H. (2016). Impact of Climate Change on Hydrology of the Upper Awash River Basin (Ethiopia): Inter-Comparison of Old SRES and New RCP Scenarios. Master's Thesis, Wageningen University, Wageningen, The Netherlands, 2016

Giorgi, Filippo, Jones, Colin, & Asrar, Ghassem R. (2009). Addressing climate information needs at the regional level: the CORDEX framework. World Meteorological Organization (WMO) Bulletin, 58(3), 175.

Gómez-Rubio, Virgilio, Cameletti, Michela, & Blangiardo, Marta. (2019). Missing data analysis and imputation via latent Gaussian Markov random fields. arXiv preprint arXiv:1912.10981.

Gordon, Neil David, & Shaykewich, Joseph. (2000). Guidelines on performance assessment of public weather services: World Meteorological Organization.

Graham, L Phil, Andréasson, Johan, & Carlsson, Bengt. (2007). Assessing climate change impacts on hydrology from an ensemble of regional climate models, model scales and linking methods–a case study on the Lule River basin. Climatic Change, 81(1), 293-307.

Graham, L Phil, Andréasson, Johan, & Carlsson, Bengt %J Climatic Change. (2007). Assessing climate change impacts on hydrology from an ensemble of regional climate models, model scales and linking methods–a case study on the Lule River basin. 81(1), 293-307.

Gustafson Jr, William I, & Leung, L Ruby. (2007). Regional downscaling for air quality assessment: A reasonable proposition? Bulletin of the American Meteorological Society, 88(8), 1215-1228.

Hailemariam, Kinfe. (1999). Impact of climate change on the water resources of Awash River Basin, Ethiopia. Climate Research, 12(2-3), 91-96.

Harmel, R Daren, Smith, Patricia K, & Migliaccio, Kati W. (2010). Modifying goodness-of-fit indicators to incorporate both measurement and model uncertainty in model calibration and validation. Transactions of the ASABE, 53(1), 55-63.

Hatfield, JL, & Allen, RG. (1996). Evapotranspiration estimates under deficient water supplies. Journal of irrigation and drainage engineering, 122(5), 301-308.

Hemel, Ronald, & Loijenga, H. (2013). Set up of a water governance program in the Awash river basin, central Ethiopia: Assessment of water governance capacity in the Awash river basin. Report, Water Governance Centre.

Hempel, Sabrina, Frieler, Katja, Warszawski, Lila, Schewe, Jacob, & Piontek, Franziska. (2013). A trend-preserving bias correction–the ISI-MIP approach.

Hirt, Christian. (2016). Digital terrain models.

Houghton, John T, Meira Filho, L Gylvan, Griggs, David J, & Maskell, Kathy. (1997). An introduction to simple climate models used in the IPCC Second Assessment Report: WMO.

IPCC, Climate Change. (2007). The physical science basis. Contribution of working group I to the fourth assessment report of the Intergovernmental Panel on Climate Change. Cambridge University Press, Cambridge, United Kingdom and New York, NY, USA, 996, 2007.

IPPC, Intergovernmental Panel On Climate Change. (2007). Climate change 2007: synthesis report (pp. 104): IPCC Geneva.

Irannezhad, M, Chen, Deliang, & Kløve, B. (2015). Interannual variations and trends in surface air temperature in Finland in relation to atmospheric circulation patterns, 1961–2011. International Journal of Climatology, 35(10), 3078-3092.

Jakob Themeßl, Matthias, Gobiet, Andreas, & Leuprecht, Armin. (2011). Empirical-statistical downscaling and error correction of daily precipitation from regional climate models. International Journal of Climatology, 31(10), 1530-1544.

James, LD, & Burges, SJ. (1982). Precipitation-runoff modeling: Future directions. Applied modeling in catchment hydrology, 291-312.

Jones, Peter G, Thornton, Philip K, & Heinke, Jens. (2009). Generating characteristic daily weather data using downscaled climate model data from the IPCC's Fourth Assessment.

Kim, J, Waliser, Duane E, Mattmann, Chris A, Goodale, Cameron E, Hart, Andrew F, Zimdars, Paul A, Hewitson, Bruce. (2014). Evaluation of the CORDEX-Africa multi-RCM hindcast: systematic model errors. Climate dynamics, 42(5-6), 1189-1202.

Kumar, Pankaj, Kotlarski, Sven, Moseley, Christopher, Sieck, Kevin, Frey, Holger, Stoffel, Markus, & Jacob, Daniela. (2015). Response of Karakoram-Himalayan glaciers to climate variability and climatic change: A regional climate model assessment. Geophysical Research Letters, 42(6), 1818-1825.

Li, Tianjing, Vedula, S Swaroop, Hadar, Nira, Parkin, Christopher, Lau, Joseph, & Dickersin, Kay. (2015). Innovations in data collection, management, and archiving for systematic reviews. Annals of internal medicine, 162(4), 287-294.

Liersch, Stefan, Tecklenburg, Julia, Rust, Henning, Dobler, Andreas, Fischer, Madlen, Kruschke, Tim, Hattermann, Fred Fokko. (2018). Are we using the right fuel to drive hydrological models? A climate impact study in the Upper Blue Nile. Hydrology and Earth System Sciences, 22, 2163-2185.

Mamalakis, Antonios, Langousis, Andreas, Deidda, Roberto, & Marrocu, Marino. (2017). A parametric approach for simultaneous bias correction and high-resolution downscaling of climate model rainfall. Water Resources Research, 53(3), 2149-2170.

Masui, Toshihiko, Matsumoto, Kenichi, Hijioka, Yasuaki, Kinoshita, Tsuguki, Nozawa, Toru, Ishiwatari, Sawako, Kainuma, Mikiko. (2011). An emission pathway for stabilization at 6 Wm-2 radiative forcing. Climatic change, 109(1-2), 59.

Maurer, EP, Ficklin, DL, & Wang, W. (2015). The impact of spatial scale in bias correction of climate model output for hydrologic impact studies. Hydrology & Earth System Sciences Discussions, 12(10).

McPherson, Michelle, García-García, Almudena, Cuesta-Valero, Francisco José, Beltrami, Hugo, Hansen-Ketchum, Patti, MacDougall, Donna, & Ogden, Nicholas Hume. (2017). Expansion of the Lyme disease vector Ixodes scapularis in Canada inferred from CMIP5 climate projections. Environmental Health Perspectives, 125(5), 057008.

Mearns, LO, Giorgi, F, Whetton, P, Pabon, D, Hulme, M, & Lal, M. (2003). Guidelines for use of climate scenarios developed from regional climate model experiments.

Meinshausen, M, Smith, SJ, Calvin, K, Daniel, JS, Kainuma, MLT, Lamarque, JF, . . . Riahi, K. (2011). The paleoclimate modeling intercomparison project contribution to CMIP5. WCRP Coupled Model Intercomparison Project-Phase 5-CMIP5, 15.

Moriasi, Daniel N, Arnold, Jeffrey G, Van Liew, Michael W, Bingner, Ronald L, Harmel, R Daren, & Veith, Tamie L. (2007). Model evaluation guidelines for systematic quantification of accuracy in watershed simulations. Transactions of the ASABE, 50(3), 885-900.

Motiee, Homayoun, & McBean, Edward. (2009). An assessment of long-term trends in hydrologic components and implications for water levels in Lake Superior. Hydrology Research, 40(6), 564-579.

Musau, J, Sang, J, Gathenya, J, & Luedeling, Eike. (2015). Hydrological responses to climate change in Mt. Elgon watersheds. Journal of Hydrology: Regional Studies, 3, 233-246.

Najafi, Mohammad Reza, & Moradkhani, Hamid. (2015). Multi-model ensemble analysis of runoff extremes for climate change impact assessments. Journal of Hydrology, 525, 352-361.

Navarro-Racines, Carlos E, & Tarapues, JE. (2015). Bias-correction in the CCAFS-Climate Portal: A description of methodologies.

Neitsch, SL, Arnold, JG, Kiniry, JR, Srinivasan, R, & Williams, JR. (2002). Soil and water assessment tool user's manual version 2000. GSWRL report, 202(02-06).

Neitsch, SL, Arnold, JG, Kiniry, JR, Williams, JR, & King, KW. (2001). SWAT: Soil and water assessment tool theoretical documentation. Temple, TX: USDA Agricultural Research Service.

Penner, Joyce E, Lister, DH, Griggs, DJ, Dokken, DJ, & McFarland, Mack %J Intergovernmental panel on climate change, Geneva, Switzerland. (1999). IPCC special report on aviation and the global atmosphere.

Piani, C, Haerter, JO, & Coppola, E. (2010). Statistical bias correction for daily precipitation in regional climate models over Europe. Theoretical and Applied Climatology, 99(1-2), 187-192.

Pielke Sr, Roger A, & Wilby, Robert L. (2012). Regional climate downscaling: What's the point? Eos, Transactions American Geophysical Union, 93(5), 52-53.

Price-Williams, Douglass Richard. (1969). Cross-cultural studies: selected readings (Vol. 20): Penguin Books.

Priestley, Charles Henry Brian, & Taylor, RJ. (1972). On the assessment of surface heat flux and evaporation using large-scale parameters. Monthly weather review, 100(2), 81-92.

Ramírez Villegas, Julian, & Jarvis, Andy. (2010). Downscaling global circulation model outputs: the delta method decision and policy analysis Working Paper No. 1.

Riahi, Keywan, Rao, Shilpa, Krey, Volker, Cho, Cheolhung, Chirkov, Vadim, Fischer, Guenther,Rafaj, Peter. (2011). RCP 8.5—A scenario of comparatively high greenhouse gas emissions. Climatic change, 109(1-2), 33.

Riggs, Henry C. (1985). Streamflow characteristics: Elsevier.

Rosenzweig, Cynthia, & Hillel, Daniel. (2008). Climate variability and the global harvest: Impacts of El Niño and other oscillations on agro-ecosystems: Oxford University Press.

Sahele, M. (2001). Hydrogeological investigation of the upper and middle borkena rivercatchment thesis. Addis Ababa: Addis Ababa university

Samuelsson, Patrick, Jones, Colin G, Will´ En, Ulrika, Ullerstig, Anders, Gollvik, Stefan, Hansson, ULF, Wyser, Klaus. (2011). The Rossby Centre Regional Climate model RCA3: model description and performance. Tellus A: Dynamic Meteorology and Oceanography, 63(1), 4-23.

Sanderson, Marie. (1948). The climates of Canada according to the new Thornthwaite classification. Scientific Agriculture, 28(11), 501-517.

Schmidli, Jürg, Frei, Christoph, & Vidale, Pier Luigi. (2006). Downscaling from GCM precipitation: a benchmark for dynamical and statistical downscaling methods. International Journal of Climatology: A Journal of the Royal Meteorological Society, 26(5), 679-689.

Sevruk, B, Ondrás, M, & Chvíla, B. (2009). The WMO precipitation measurement intercomparisons. Atmospheric Research, 92(3), 376-380.

Shiklomanov, Alexander I, Lammers, Richard B, Lettenmaier, Dennis P, Polischuk, Yuriy M, Savichev, Oleg G, Smith, Laurence C, & Chernokulsky, Alexander V. (2013). Hydrological changes: historical analysis, contemporary status, and future projections Regional environmental changes in siberia and their global consequences (pp. 111-154): Springer.

Singh, Pratap, & Kumar, Naresh %J Journal of Hydrology. (1997). Effect of orography on precipitation in the western Himalayan region. 199(1-2), 183-206.

Sinha, Tushar, & Cherkauer, Keith A. (2008). Time series analysis of soil freeze and thaw processes in Indiana. Journal of hydrometeorology, 9(5), 936-950.

Smakhtin, Vladimir U. (2001). Low flow hydrology: a review. Journal of hydrology, 240(3-4), 147-186.

Strauch, Michael, Bernhofer, Christian, Koide, Sérgio, Volk, Martin, Lorz, Carsten, & Makeschin, Franz. (2012). Using precipitation data ensemble for uncertainty analysis in SWAT streamflow simulation. Journal of Hydrology, 414, 413-424.

Sui, Qian, Huang, Jun, Deng, Shubo, Yu, Gang, & Fan, Qing %J Water research. (2010). Occurrence and removal of pharmaceuticals, caffeine and DEET in wastewater treatment plants of Beijing, China. 44(2), 417-426.

Sun, Shanlei, Sun, Ge, Mack, Erika Cohen, McNulty, Steve, Caldwell, Peter V, Duan, Kai, & Zhang, Yang. (2016). Projecting water yield and ecosystem productivity across the United States by linking an ecohydrological model to WRF dynamically downscaled climate data. Hydrology and Earth System Sciences, 20(2), 935-952.

Tabari, Hossein, Marofi, Safar, Aeini, Ali, Talaee, Parisa Hosseinzadeh, & Mohammadi, Kurosh. (2011). Trend analysis of reference evapotranspiration in the western half of Iran. Agricultural and forest meteorology, 151(2), 128-136.

Taye, Meron, Dyer, Ellen, Hirpa, Feyera, & Charles, Katrina. (2018). Climate Change Impact on Water Resources in the Awash Basin, Ethiopia. Water, 10(11), 1560. doi: 10.3390/w10111560

Teutschbein, Claudia, & Seibert, Jan. (2012). Bias correction of regional climate model simulations for hydrological climate-change impact studies: Review and evaluation of different methods. Journal of hydrology, 456, 12-29.

Thomson, Allison M, Calvin, Katherine V, Smith, Steven J, Kyle, G Page, Volke, April, Patel, Pralit, Clarke, Leon E. (2011). RCP4. 5: a pathway for stabilization of radiative forcing by 2100. Climatic change, 109(1-2), 77.

Tibebe, Mahtsente, Melesse, Assefa M, & Zemadim, Birhanu. (2016). Runoff estimation and water demand analysis for Holetta River, Awash Subbasin, Ethiopia using SWAT and CropWat models Landscape Dynamics, Soils and Hydrological Processes in Varied Climates (pp. 113-140): Springer.

Turco, Marco, Quintana-Seguí, Pere, Llasat, MC, Herrera, S, & Gutiérrez, José M. (2011). Testing MOS precipitation downscaling for ENSEMBLES regional climate models over Spain. Journal of Geophysical Research: Atmospheres, 116(D18).

van Griensven, A van, Meixner, Thomas, Grunwald, S, Bishop, T, Diluzio, M, & Srinivasan, R. (2006). A global sensitivity analysis tool for the parameters of multi-variable catchment models. Journal of hydrology, 324(1-4), 10-23.

Van Vuuren, Detlef P, Edmonds, Jae, Kainuma, Mikiko, Riahi, Keywan, Thomson, Allison, Hibbard, Kathy, Lamarque, Jean-Francois. (2011). The representative concentration pathways: an overview. Climatic change, 109(1-2), 5.

Van Vuuren, Detlef P, Kriegler, Elmar, O'Neill, Brian C, Ebi, Kristie L, Riahi, Keywan, Carter, Timothy R, Mathur, Ritu. (2014). A new scenario framework for climate change research: scenario matrix architecture. Climatic Change, 122(3), 373-386.

Van Vuuren, Detlef P, Stehfest, Elke, den Elzen, Michel GJ, Kram, Tom, van Vliet, Jasper, Deetman, Sebastiaan, Beltran, Angelica Mendoza. (2011). RCP2. 6: exploring the possibility to keep global mean temperature increase below 2 C. Climatic change, 109(1-2), 95.

Vermeer, Martin, & Rahmstorf, Stefan. (2009). Global sea level linked to global temperature. Proceedings of the national academy of sciences, 106(51), 21527-21532.

Vogel, Richard M, & Fennessey, Neil M. (1994). Flow-duration curves. I: New interpretation and confidence intervals. Journal of Water Resources Planning and Management, 120(4), 485-504.

Wang, Dingbao, Hejazi, Mohamad, Cai, Ximing, & Valocchi, Albert J. (2011). Climate change impact on meteorological, agricultural, and hydrological drought in central Illinois. Water Resources Research, 47(9).

Watanabe, Satoshi, Kanae, Shinjiro, Seto, Shinta, Yeh, Pat J-F, Hirabayashi, Yukiko, & Oki, Taikan. (2012). Intercomparison of bias-correction methods for monthly temperature and precipitation simulated by multiple climate models. Journal of Geophysical Research: Atmospheres, 117(D23).

Water, UN. (2015). Wastewater Management: A UN-Water Analytical Brief. New York.

Whitehead, Paul G, Wilby, Robert L, Battarbee, Richard W, Kernan, Martin, & Wade, Andrew John. (2009). A review of the potential impacts of climate change on surface water quality. Hydrological Sciences Journal, 54(1), 101-123.

Wilby, Robert L, Charles, SP, Zorita, Eduardo, Timbal, Bertrand, Whetton, Penny, & Mearns, LO. (2004). Guidelines for use of climate scenarios developed from statistical downscaling methods. Supporting material of the Intergovernmental Panel on Climate Change, available from the DDC of IPCC TGCIA, 27, -.

Wilby, Robert L, & Dawson, Christian W. (2013). The statistical downscaling model: insights from one decade of application. International Journal of Climatology, 33(7), 1707-1719.

Yang, Jing, Reichert, Peter, Abbaspour, Karim C, Xia, Jun, & Yang, Hong. (2008). Comparing uncertainty analysis techniques for a SWAT application to the Chaohe Basin in China. Journal of Hydrology, 358(1-2), 1-23.

Yılmaz, Fatma. (2008). Avrupa'da Irkçılık ve Yabancı Düşmanlığı (Vol. 6): International Strategic Research Organization (USAK).

You, Gene Jiing-Yun, & Ringler, Claudia. (2010). Hydro-economic modeling of climate change impacts in Ethiopia: International Food Policy Research Institute (IFPRI).

Zafar, Muhammad Usama, Ahmed, Moinuddin, Rao, Mukund Palat, Buckley, Brendan M, Khan, Nasrullah, Wahab, Muhammad, & Palmer, Jonathan. (2016). Karakorum temperature out of phase with hemispheric trends for the past five centuries. Climate Dynamics, 46(5-6), 1943-1952.

Zhang, Qiang, Xu, Chong-Yu, Chen, Xiaohong, & Zhang, Zengxin. (2011). Statistical behaviours of precipitation regimes in China and their links with atmospheric circulation 1960–2005. International Journal of Climatology, 31(11), 1665-1678.

7. APPENDIX

Appendix A: Annual observed rainfall in Borkena watershed

Year	Dessie	Chefa	kombolcha	Harbu	kemis	Majetie
1986	1251.5	824.0	1094.0	1114.7	1144.1	1010.9
1987	1020.4	1138.9	811.6	1070.8	829.8	1086.3
1988	1348.4	1110.7	1194.8	1189.6	1131.4	1214.4
1989	953.4	976.9	1169.2	1207.4	901.3	1152.8
1990	933.2	1002.3	893.3	561.5	671.6	1025.2
1991	1171.8	898.0	823.8	882.2	695.0	1003.3
1992	1253.8	1171.1	1054.5	814.3	616.3	1130.7
1993	1458.7	1110.8	1317.0	981.9	1128.1	1171.2
1994	1314.3	1407.9	1201.1	1210.7	1122.9	1014.8
1995	1435.2	830.7	1128.3	795.1	1399.5	1390.8
1996	1533.3	1024.6	1167.1	1200.0	1455.7	1356.4
1997	1242.7	1242.7	1048.0	911.2	1328.4	1289.6
1998	1646.3	995.4	1377.8	680.1	1137.2	1516.7
1999	1378.9	1101.8	1059.9	502.9	1209.0	1620.4
2000	1375.3	1208.0	1223.7	852.1	1240.9	1226.3
2001	1263.1	1229.4	1009.4	1642.7	1016.5	1151.7
2002	1289.4	739.4	908.5	1297.6	1074.9	1171.1
2003	1226.5	1176.5	1023.4	1142.4	919.9	1067.3
2004	1001.6	1104.0	943.4	818.9	1112.1	1093.6
2005	1349.5	1227.1	1061.1	1052.2	932.5	1156.5

Appendix B: Parameters considered for sensitive analysis in global sensitivity analysis

Hydrological Parameters	Description	min value	Max-value
r__CN2.mgt	Initial Curve No. at Moisture Condition II	-0.25	0.25
v__ALPHA_BF.gw	Base flow alpha fact	0	1

v__ALPHA_BNK.rte	Baseflow alpha factor for bank storage	0	1
v__GW_DELAY.gw	Groundwater delay	0	500
v__GWQMN.gw	Threshold depth of water in the shallow aquifer	0	2
v__SURLAG.bsn	Surface runoff lag time	2.24	16.78
v__GW_REVAP.gw	Groundwater ‘’revap’’ coefficient	0.02	0.2
v__REVAPMN.gw	Threshold water depth in the shallow aquifer	0	1
v__RCHRG_DP.gw	Deep aquifer percolation fraction	0	1
r__SLSUBBSN.hru	Average slope length	-0.25	0.25
v__LAT_TTIME.hru	Lateral flow travel time	0.25	120.3
v__ESCO.hru	Soil evaporation compensation	0	1
r__CANMX.hru	Maximum canopy storage	0	10
r__CH_K2.rte	Channel effective hydraulic conductivity	0	150
r__CH_N2.rte	Manning’s roughness value for the main channel	0	1
r__EPCO.hru	Plant uptake compensation factor	0	1
r__SOL_Z(..).sol	Soil depth	-0.25	0.25
r__SOL_AWC (..).sol	Available water capacity	-0.25	0.25
r__SOL_K(..).sol	Saturated hydraulic conductivity	-0.25	0.25
r__SOL_ALB (..).sol	Moisture soil albedo	-0.25	0.25
r__TLAPS.sub	Temperature lapse rate	0	50
r__OV_N.hru	Manning's "n" value for overland flow	0.01	30

Appendix C: Rank of sensitive Parameters using global sensitivity analysis

S\NO	Parameter Name	t-Stat	P-Value
1	19:R__SOL_ALB (..).sol	0.068425506	0.945475652
2	5:V__SURLAG.bsn	0.246021528	0.805771617
3	7:V__REVAPMN.gw	0.277455408	0.781550900
4	9:R__SLSUBBSN.hru	0.403837746	0.686513400
5	12:R__CANMX.hru	-0.439728704	0.660333187
6	18:R__SOL_K(..).sol	0.449627988	0.653183374
7	15:R__EPCO.hru	-0.624366116	0.532686305
8	20:R__TLAPS.sub	-0.876256737	0.381332462
9	13:R__CH_K2.rte	1.043795815	0.297109671

10	22:V__ALPHA_BNK.rte	-1.152791248	0.249574656
11	8:V__RCHRG_DP.gw	1.160796139	0.246306630
12	4:V__GWQMN.gw	-1.276854008	0.202276322
13	16:R__SOL_Z(..).sol	1.423039063	0.155379884
14	2:V__ALPHA_BF.gw	1.738754207	0.082724557
15	21:R__OV_N.hru	2.197099049	0.028494563
16	6:V__GW_REVAP.gw	2.675325085	0.007722868
17	3:V__GW_DELAY.gw	2.854684527	0.004495992
18	14:R__CH_N2.rte	2.892612079	0.003995586
19	17:R__SOL_AWC (..).sol	3.879835054	0.000119252
20	11:V__ESCO.hru	-6.315733055	0.000000001
21	10:V__LAT_TTIME.hru	7.777563205	0.000000000
22	1:R__CN2.mgt	-36.96959733	0.000000000

APPENDIX D: Monthly Projected stream flow (m3/s) for the future three time horizons (2030s, 2050, and 2070)

year	2030.00					
RCM	IPSL		MIROC5		MPI	
Month	RCP4.5	RCP8.5	RCP4.5	RCP8.5	RCP4.5	RCP8.5
Jan	18.0	19.6	-14.8	32.6	-2.7	-6.9
Feb	-24.0	14.3	-1.8	-0.4	91.8	32.2
Mar	-40.0	-14.9	56.3	67.9	-18.4	-44.3
Apr	18.5	15.0	-13.3	-18.3	7.2	0.3
May	57.0	74.4	38.5	28.6	-6.2	-37.2
Jun	45.0	46.7	-31.9	-8.4	-7.2	-30.3
Jul	-42.3	-22.8	71.7	23.3	-52.8	-59.8
Aug	-48.0	-22.6	42.0	45.7	-15.9	-26.7
Sep	-22.4	5.8	47.2	21.9	-7.4	-5.8
Oct	-6.4	23.2	31.2	20.6	19.6	-8.6
Nov	38.2	19.5	-1.4	2.6	-1.7	-3.2
Dec	17.1	2.0	-36.0	-8.6	1.5	-25.4
Year	2050.00					
RCM	IPSL		MIROC5		MPI	
Month	RCP4.5	RCP8.5	RCP4.5	RCP8.5	RCP4.5	RCP8.5

Jan	0.0	49.2	21.7	21.1	27.3	51.3
Feb	-10.0	-24.9	-1.1	7.2	0.7	93.4
Mar	9.9	-54.7	-27.6	90.5	-55.6	-36.6
Apr	82.8	10.6	-25.5	27.7	15.4	-16.5
May	46.9	93.8	20.6	37.3	-34.6	-32.0
Jun	72.8	77.8	-7.6	3.7	-28.3	-25.0
Jul	21.0	21.0	65.9	71.7	-53.6	-45.3
Aug	4.2	-8.0	41.2	103.2	-29.4	-22.5
Sep	37.4	2.6	72.8	70.5	-23.5	-16.4
Oct	79.2	-2.3	59.2	86.7	-2.4	10.3
Nov	40.5	34.2	24.2	35.2	-5.2	48.0
Dec	63.9	-2.5	-2.7	37.0	4.9	21.7

Year	2070.00					
RCM	IPSL		MIROC5		MPI	
Month	RCP4.5	RCP8.5	RCP4.5	RCP8.52	RCP4.5	RCP8.5
Jan	19.1	94.1	25.5	12.1	7.7	7.3
Feb	-18.4	-6.0	-14.4	-23.2	19.1	61.1
Mar	-48.0	-12.2	4.0	19.7	-39.4	-43.8
Apr	-48.0	54.7	-6.2	39.7	4.4	-59.3
May	88.2	79.7	19.8	38.6	-22.3	-37.5
Jun	91.4	132.2	-16.2	4.4	-15.3	-30.5
Jul	9.1	62.3	99.4	76.6	-54.7	-54.9
Aug	-20.3	10.6	97.6	49.7	-29.3	-19.6
Sep	-19.4	23.6	94.5	58.9	-13.7	-13.8
Oct	13.8	82.3	45.1	49.5	9.7	26.1
Nov	90.2	83.6	17.0	38.2	58.9	34.7
Dec	17.4	83.6	-11.0	-6.7	32.2	10.5

Appendix E: Annually projected maximum stream flow (m3/s) for the future three-time horizons (2030s, 2050, and 2070)

2030s						
RCM	RCA4(IPSL)		RCA4(MIROC5)		RCA4(MPI)	
Senario	RCP4.5	RCP8.5	RCP4.5	RCP8.5	RCP4.5	RCP8.5
2021	57.1	89.3	126.9	110.5	69.7	59.2
2022	61.2	97.2	126.5	124.5	73.1	61.3
2023	31.16	97.81	90.4	79.37	58.59	28.52
2024	46.09	50.62	144.6	94.11	89.13	73.37
2025	34.77	117.2	189.3	184.2	93.94	63.94

2026	48.03	90.88	43.01	152.1	54.14	43.41
2027	61.57	97.56	128.6	59.03	72.95	99.96
2028	100.9	81.77	97.54	38.64	48.53	56.38
2029	36.58	49.99	159.2	65.12	75.77	38.5
2030	97.99	128.6	162.4	211.7	64.64	69.13
2031	63.6	160.9	87.41	191.2	85.82	45.48
2032	35.98	113.1	157.5	221.6	70.41	116
2033	92.16	90.72	133.3	174.9	97.38	59.43
2034	147.7	93.25	330.8	120.6	75.82	120.6
2035	57.46	87.57	187.8	333.6	59.26	65.77
2036	56.78	79.1	145.6	118.5	52.7	77.68
2037	43.34	93.38	133.3	212.1	102.5	65.35
2038	82.45	50.34	133.2	73.47	71.78	79.23
2039	137.1	96.56	170.3	283.2	123.5	65.79
2040	119.8	88.27	219.2	130.6	74.2	39.44
2050s						
RCM	RCA4(IPSL)		RCA4(MIROC5)		RCA4(MPI)	
Scenario	RCP4.5	RCP8.5	RCP4.5	RCP8.5	RCP4.5	RCP8.5
2041	144.6	89.4	137.4	221.6	72.8	57.4
2042	153.0	96.5	144.9	252.4	70.9	59.1
2043	68.1	49.4	63.1	90.4	62.1	49.9
2044	173.8	96.2	171.4	282.8	81.4	78.3
2045	201.6	113.1	132.2	282.6	68.9	82.2
2046	146.2	92.5	158.1	330.5	65.7	48.8
2047	79.7	99.2	95.4	177.6	114.3	55.2
2048	111.4	64.5	63.6	75.3	60.3	61.1
2049	93.2	127.6	279.4	253.6	79.0	26.6
2050	282.4	72.9	136.1	280.0	50.9	57.2
2051	135.4	106.0	123.1	337.1	46.6	63.7
2052	79.4	139.0	106.0	126.7	50.2	53.5
2053	134.6	248.9	88.6	325.3	44.7	51.4
2054	184.0	40.3	125.1	267.4	45.2	76.9
2055	72.3	59.7	59.1	218.0	54.7	63.3
2056	137.8	279.9	223.5	211.6	97.9	124.1
2057	187.4	123.1	277.9	71.6	62.4	121.6
2058	180.2	85.2	320.0	195.4	39.0	43.8
2059	159.7	132.7	96.8	97.6	69.2	96.6
2060	101.8	121.6	147.0	220.8	53.1	49.6
2070s						

RCM	RCA4(IPSL)		RCA4(MIROC5)		RCA4(MPI)	
Senario	RCP4.5	RCP8.5	RCP4.5	RCP8.5	RCP4.5	RCP8.5
2061	83.3	134.9	156.0	235.5	69.9	68.9
2062	85.3	140.0	142.3	222.0	63.4	72.5
2063	56.9	136.9	243.4	216.7	117.4	62.9
2064	52.7	130.7	69.8	255.7	59.8	63.7
2065	125.2	51.0	107.0	148.7	26.9	89.0
2066	61.2	157.7	191.1	164.9	54.2	63.7
2067	109.0	83.0	345.5	189.3	66.4	75.3
2068	48.4	194.4	153.6	325.7	75.8	54.0
2069	82.0	138.1	104.3	319.4	108.8	60.2
2070	131.0	187.2	33.6	213.8	49.6	82.4
2071	72.6	177.7	133.4	108.5	65.2	91.9
2072	87.8	153.6	345.3	322.8	60.6	83.9
2073	136.0	80.6	352.4	312.5	88.9	69.9
2074	100.6	74.2	330.0	322.4	96.5	79.7
2075	72.1	189.3	234.0	120.4	80.4	71.4
2076	115.8	143.1	316.9	179.2	107.2	84.2
2077	159.2	200.6	220.9	214.0	73.4	75.8
2078	80.9	102.6	232.8	296.6	118.5	61.7
2079	75.8	154.7	190.6	324.7	66.7	73.5
2080	101.3	92.0	62.8	328.0	126.9	72.8

Appendix F: Percentage change of mean monthly rainfall during future periods of the 2030s, 2050s and 2070s.

near term(2030s)						
MONTH	IPSL		MPI		MIROC5	
	RCP4.5	RCP8.5	RCP4.5	RCP8.5	RCP4.5	RCP8.5
Jan	5.5	15.1	24.48	43.79	13	23.2
Feb	2.5	57.5	44.83	-31.93	5	12.6
Mar	-8.9	-8.9	-40.08	-35.98	20.2	20.6
Apr	44.7	54.4	26.39	3.74	-22.5	-19.6
May	2.3	46	9.21	-13.42	-2.3	17.2
Jun	52	48.1	-47.72	-56.49	-42.8	-24.8
Jul	-53.4	-30	-37.16	-44.96	36	34.5
Aug	-32.5	-7.6	-27.77	-13.16	34.8	41.4
Sep	7.6	28.7	14.05	21.99	32.1	9.3
Oct	23.6	22.4	-0.87	-27.78	7.7	-8.9
Nov	114.1	-33.4	5.52	61.77	-2.2	27.3

Dec	28.4	2.1	-0.91	-50.04	-80.9	-47.9
Mid- term(2050s)						
MONTH	IPSL		MPI		MIROC5	
	RCP4.5	RCP8.5	RCP4.5	RCP8.5	RCP4.5	RCP8.5
Jan	60.7	41.6	61.13	99.09	8.5	-17.5
Feb	-42.5	-20	-47.03	9.81	-12.9	-3.3
Mar	4.4	-57.8	-38.86	-38.03	-8	84.1
Apr	87.6	42.1	17.24	-1.52	-34.4	-29.3
May	32.3	40.2	-36.22	-35.68	23.3	15.6
Jun	103.9	100.6	-35.3	-32.29	-17.9	0.8
Jul	-15	-3.2	-41.67	-31.7	50.7	93.1
Aug	22.3	-4.1	-12.87	-23.55	41.2	50.8
Sep	21.7	3.9	0.2	14.61	52.3	37.6
Oct	141.4	37.1	-5.01	34.37	40.3	31.8
Nov	25.3	113.4	57.3	85.27	-37.9	-1.5
Dec	17.7	-18.1	45	-15.29	-48.1	-7.3
Late- term(2070s)						
MONTH	IPSL		MPI		MIROC5	
	RCP4.5	RCP8.5	RCP4.5	RCP8.5	RCP4.5	RCP8.5
Jan	-9.6	30.9	61.58	46.46	-0.2	-23.5
Feb	-27.5	-15	-50.63	-0.27	-23.4	-35.6
Mar	-46.7	-12.9	-33.46	-68.13	27.9	34.1
Apr	-21	112.1	18.25	-33.08	-31.5	-18.1
May	97	77.8	-20.31	-13.46	2.6	28.9
Jun	110.7	131.3	-21.45	-42.68	-27.6	15
Jul	-20.3	18.4	-46.31	-39.5	69.4	119.6
Aug	-7.3	5.3	-19.07	-3.3	67.3	99.7
Sep	-11.7	34.7	22.3	12.99	47.9	73.1
Oct	81.3	117.2	48.34	44.72	12.7	86.9
Nov	73.5	73.3	65.32	120.23	-73.9	-90.3
Dec	32.1	73.3	41.54	-2.26	-65.3	-83.6

Appendix G: Percentage change of mean monthly maximum temperature during future periods of the 2030s, 2050s and 2070s.

near term(2030s)						
MONTH	IPSL		MPI		MIROC5	
	RCP4.5	RCP8.5	RCP4.5	RCP8.5	RCP4.5	RCP8.5
Jan	-0.1	0.1	-0.2	-0.2	0.3	0.2
Feb	0	0	-0.6	-0.8	0.3	0.5
Mar	0	0	-1.9	-1.7	0.8	0.8

Apr	-0.2	-0.1	-2	-1.9	1	1.3
May	-0.2	-0.2	-0.6	-0.6	0.6	0.7
Jun	-0.3	-0.1	0.7	0.5	-0.9	-0.5
Jul	0.2	0.1	2.1	2	-1	-1.2
Aug	0.6	0.4	0.9	1.1	-0.5	-1
Sep	0.1	0	0.7	0.9	0.4	0
Oct	0	-0.2	0.3	0.5	0.3	0.3
Nov	-0.1	0.2	0.3	0.2	-0.7	-0.6
Dec	-0.1	0	0.2	0	-0.6	-0.5
Mid- term(2050s)						
MONTH	IPSL		MPI		MIROC5	
	RCP4.5	RCP8.5	RCP4.5	RCP8.5	RCP4.5	RCP8.5
Jan	0.1	0.2	-0.4	0.1	0	0.2
Feb	0.3	0.1	-0.9	-0.8	0.5	0.1
Mar	0.1	0.1	-1.6	-2.1	1.2	0.8
Apr	-0.1	0	-2	-1.8	1	1.1
May	-0.1	-0.1	-0.4	-0.4	1	1.1
Jun	-0.1	-0.3	0.4	0.6	-1	-0.5
Jul	0	-0.1	2.1	1.7	-1.1	-1.1
Aug	0.2	0.4	1.1	1.1	-0.6	-0.6
Sep	0.1	0.2	0.6	0.7	0.2	0.3
Oct	-0.2	-0.3	0.2	0.3	0.3	0.2
Nov	-0.3	-0.1	0.3	0.3	-0.6	-0.8
Dec	-0.1	0	0.4	0.1	-1	-0.7
Late- term(2070s)						
MONTH	IPSL		MPI		MIROC5	
	RCP4.5	RCP8.5	RCP4.5	RCP8.5	RCP4.5	RCP8.5
Jan	0.6	1	0.2	0.9	0.5	1.1
Feb	0.6	1.2	-0.4	0.7	0.6	1.5
Mar	0.7	1.2	-1.5	-0.6	1.3	2.3
Apr	0.8	0.6	-1.7	-1	1.7	3
May	0.2	0.7	-0.2	0.3	1.2	2
Jun	0.3	0.6	0.8	1.4	-0.2	0.6
Jul	0.5	0.9	2.4	2.6	-0.3	0.4
Aug	1.2	1.5	1.1	1.5	-0.3	0.6
Sep	1	1.4	0.9	1.4	0.6	1.3
Oct	0.5	0.7	0.5	0.9	0.4	1.2
Nov	0.3	0.5	0.7	1.2	-0.6	0.4
Dec	0.4	0.3	0.7	1.5	-0.4	0.2

APPENDIX H: Percentage change of mean monthly minimum temperature during future periods of the 2030s, 2050s and 2070s

2030S						
month	IPSL RCP4.5	IPSL RCP8.5	MIROC RCP4.5	MIROC RCP8.5	MPI RCP4.5	MPI RCP8.5
Jan	0.1	0.3	0.5	-0.2	0	0.1
Feb	0.2	0.4	0.3	0.6	0.4	-0.3
Mar	-0.1	0.3	0	0	-0.7	-0.5
Apr	-0.1	0.2	0	0	0.3	0.1
May	-0.2	0.3	-0.1	-0.1	0.2	0.2
Jun	-0.4	-0.2	0.4	0.1	-0.1	0
Jul	0.1	0.1	-0.2	-0.2	-0.1	-0.2
Aug	0.4	0	0	0	-0.1	0.1
Sep	0	-0.2	-0.2	-0.4	0.1	0.4
Oct	0.2	-0.1	0.5	0.5	-0.3	0
Nov	0.1	-0.5	-0.2	0.3	0.3	0.5
Dec	-0.3	-0.6	-1.2	-0.6	0	-0.1
2050s						
month	IPSLRCP 4.5	IPSL RCP8.5	MIROC RCP4.5	MIROC RCP8.5	MPI RCP4.5	MPI RCP8.5
Jan	0.3	0.1	0	-0.2	-0.1	-0.2
Feb	-0.1	-0.2	0.6	0.5	-0.2	0.2
Mar	0	-0.2	0.1	0.3	-0.5	-0.9
Apr	0.3	0.3	-0.3	-0.4	0.2	0.2
May	0.4	0.8	0.3	0.4	0.1	0.4
Jun	0	-0.4	0.1	0.1	-0.2	0.1
Jul	-0.4	-0.3	0.1	-0.1	-0.1	-0.3
Aug	0.1	0.2	-0.1	0	0	-0.2
Sep	0	0	0	-0.3	0.2	0.1
Oct	0.3	0.6	0.7	0.7	0.1	0.2
Nov	0	-0.5	-0.5	-0.1	0.6	0.6
Dec	-0.9	-0.4	-1	-0.7	0	-0.2
2070S						
month	IPSL RCP4.5	IPSL RCP8.5	MIROC RCP4.5	MIROC RCP8.5	MPI RCP4.5	MPI RCP8.5
Jan	0.5	1.3	0.6	0.4	0.4	0.8
Feb	0.4	1.5	0.7	0.7	0.1	1.2
Mar	0.8	1.5	0.4	0.6	-0.4	-0.1
Apr	0.8	1.8	-0.2	0.5	0.9	1.1
May	1.1	2	0.7	1	0.6	1.4
Jun	0.5	1.4	0.5	1.1	0.6	0.8

Jul	0.2	0.7	0.3	0.7	0.2	0.6
Aug	0.6	1.2	0.2	0.7	0.3	0.6
Sep	0.8	1.4	0.3	0.7	0.6	0.9
Oct	1	2	1.1	2.4	1.1	1.8
Nov	0.8	1.7	-0.3	0.2	0.9	2
Dec	0.2	1.4	-1	-0.9	0.6	1.1

APENDIX I: The description of the Global Climate Models (GCMs) dynamically downscaled by RCA4 CORDEX.

	Institute	GCM name	Abbreviated name
1	Canadian center for climate modeling and analysis (Canada)	CCCma-CanESM2	CanESM2
2	Centre national research meteorologists (France)	CNRM-CRAFACS-CNRM-CM5	CNRM-CM5
3	Met office hadley center	MOHC-HadGEM2-ES	HadGEM2-ES
4	Consortium of European research institution and researchers	ICHEC-EC-EARTH	EC-EARTH
5	NOAA geophysical fluid dynamics laboratory, USA	NOAA-GFDL-GFDL-ESM2M	GFDL-ESM2M
6	Institut pierre-simon laplace, France	IPSL-IPSL-CM5A-MR	IPSL-CM5A-MR(IPSL)
7	National institute for environmental studies, and japan agency for marine-earth science and technology (MIROC),Japan	MIROC-MIROC5	MIROC5
8	Commonwealth scientific and industrial research organization	CSIRO-MK3-6-0	CSIRO
9	Max planck institute for meteorology (Germany)	MPI-M-MPI-ESM-LR	MPI-ESM-LR(MPI)
10	Norwegian climate center (Norway)	NCC-NorESM1-M	NorESM1-M

Appendix J: List of the CORDEX Africa RCMs, their driving GCMs and RCPs downscaled by each RCM

		AFR-44 CORDEX simulations		
No	RCM	Driving GCM	RCPs	Period
1		CCCma-CanESM2	4.5,8.5	1951–2100
		CNRM-CERFACS-CNRM-CM5	2.6,4.5,8.5	1951–2100
		MOHC-HadGEM2 E S	2.6,4.5,8.5	1951–2100
		NCC-NorESM1 M	2.6,4.5,8.5	1951–2100
	SMHI-RCA4	ICHEC-EC-EARTH	2.6,4.5,8.5	1951–2100
		MIROC-MIROC5	2.6,4.5,8.5	1951–2100
		NOAA-GFDL-GFDL-ESM2M	4.5,8.5	1951–2100
		MPI-M-MPI-ESM-LR	2.6,4.5,8.5	1951–2100
		IPSL-IPSLCM5A-MR	2.6,4.5,8.5	1951–2100
		CSIRO_QCCCE-CSIRO-Mk3–6-0	4.5,8.5	1951–2100
2		ICHEC-EC-EARTH	4.5,8.5	1951–2100
	KNMI-RACMO22T	ICHEC-EC-EARTH	2.6	1951–2100
		MOHC-HadGEM2 E S	2.6,4.5,8.5	1951–2100
3	DMI-HIRHAM5	ICHEC-EC-EARTH 45, 85 1951–2100	4.5,8.5	1951–2100
		NCC-NorESM1 M	4.5,8.5	1951–2100
4		CNRM-CERFACS-CNRM-CM5	4.5,8.5	1951–2100
	CLMcom-CCLM4–8-17	MOHC-HadGEM2 E S	4.5,8.5	1951–2100
		ICHEC-EC-EARTH	4.5,8.5	1951–2100
		MPI-M-MPI-ESM-LR	4.5,8.5	1951–2100
5	CCCma-CanRCM4	CCCma-CanESM2	4.5,8.5	1951–2100
6	BCCR-WRF331C	NCC-NorESM1 M	4.5,8.5	1951–2100
7	MPI-CSC-REMO2009	ICHEC-EC-EARTH	2.6,4.5,8.5	1951–2100
		MPI-M-MPI-ESM-LR	2.6,4.5,8.5	1951–2100
		IPSL-IPSLCM5A-LR	2.6,85	1951–2100
8	GERICS-REMO2009	MIROC-MIROC5	2.6	1951–2100
		MOHC-HadGEM2-ES	2.6	1951–2100
		NOAA-GFDL-GFDL-ESM2G	2.6	1951–2100
9	UQAM-CRCM5	CCCma-CanESM2	4.5	1951–2100
		MPI-M-MPI-ESM-LR	4.5	1951–2100
10	CNRM-ALADIN53	CNRM-CERFACS-CNRM-CM5	4.5,8.5	1951–2100
11	ICTP-RegCM4-3	MPI-M-MPI-ESM-LR	4..5	1951–2100

Source (Osima et al., 2018)